Marianne Leinikka

Recombinant antibody coated SU-8 microfluidic devices

School of Electrical Engineering

Thesis submitted for examination for the degree of Master of Science in Technology.

Espoo 26.5.2014

Supervisor:

Prof. Sami Franssila

Instructors:

PhD Tarja Nevanen

PhD Ville Jokinen

Aalto University
School of Electrical
Engineering

AALTO UNIVERSITY ABSTRACT OF THE

SCHOOL OF ELECTRICAL ENGINEERING MASTER'S THESIS

Author: Marianne Leinikka

Title: Recombinant antibody coated SU-8 microfluidic devices

Date: 26.5.2014 Language: English Number of pages: 97 +15

Degree programme: Bioinformation technology

Supervisor: Prof. Sami Franssila

Instructors: PhD Tarja Nevanen, PhD Ville Jokinen

Immunoassay is a bioanalytical test, which utilizes the specific binding capability the antibody and the target analyte have towards each other, in order to detect different analytes from the samples. The miniaturized, polymeric microfluidic immunoassays, called as immunochips combine the cheap material costs, disposability and fast analysis. They enable large amounts of samples to be screened fast, which assists prognostication of many hazardous diseases. However, the development is not a straightforward process as the antibodies are delicate molecules and easily denatured when coupled to polymers. The functional application demands both careful planning regarding the surface modification of the substrate and the choice of the antibody immobilization method as they both have a major impact on the functioning of the application.

In this thesis, the preliminary results of α-MPA Fab F5 immobilization onto SU-8 surface via residual epoxy groups are shown. Two different approaches are presented: random covalent and IDA-Co chelation, oriented immobilization. Both methods were studied in terms of different immobilization parameters (antibody incubation time, antigen amount, incubation buffer, SU-8 surface modification and both, SU-8 and antibody stability) and compared to each other. In addition, the possibility to use bare SU-8 as a MALDI base was studied and construction of a SU-8 immunoassay chip, where an innovative immobilization method based on position-selectivity and capillary action as the power source were used, was presented.

This thesis serves as a comprehensive guideline for the follow-up studies of the antibody immobilization onto SU-8 surface. These preliminary results indicate that the antibody immobilization onto SU-8 with both of the presented immobilization methods is feasible. The comparison studies showed that the random immobilization was better in over 80 % of the studied cases. Despite the higher antibody efficiency responses the random immobilization offered, the better repeatability obtained in the oriented immobilization would favor it at least while thinking the functional applications. In MALDI studies, the sensitivity was still inadequate. In the immunochip studies, a correct contact angle (42º) and the layer parameters (thickness: 14.8 μm, consecutive row distance: 23 μm), which yielded the correct functioning of the presented application, were determined.

Keywords: SU-8, Fab, recombinant antibody, microfluidics, polymer, antibody immobilization

AALTO-YLIOPISTO DIPLOMITYÖN

SÄHKÖTEKNIIKAN KORKEAKOULU TIIVISTELMÄ

Tekijä: Marianne Leinikka

Työn nimi: Rekombinanttivasta-aineilla pinnoitetut, mikrofluidistiset SU-8 sovellukset

Päivämäärä: 26.5.2014 Kieli: Englanti Sivumäärä: 97 +15

Koulutusohjelma: Bioinformaatioteknologia

Valvoja: Prof. Sami Franssila

Ohjaajat: FT Tarja Nevanen, FT Ville Jokinen

Vasta-ainemääritys perustuu vasta-aineen ja antigeenin väliseen spesifiseen sitoutumiseen, jonka avulla voidaan määrittää erilaisia aineita näytteistä. Mikrofluidistiset, polymeeriset vasta-ainesirut, jotka ovat perinteisen määrityksen miniaturisointeja, mahdollistavat halvat materiaalikustannukset, kertakäyttöisyyden ja nopean analysoinnin. Niiden avulla pystytään seulomaan nopeasti suuriakin näytemääriä, mikä edesauttaa mm. useiden tautien diagnosointia. Tällaisten sirujen valmistus ei kuitenkaan ole yksinkertaista, koska vasta-aineet herkkinä molekyyleinä denaturoituvat helposti kiinnityksen yhteydessä. Toimiva vasta-ainesiru vaatii sekä tarkkaa suunnittelua alustan että kiinnitysmenetelmän valinnan suhteen.

Tässä diplomityössä esitetään ensimmäiset tulokset α-MPA Fab F5 rekombinanttivasta-aineen kiinnittämisestä SU-8:n pintaan valottumisessa vapaaksi jäävien epoksiryhmien avulla. Työssä käsitellään kahden eri kiinnitysmenetelmän, suoran (satunnainen, kovalenttinen) ja suunnatun (IDA-Co), optimointia vasta-aineen inkubaatioajan, antigeenin määrän, inkubaatioliuoksen, pinnan käsittelyn sekä pinnan että vasta-aineen stabiilisuuden suhteen. Menetelmiä myös verrattiin toisiinsa. Työssä tutkittiin SU-8:n soveltuvuutta MALDI-mittausalustaksi. Lisäksi työssä toteutettiin täysin SU-8:sta valmistettu siru, jonka toiminta perustuu kapillaari-ilmiöön ja kanavien rakenteeseen koodattuun ja täysin uudenlaiseen, paikka-selektiiviseen kiinnitykseen.

Diplomityö toimii kattavana ohjeena jatkotutkimuksille vasta-aineiden kiinnittämisestä SU-8 pintaan. Työssä saadut tulokset osoittavat, että vasta-aineen kiinnitys SU-8 pintaan on mahdollista molemmilla menetelmillä. Suora kiinnitysmenetelmä osoittautui yli 80 % kokeista orientoitua menetelmää paremmaksi. Lopputuotetta ajatellen, orientoidun kiinnityksen tulosten parempi toistettavuus on kuitenkin toivottavampaa. MALDIn sensitiivisyys ei vielä ollut riittävä SU-8 käyttöön mittausalustana. Vasta-ainesirututkimuksissa sen sijaan pystyttiin osoittamaan oikea kontaktikulma (42º) ja SU-8 kanavarakenteiden oikeat parametrit (paksuus: 14.8 μm ja kuvioriviväli: 23 μm), joiden avulla siru toimi halutunlaisesti.

Avainsanat: SU-8, Fab, rekombinanttivasta-aine, mikrofluidistiikka, polymeeri, vasta-aineen kiinnitys

Preface

First of all, I want to thank my supervisor Dr. Sami Franssila, who has been more than patient with me and my thesis. The instructions and endless encouragement you gave me were valuable. You did not let me settle with the text, but pushed the best out of me even though I let you down more than couple of times. Secondly, I want to thank my instructor PhD Tarja Nevanen who introduced me to the fascinating world of antibodies and especially recombinant antibodies. The trust you had for my abilities to work with antibodies was unforgettable. I hadn't got any experience prior this thesis. I am also grateful, that you donated serum for my research studies. Most of all I want to thank my dear friend and instructor PhD Ville Jokinen, who managed to graduate to PhD before I managed to finish my Master's studies. You have always trusted my abilities to write this thesis! You have given valuable comments to the text and especially related to the structure of the thesis. Without you, this thesis wouldn't be what it is now. I also want to thank my work colleagues both in Micronova and VTT laboratories, especially Susanna, Piia, Mikko and Antti. The coffee breaks and interesting stories kept me going even though work days were sometimes long. However, I think the one person most interested in my thesis has been my father. The passion he has had towards the writing process has been incredible. He even offered to help with the text even though microfabrication is not his specialty. Therefore this thesis is dedicated especially to you, my Dad. But also equally to my loving Mum, who knows how to cheer me up. I also want to thank my siblings and friends, you are priceless.

The writing of this thesis has been an extremely long journey. Research work is certainly my passion in life, but somehow this writing process was exhausting and almost too difficult for me. Luckily, I know myself. I knew, when all the other doubted, that this day would come - me with a fully written thesis.

Helsinki, 26.5.2014

Marianne Leinikka

Table of Contents

Appendices:

Symbols

a	atto
α	anti
IU	international unit
k	kilo
m	milli
μ	micro
n	nano

Abbreviations

AEAPS	[3-(2-aminoethyl)aminopropyl]-trimethoxysilane
Ag	Silver
AP	Alkaline phosphatase
APTES	Aminopropyltriethoxysilane
AR	Aspect ratio
ATIR-FTIR	Attenuated total reflection fourier transform infrared
BioMEMS	Biological microelectromechanical system
BSA	Bovine serum albumine
c	Constant domain
CAN	Cerium ammonium nitrate
Co	Cobalt
$CoCl_2$	Cobalt(II)-chlorid hexahydrat
COC	Cycloolefic copolymer
COOH	Carboxyl acid group
CRP	C-Reactive protein
CTE	Thermal expansion coefficient
Cy3	Red fluorescent dye of the cyanine dye family
Da	Dalton
3D	3-Dimensional
DDIW	Double-distilled water
DNA	Deoxyribonucleic acid
DRIE	Deep reactive ion etching
E. coli	Escherichia coli
Fab	Antigen-binding fragment
Fc	Fragment crystallizable region
FITC	Fluorescein isothiocyanate
Fv	Active antibody fragment
GBL	γ-butyrolactone
HB	Hard bake
HCCA	α-cyano-4-hydroxycinnamic acid
HCPK	1-hydroxycyclohexyl phenyl ketone
HDMS	Hexamethyldisilazane
He	Helium
HEMA	2-hydroxyethylmethacrylate-based
His	Histidine
His6	Histidine6
H_2O	Hydrogen peroxide

hPDMS	Hard polydimethylsiloxane
HWCVD	Hot wire chemical vapour deposition
IgG	Immunoglobulin G
IPA	Isopropanolacetate
IDA	Iminodiacetic acid
LIGA	German acronym for Lithography, Electroplating and Molding
Lys	Lysine
LOC	Lab-on-a-chip
M	Molar
MALDI	Matrix-assisted laser desorption / ionization
MEMS	Microelectromechanical system
MHA	Mercaptohexadeconic acid
MPA	Mycophenolic acid
MS	Mass Spectrometer
MUA	11-mercapto undecanoic acid
$Na_2B_4O_7$	Sodium borate
NaOH	Sodium hydroxide
NH_2	Amine group
NIL	Nanoimprint lithography
NUV-NIL	nanoimprint lithography
o/n	Overnight
ODTS	Octadecyltrichlorisilane
PAA	Poly(acrylic acid)
PAG	Photoacid generator
PAM	Poly(acrylamide)
PBS	Phosphate buffered saline
PC	Polycarbonate
PCR	Polymerase chain reaction
PDMS	Polydimethylsiloxane
PE	Polyethyl
PEB	Post-exposure bake
PEG	Polyethylene glycol
PGMEA	Propylene glycol methyl ether acetate
PMMA	Polymethyl methacrylate
PNPP	4-Nitrophenyl phosphate disodium salt hexahydrate
POC	Point-of-care
PS	Polystyrene
RIE	Reactive ion etching
RM	Replica moulding
rpm	Rounds per minute
RT	Room temperature
SAM	Self-assembled monolayer
SAV	Surface-to-volume ratio
SB	Soft bake
SEM	Scanning electron microscope
Si	Silicon
SiO_2	Silicon oxide
SPR	Surface plasmon resonance
SU-8	Negative photoresist SU-8
TBS	Tris-buffered saline

TD	Decomposition temperature
TiO_2	Titanium dioxide
T_g	Glass transition temperature
TSH	Thyroid-stimulating hormone
μTAS	Micro total analysis system
UV	Ultraviolet light
UV-NIL	Ultraviolet-nanoimprint lithography
v	Variable domain

1 Introduction

1.1 Microfluidics and immunoassays

Immunoassay is a bioanalytical test to detect the concentrations of analytes from the samples by utilizing the specific binding capability the antibody and the target analyte have towards each other. By combining microfluidics, the art of handling small amounts of liquids in micro scale, to immunoassays a new diagnostic platform is created. Even though the history of this platform is still rather short, both immunoassay types, homogenous (immunoreaction happens in soluble phase) and heterogenous (one of the immunoreagents requires to be immobilized) have already been successfully implemented to the microfluidics [1]. Immunoassay markets are attractive as assays are performed in high quantities by centralized laboratories and there is a wide range of potential users both in developed and developing countries (e.g. point-of-care (POC) and home diagnostics applications for the former and simple diagnostic devices for the latter [2]).

The reason why these miniaturized immunoassay chips has gained attention from the conventional immunoassays is the improvements they offer: lower consumption of reagents (from 100 µl to 1 µl), decreased analysis time, disposability and increased sensitivity to mention a few [3-4]. In addition, these devices can be controlled passively by means of diffusion and / or capillary action [3] or by utilizing interesting innovations (e.g. liquid control by air evacuation [4]). The lack of need of external energy source makes possible to fabricate simple and easy-to-use, portable devices with impressively low detection limit in the attomolar (aM) range [5-6]. In addition to more technical reasons, one motivation fact is the urging need to be able to screen fast different clinically important antigens, like C-reactive protein (CRP). CRP is a major acute-phase reactant protein (117.5 kDa), which is often used as a biomarker for the prognostication of cardiovascular events [7]. The clinically relevant detection limit of CRP is 3 mg/l [8].

The idea to implement antibodies to the microfluidic platform originates from the successful implementation of the deoxyribonucleic acid (DNA) to the chip structure. One example of a functional DNA chip is the polymerase chain reaction (PCR) chip, which multiplies the DNA sequence thousands of times [9]. But the construction of a functional immunoassay chip similar to DNA chip is not that simple. There are several reasons to support the argument: antibodies (and proteins in general) are chemically and structurally much more complex and heterogenous compared to DNA, their concentration varies a lot in a single biological sample, they have a

poor resistance towards heat and they are also amphiphilic molecules with pronounced surface activity (DNA constitutes of equally negatively charged nuclei acids). Antibodies may denature when immobilized to foreign surfaces like polymers, which makes the coupling of them to microfluidic devices challenging [5].

Microfluidic immunoassays are fabricated in silicon, glass, polymer or their combinations [1, 3,5]. Silicon, which is a traditional semiconductor industry material, and glass have several limitations set by their material properties and fabrication processes, which have directed the material choice to polymers [1,3,5]. Silicon, for instance, is not optically transparent within the ultraviolet (UV) / visible area and the microfabricated glass channels have often a curved bottom, which complicates the detection. Instead, polymers are a wide group with highly diverse physical and chemical properties. They have reduced material costs, which allow the fabrication of disposable devices (elimination of cross-contamination). Besides polymers are available in multiple different formats from foams to films, wafers to powders and have high gas permeability (depending on the application, this may be advantage or disadvantage). Many polymers are also transparent allowing the use of different optical detection methods suitable for diagnostics (e.g. fluorescence) and are often naturally biocompatible. The copolymerization of two or more polymers enables further increase in material properties. [10-11]

Nevertheless, the most dominant feature to support the use of polymers is the diversity they offer with fabrication methods [11]. Polymers can be fabricated with wide range of methods, which are also compatible with the conventional microfabrication techniques. Harmful particles or residues, which are often generated during the processing of the traditional materials (e.g. due to usage of harsh chemicals), can be prevented by the choice of less contaminating processes.

Roughly, the polymer fabrication techniques can be divided into two: direct and replication techniques. The difference between these groups is the principle of how the modification is applied. Direct techniques aim to transfer the designed pattern to polymer by irradiating the polymer with energy source either through mask or by beam scanning without the mask. The energy source can be UV-light, laser, X-ray or a charged particle beam. Direct techniques are highly developed and mainly used in the academic world, because they are well suited for prototype fabrication.

In replication techniques, the inverse structure of the master (also called as mould) is transferred to the polymer either by casting, moulding or embossing. The master is either hard (e.g. silicon [12]) or soft (e.g. polymer [13]). The fabrication of master is the most time-consuming and

expensive step within the replication techniques. But because the single master can produce even hundreds of thousands of replicas, different replication methods possess great industrial and economical potential. [10] In casting (e.g. replica moulding) and moulding (e.g. injection moulding) processes polymer in its liquid form is either poured or injected to the master, respectively. Embossing shapes the softened but still solid polymer by pressing the master against the surface of the polymer. Pressure, light, heat or their combination is often applied to enhance the embossing process (e.g. pressure in nanoimprint lithography (NIL), light in UV-NIL and heat in hot-embossing).

Currently, the most dominant material for microfluidic immunoassays is polydimethylsiloxane (PDMS) [1,3,5]. There are several studies showing PDMS is a suitable material for antibodies [4, 6, 14-17]. The immunoassays are made either entirely on PDMS [15] or by combining several materials [14]. The advantages of PDMS are the well-known material properties, a high degree of biocompatibility and fast and cheap fabrication method, which does not involve the cleanroom environment [3]. The PDMS based applications are usually fabricated via casting (replication technique, figure 1). Li et al. [7], for instance, fabricated a PDMS microfluidic immunoassay based on heterogenous sandwich assay to detect CRP by fluorescence (figure 1). The chip (length: 28 mm, width: 28 mm, thickness: 3 mm) was constructed of two separate PDMS layers bonded to each other by oxidation treatment in a plasma system. Both layers were obtained using previously mentioned casting: the base (flat slab) without and the layer with five microfluidic channels (length: 17 mm, width: 150 µm width, thickness: 35 µm) with silicon master. The fluids were delivered to the chip by pressure-driven flow utilizing syringe pumps. They reached detection limit of 0.54 µg/ml. Other implemented polymers in microfluidic immunoassays include polystyrene (PS) [18], cycloolefic copolymers (COC) [19], polymethyl methacrylate (PMMA) [12, 20] and polycarbonate (PC) [1, 5].

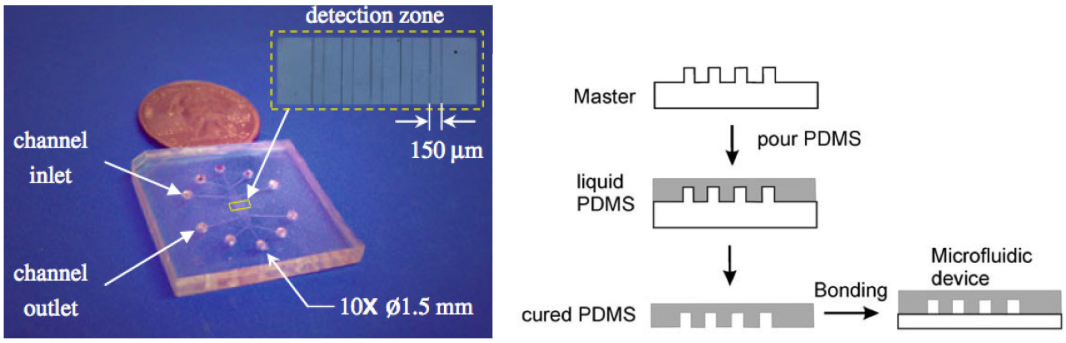

Figure 1. Microfluidic PDMS immunoassay chip for CRP detection (on left). The chip was fabricated by PDMS casting (on right). From ref. [7, 10 (adapted)].

1.2 Surface modification and antibody coupling

The most crucial step in construction of a heterogenous immunoassay chip is the coupling of the antibody as it defines the achievable detection limit for the assay [4]. The large surface-to-volume ratio, which on the other hand enables short diffusion distances and therefore fast reactions, allows a large surface for immunoagents to interact with. Antibodies (and proteins in general) are highly prone to nonspecific adsorption by e.g. hydrophobic interactions [1]. This tendency is enhanced by the hydrophobic nature the polymers (e.g. PDMS and PMMA), which are often used in microfabrication, have [5]. As the nonspecific adsorption results in high degree of background signal, the assay performance is degraded both in sensitivity and selectivity [1,4]. Therefore different surface modification methods are applied to improve the surface control during antibody coupling to the microfluidic surface.

Potential surface modifications are either physical or chemical [5]. One example of a familiar physical surface modification is the Reactive Ion Etching (RIE), which is an oxygen plasma treatment, which both activates hydroxyl groups and increases surface roughness [21]. There are many studies indicating the RIE-treated surface both alleviates the nonspecific adsorption and increases surface roughness thereby improving the assay sensitivity [1, 21-22]. For example, in the study of Yuan et al. [22], root mean square (RMS) roughness value for PMMA increased from 0.232 to 2.608 with plasma oxidation treatment. Examples of chemical surface treatments are polymer grafting (e.g. UV-grafting of polyacrylic acid (PAA) on PMMA [20]), addition of self-assembled monolayers (SAMs) (e.g. 16-mercapto-hexadeconic acid (16-MHA) on gold coated PS substrate [18]) or amphiphilic polymers (e.g. second generation amphiphilic polymers poly(DMA-r-mPEGMA-r-NAS) and poly(BMA-r-mPEGMA-r-NAS on COC [19]) and sol-gel technology (e.g. Al_2O_3 sol-gel in $(BMA)_x$-$(MAOPTMS)_y$ modified microchannels) [12]).

Another advantage often associated to surface modification is the yielding of higher surface loadings compared to the nontreated surfaces [1, 20, 22]. This is important especially with microfluidic immunoassays as the total surface area is very small compared to the conventional immunoassay surfaces and therefore it is important to have all the antibodies fully functional. Wen et al. [20], for example, were able to improve the detection limit manyfold. They treated PMMA surface with oxygen plasma (20 sccm, 300W, 30s) and then UV-grafted PAA to formed hydroxyl groups prior attaching the antibody through linker molecule. Assay sensitivity can also be improved by simple means of microstructuring. The structuring of a simple channel design by PDMS microposts of 30 μm in height increased the total surface area 1.75-fold compared to

the flat area [23]. The fluorescence signal amplification in the performed sandwich assay showed linear dependence of the relative surface area of the post structures.

The actual coupling of antibodies to polymer is done either via physical adsorption, covalent coupling or bio-specific immobilization [24]. The chosen method is decided case-specific, but with microfluidic applications, the covalent coupling has been the mainstream method [5]. The main target in immobilization is to maintain the conformation and functionality of the antibody by positioning the antigen-binding site towards solution phase in a correct incubation conditions (figure 2). Even though the high surface coverage is desired, the orientation of the antibodies should be loose enough to avoid steric obstruction [24]. The latter two immobilization methods, covalent coupling and bio-specific immobilization, are often associated to optimal orientation due to more controlled and specific reactions between the surface and the antibody molecule and therefore higher antibody activity compared to physical adsorption [25]. Physical adsorption is based on the weak interactions and antibodies can land in any possible orientation on the surface (figure 2).

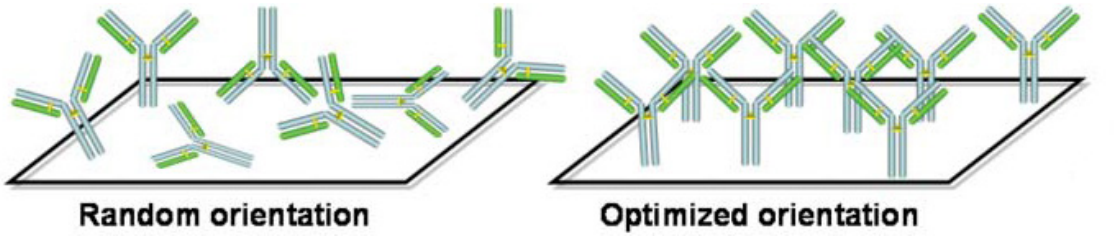

Figure 2. In optimized orientation of antibody, antigen-binding site is towards the solution phase which yields high surface coverage and maintained antibody activity. Adapted from ref. [24].

The immobilized antibody is often a natural antibody, like immunoglobulin G (IgG) with mammalian origins [12, 18-19]. However, the detection sensitivity would be enhanced by the usage of genetically engineered, recombinant antibody fragments, like antigen-binding fragment (Fab). Their small size enables more fragments to be immobilized in the same area compared to the intact antibodies. Recombinant Fabs are truncated antibodies, which lack the Fc part of the IgG. One way to develop recombinant antibodies is the phage display technique [26], which links the phenotype to the genotype (antigen-binding behaviour to coding genes). Antibodies binding to desired targets can be selected from the phage display antibody libraries. Furthermore, it is possible to tailor the properties of the antibody fragment e.g. by adding

affinity tags to the C-terminus of the heavy chain. An example of a tag is a histide (His) -tag [27]. The tag is especially advantageous in the antibody coupling as it enables the immobilization of the fragment in an oriented manner [24]. Moreover, fast and efficient production, small size and high surface loadings are numbered among the advantages of the antibody fragment [27]. In the study of Brockmann et al. [27], Fabs offered 3-folds higher binding capacity, faster kinetics and better detection limit of thyroid-stimulating hormone (TSH) compared to the whole monoclonal antibodies (0.09 mIU/L TSH and 0.26 mIU/L TSH, respectively). Despite the advantages the recombinant fragments offer, their utilization is not widespread within the conventional immunoassays [27]. Therefore, the studies based on microfluidic supports are also scarce or lacking completely.

1.3 Scope of the thesis

In this thesis we study the recombinant Fab fragment immobilization onto SU-8, an epoxy-based photoresist. SU-8 is widely used in microfluidics, because of mechanical reliability, chemical resistance to solvents, acids and bases as well as easy fabrication by photolithography [27]. Even though SU-8 has adequate biocompatibility [29] and reactive epoxy groups capable of biomolecule coupling after fabrication [28, 30-32], comparatively few studies exist on antibody immobilization. In most of the previous studies, antibodies have been immobilized via covalent attachment onto SU-8 surface [28, 31-33].

We demonstrate the feasibility of His6-tagged Fab (mycophenolic acid (MPA) Fab) immobilization onto SU-8 surface and the construction of an immunoassay chip, which is made entirely of SU-8. Two different immobilization methods, random covalent and iminodiacetic acid (IDA) - cobalt (Co) chelation immobilizations [34] were optimized. Also, the comparison between these in terms of antibody incubation time, antigen concentration, biofouling resistance, wet and dry storing, pH of the immobilization buffer and the effect of surface patterning is presented. At least to our knowledge, studies on immobilization of recombinant Fab fragments with His-tags have not been presented before for SU-8 surface. In addition, the few intact antibody immobilization studies found utilized planar SU-8 excluding one study where antigens were immobilized instead of antibodies on nanopatterned SU-8 [35].

At the moment, the detection methods in microfluidic immunoassays are mainly comprised by fluorescence, surface plasmon resonance (SPR) and electrochemical detection [5]. The previous studies with SU-8 have always been based on fluorescence detection. Therefore, the potential to use SU-8, either as planar or nanopatterned surface, in detection of the interaction between

antibody and antigen with matrix assisted laser desorption / ionization (MALDI) mass spectrometry (MS) is incorporated to this thesis. Previous study of Hua et al. [36] demonstrated the usage of SU-8 as a MALDI base, but with a bulk modified version. They coupled the typical MALDI matrix material α-cyano-4-hydroxycinnamic acid (HCCA) covalently into SU-8 via cationic photopolymerization reaction.

In addition to recombinant antibody immobilization the novelty presented in this thesis lies in the directed capillary flow by which the recombinant antibody solution is selectively positioned only to a certain compartment of the chip structure. The technique is based on our own findings [37]. Position-selective immobilization enables the simultaneous analysis of different antigens in a single microfluidic device [5]. It is not a new technique within the microfluidic immunoassays as Bernard et al. [15] and Hashimoto et al. [23] have shown. However, in their studies the position-selectivity was incorporated into the fabrication process. In our application the position-selectivity is encoded in the design of the microfluidic structure.

In order to assess the aims, three main questions were identified:

1. Which of the two developed immobilization concepts, random or oriented immobilization offer higher antibody fragment activity after immobilization process?
2. Is bare SU-8 surface suitable for MALDI detection?
3. Is it possible to create a functional immunoassay prototype made entirely of SU-8?

1.4 Structure of the thesis

The literature part of this thesis is divided into five chapters. Chapter two explains the basic principles of passive microfluidics – how spontaneous flow of liquids is possible in micro scale channels and what unique properties micro world brings not seen in the macro world. Chapter three concentrates on the base material of all the tests: negative photoresist SU-8. This chapter explains widely the properties and fabrication and modification of SU-8. The antibody structure, the concept of immunoassay and the recombinant Fab fabrication are explained in chapter four. Chapter five describes the existing antibody immobilization methods on substrate surface and explains which part of the antibody molecule enables the immobilization. The differences between the intact antibody and fragment immobilizations are reviewed. This chapter also reviews the current state of antibody immobilization onto SU-8 substrate. The main points in the literature part of this thesis are the base material SU-8 and its properties as well as antibody

immobilization on polymer support. Therefore homogenous immunoassays and other supports than polymers and SU-8 are excluded.

The experimental part consists of three parts: preliminary planning, system-setup and proof-of-concept (figure 3). Preliminary planning has been done prior this thesis. System-setup step involves the development of two different immobilization concepts, which were both developed to be suitable for SU-8 immobilization. The last part, the proof-of-concept presents the drafting and preliminary testing of the easy-to-use heterogenic assay based on the capillary flow, which demands only minimal activity of the end user and is made entirely of SU-8.

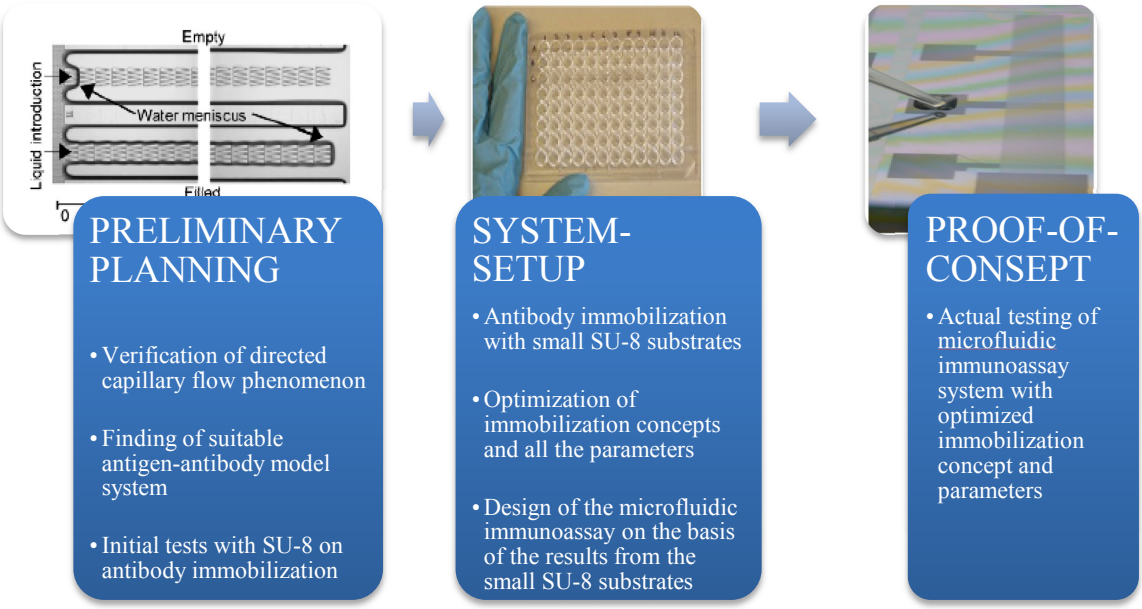

Figure 3. A three-step process flow diagram of the experimental part. Adapted from refs. [37-38].

2 Microfluidics and wetting

The evolution of microfluidics started in the early 1950s when first demonstrations of inkjet nozzles and liquid analysis at high precision by chromatographic systems were developed [2]. However, it took more than three decades before the real benefits of microfluidics, especially in improving the analytical performance, were discovered and it evolved to a discipline of its own: a discipline, which combines different branches of science in order to manipulate the fluid flow and analyse the components of a solution in the micro scale channels. The turning point can be traced back to the early 1990s, when Manz et al. [39] introduced the concept of micro total analysis systems (uTAS) by combining sample processing and electrophoretic separation on the same micro sized glass chip. The evolution of the microfluidic technology in short is presented in figure 4.

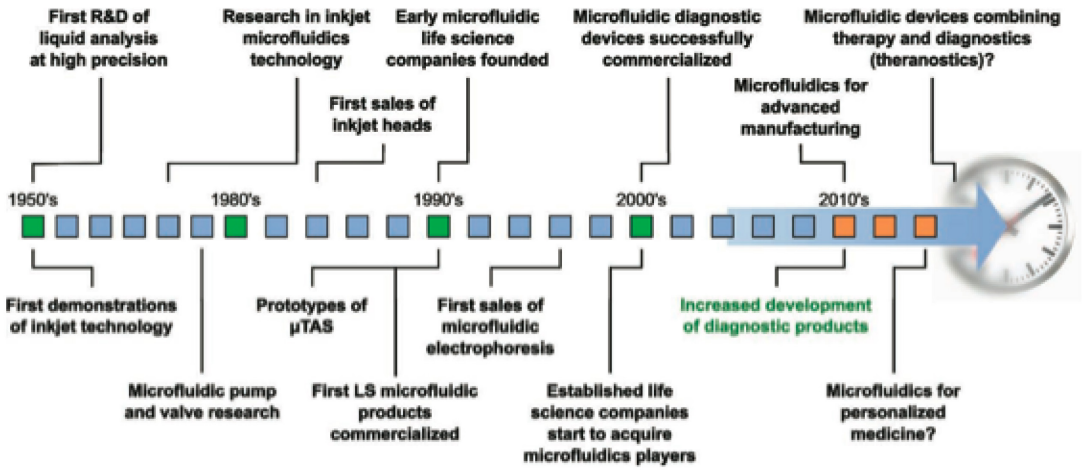

Figure 4. Evolution of the microfluidic technology within the past 60 years. From ref. [2].

Minituarization brings about substantial changes in the importance of different phenomena due to large surface-to-volume ratio (e.g. surface tension, flow profile and diffusion). This enables unique and useful phenomena not seen in the macro world, which are shown e.g. as the negligible effect of gravitational forces, fast diffusion, capillary action, self-cleaning surfaces of lotus leaves and the capability of small insects, like water springtails, to walk on water. In this chapter, we present the concept of microfluidics, explain the new features of liquid flow and elaborate key physical phenomena common for fluids at the micro scale.

2.1 Basics of microfluidics

Microfluidics is a scientific discipline, where the interdisciplinary understanding of surfaces and fluid reactions, material properties of the channel and fundamentals of physics, material science, chemistry and biology are needed. Microfluidics aim to manipulate microlitre volumes of liquids (e.g. urine, blood, saliva, water) on micro sized channels either passively utilizing the capillary action arising from the large surface-to-volume ratio or actively using different components like pumps and valves.

The term microfluidic channel usually indicates that at least two dimensions are in the micro scale. Typically they are the depth and width of the channel, while the length of the channel can be in the millimetre or centimetre range. For example, an extraction channel in a SU-8 based capillary-electrophoresis chip has a length of 5 cm, width of 10 µm and depth of 50 µm [40]. Due to the micro sized diameter, the liquid flow is almost always laminar. Reynolds number is defined as (1),

$$Re = \frac{\rho v D_h}{\eta} \tag{1}$$

where ρ is the fluid density, υ the characteristic velocity of the fluid, D_h the channel diameter and η the fluid viscosity. The Re-values below 2000 indicate laminar flow. Laminar flow enables two or more streams to proceed without turbulent mixing in the microfluidic channel leading to a controlled flow profile. In laminar flow the mixing is dominated by diffusion. It is a fast process on microsystems as the diffusion distance d is squared in equation (2),

$$d^2 = 2Dt \tag{2}$$

where t is time and D the characteristic diffusion coefficient. The effect of gravity can be neglected in microfluidic channels, because surface tension is dominating. The relationship of gravitational forces and surface tension is described with Bond number (3),

$$Bo = \frac{\rho g L^2}{\gamma} \tag{3}$$

where ρ is the fluid density, g the acceleration of gravity, L a characteristic length scale (e.g. diameter of the channel) and γ the surface tension. A typical value of Bond number for micro sized channel is below 1, because L is in its maximum gets values in centimetre scale ($L < 10^{-2}$

m). Another dimensionless number related to the microfluidics is Capillary number (4), which describes the relative strength of viscosity and surface tension

$$Ca = \frac{\eta v}{\gamma} \quad (4)$$

where η is the fluid viscosity, v the characteristic velocity of the fluid and γ the surface tension. A typical value for microfluidic systems is of order of 10^{-2} [41].

2.2 Surface free energy

Surface free energy, which in liquid-vapor systems is called surface tension, rise from the dissimilar forces the bulk and the surface molecules of the liquid experience. A molecule within the bulk of the liquid is surrounded in all directions by neighboring molecules. Cohesive interactions between liquid molecules, which are either hydrogen bonds or Van der Waals forces [42, p. 8], are balanced, yielding no net force. At the surface, the molecule is lacking upper counterparts resulting in increased potential energy compared to the bulk molecules. The interaction, which interfacial liquid molecules are experiencing, is greater between the underlying liquid molecules compared to the air molecules. Therefore, the interfacial liquid molecules are pulled towards the bulk. Surface tension, γ, is the work, which is needed to move molecules from the bulk to the surface. Surface tension (5) is calculated by the ratio of the change in free energy (dG) and the area (dA) in the surface

$$\gamma = \frac{dG}{dA} \quad (5)$$

Usually surface tensions for liquids are in the range of 20-80 mN/m. For example, the surface tension of water is 71.99 mN/m and methanol 22.07 mN/m (25°C)). [42, p.7] Optical goniometer and experimental methods, like Wilhelmy plate and Du-Noüy ring, are applied to measure the surface tension [42, p.15-16].

2.3 Wetting

Wetting, the ability of liquids to form interfaces with solid structures, is a characteristic property for the material surface in solid-liquid-vapor systems. It is governed by the combination of material's inherent chemical nature and topographic properties [43]. Three-phase system creates a contact line (wetting line), where all the phases are in contact. Contact angle, which determines the wetting behavior of the surface, results from the interfacial surface tensions

between liquid and solid, which are surrounded by vapor (figure 5). Wetting is described quantitatively by Young's equation (6)

$$ycos\theta = \gamma_{SV} - \gamma_{SL} \quad (6)$$

where γ is the liquid surface tension, θ the contact angle, γ_{SV} the solid surface free energy and γ_{SL} the solid / liquid interfacial free energy [42, p.125].

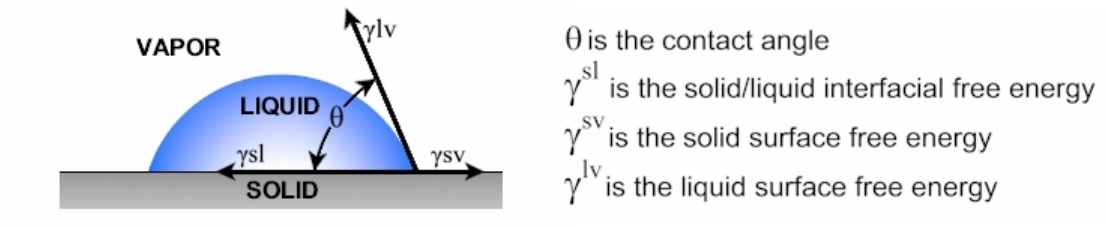

Figure 5. Contact angle in a three-phase system. From ref. [44].

Surfaces are either hydrophilic (wetting surfaces) or hydrophobic (nonwetting surfaces) depending on the measured contact angle. Contact angles between 0° and 90° result in hydrophilic whereas angles varying from 90° to 150° are hydrophobic surfaces [45]. The extreme contact angles, $\theta = 0°$ and $150° < \theta < 180°$ yield superhydrophilic and –hydrophobic surfaces, respectively. Also prefix ultra, instead of super is sometimes applied [46]. These surfaces, often found in the nature [45], offer interesting properties, which have many potential application fields in the modern world. For example, lotus leaf – like superhydrophobic surface, is water-repellent and capable of self-cleaning [47]. Lee et al. [47] succeeded to mimic the lotus leaf structure by patterning the PDMS with micro- and nano-scaled grass via electroformed nickel (Ni) mould. The resulting contact angle of 163° of PDMS surface was close to the real lotus leaf contact angle (168°), even though they did not reach the perfect replication fidelity. The variation in wetting phenomenon is illustrated in figure 6.

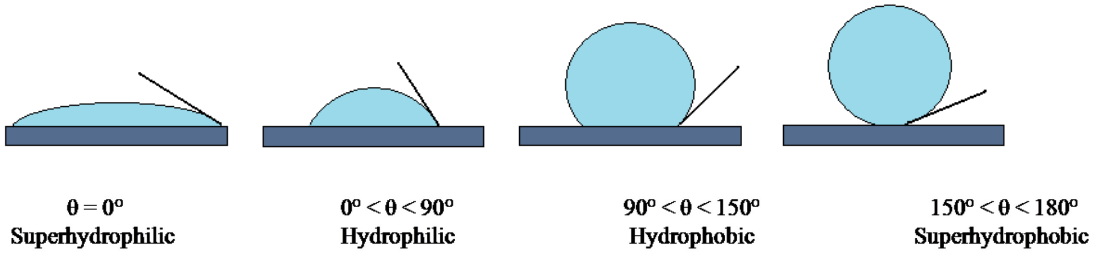

Figure 6. Behaviour of the droplet on different wetting surfaces.

A common method to measure contact angle is the sessile drop method [42, p.133], where the droplet is placed on the substrate and evaluated optically via goniometer and by fitting the droplet shape to Young-Laplace equation. Interactions at the boundary surface (e.g. evaporation of the liquid, chemical reactions between the solid and the liquid, adsorption of molecules from the solution, desorption of molecules from the surface, surface heterogeneity (chemical and structural) [42, p. 136-137]) cause hysteresis in the contact angle. Therefore, the thermodynamic equilibrium (Young's contact angle), is only applicable in ideal cases, where the surface is presumed to be perfectly smooth, flat and homogenous. With real cases, the contact angle is defined by advancing (θ_a) and receding (θ_r) contact angles, where the advancing and receding angles refer to the movement of the wetting line. The phenomenon is called contact angle hysteresis (H) (7) and it is defined as the difference between advancing and receding angles

$$H = \theta_a - \theta_r \qquad (7)$$

Surface roughness, either accidental (e.g. contaminations on the surface) or intentional (e.g. micro or nano patterning), results in situation, where Young's equation needs additional modifications to assess the proper contact angle between the surface and the liquid [48]. With rough surfaces, where the entire area under the droplet is wetted, Wenzel model (8) is used

$$cos_W = rcos\theta \qquad (8)$$

where θ_w is the contact angle of the liquid on the rough surface and r the ratio ($r \geq 1$) between the actual area of rough surface and the geometrically projected area and θ the Young's angle of the liquid with corresponding flat surface with the same chemical characteristics. Wenzel model results in enhanced intrinsic contact angle with respect to the ratio r [42, p.137]. In case of rough

hydrophobic surfaces, where air pockets are trapped under the droplet, Cassie-Baxter model (9), originally developed for chemically heterogenous surfaces, is used

$$cos\theta_{CB} = f_s[cos\theta + 1] - 1 \quad (9)$$

where θ_{CB} is the contact angle of the liquid droplet on the rough surface and f_s (> 1) the fraction of the solid surface on which the liquid is lying. The trapped air between adjacent patterns enhances the water repellency since the droplet is partially on air, thereby leading to liquid / solid and liquid / vapor interfaces [47]. Wettability is lowered and hydrophobicity increased. Both above described models apply only when the droplet size is sufficiently large compared to the surface roughness scale.

Caputo et al. [43] were able to switch the wetting mechanism from Cassie-Baxter to Wenzel model by changing the inter-pillar spacing from 14 µm to 77 µm. Pillars were 42 µm x 42 µm in width and 25 µm in height. Phenomenon was reported to occur mainly due to the gravitational forces, which become larger than the interfacial tension force between air and water during the experiment. Therefore, the water is able to seep between the pillars with larger inter-pillar spacing. The threshold value for the change was reported to be 20 µm. Contact angles were ranging from 118° to 82° with spacing 14 µm to 77 µm, respectively. The state between two previously described models is suggested to be the intermediate state, where the liquid seeps only partly between the adjacent pillar structures [47]. It is called as Cassie-Wenzel state. Wenzel, Cassie-Baxter and Cassie-Wenzel models are illustrated in figure 7.

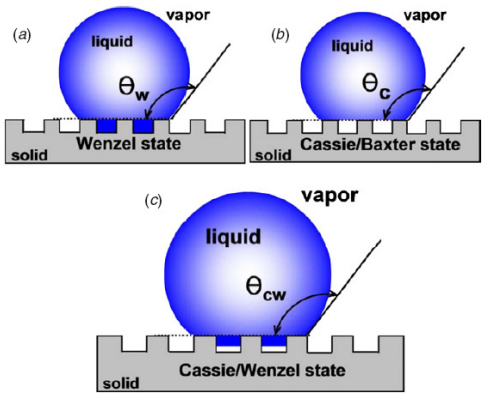

Figure 7. Contact angle on rough surfaces is determined by Wenzel, Cassie-Baxter or Cassie-Wenzel models. From ref. [47].

In addition to surface roughness, wettability can be controlled by using different coatings. For example techniques like fluoropolymer coating, which increase the contact angle of oxidized silicon nanograss surface from 0° to 170° [46], different surface modifying techniques (e.g. oxygen plasma treatment, which lowers the contact angle of SU-8 e.g. from 68° to 27° [37]), electrostatic force (e.g. the electrostatic actuator made out of copper/PDMS composite polymer membrane changed contact angle from 152° to 131° by applied 250 V electrical potential [48]) and UV-light exposure (e.g. titanium dioxide (TiO_2)-covered SU-8 surfaces change the contact angle from hydrophobic to hydrophilic upon induction to UV-light and return to hydrophobic with dark restoring conditions [43]) are used.

2.4 Capillary phenomenon

Capillary phenomenon, also known as capillarity, means the spontaneous filling of micro scale channels based on surface free energy minimization and wetting phenomena. It depends on the relative strength of the intermolecular attraction (occur between the liquid molecules and the solid material) and cohesive forces (occur between liquid molecules). Depending on the solid surface properties, nonwetting or wetting, the two-phase interface either forms a proceeding characteristic convex or concave meniscus, respectively.

Capillarity is often demonstrated by putting a narrow glass tube called a capillary on a bowl containing liquid (e.g. water). Due to large surface area and inherently higher pressure inside the capillary compared to the outside, liquid can climb in a capillary tube for centimetres without any external power source. Capillary or Laplace pressure, the pressure difference between the two-phase interphase (air-liquid) is calculated from Laplace equation (10)

$$\Delta P = \gamma \left(\frac{1}{R_1} + \frac{1}{R_2} \right) \tag{10}$$

where R_1 and R_2 are radii of curvature and γ the surface tension of the liquid. R_1 is the meniscus radius and R_2 the radius of the meniscus in the orthogonal plane. Surface tension minimizes the area of free surface yielding applied force F according to equation (11)

$$F = \gamma L = \gamma (2\pi r) \tag{11}$$

where L is the distance the tension is forced to push the liquid forward and γ the surface tension of the liquid. Gravitational force F_g pulls the liquid column downwards. The total weight of the liquid column (12) in a cylindrical tube is the product of mass and gravity,

$$w = Mg = \rho Vg = \rho g \pi r^2 h \tag{12}$$

where ρ is the density of the liquid, g is the gravitational coefficient, h the height of the liquid column and r the radius of the tube. At the equilibrium, the forces needed to support the liquid column and to minimize the surface tension are equal yielding the height (13) the liquid proceeds in the cylindrical tube

$$h = \frac{2\gamma cos\theta}{\rho g r} \tag{13}$$

Fluid flow in the microfluidic channel is determined by the channel design and surface properties [49]. Jokinen et al. [37] reported directed capillary flow by the topographic modification of the channel structure. They fabricated a double channel structure made out of SU-8, which was oxygen plasma treated and patterned with rows of triangles (base 20 µm, length 80 µm, inter-triangle distance 5 µm and thickness 12.8 µm) (figure 8). The triangles were placed either base or tip towards the liquid reservoir. They were able to show, that with a contact angle of 39° and inter-row distance of 11 µm and 14 µm, the water proceeded only in the channel, where the triangles were tips first. This is mainly explained by the fact, the proceeding meniscus gets a better support from the adjacent bases, which form an almost uniform wall whereas the tips offer a less hydrophilic support.

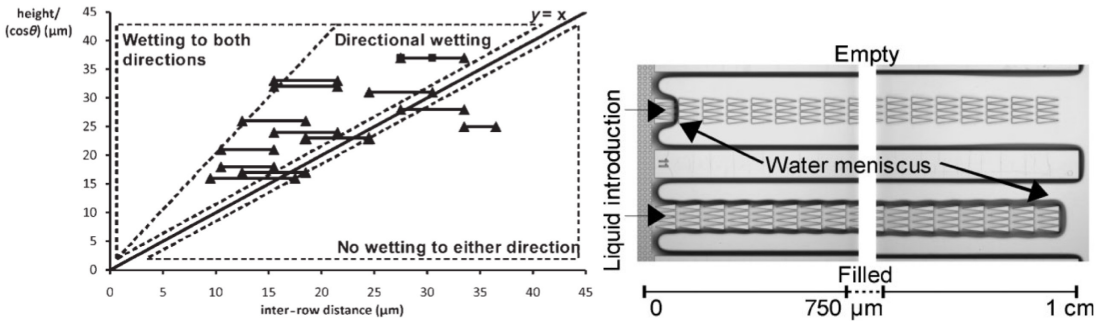

Figure 8. The theoretical and experimental reach of directional wetting with fabricated test structures (on left). The advancing meniscus is supported by the wall structure the bases of the triangles form whereas the adjacent tips are not able to offer a suitable support for the meniscus (on right). From ref. [37].

3 Thick photoresist SU-8

SU-8 is an epoxy-based thermoset photopolymer, which was invented in the late 1980s by IBM [50] as a high-resolution resist for submicron lithography. It offered an alternative solution for x-ray lithography step in the high-aspect ratio process called LIGA [German acronym for Lithographie, Galvanoformung, Abformung (Lithography, Electroplating and Molding)], which was unconvenient due to relatively high cost and limited access to synchrotron X-ray equipment [51]. Later on, the outstanding material properties of SU-8 and compatibility with conventional methods in microfabrication assisted the evolution from simple patterning material to a material of choice with structural components, especially in microfluidic MEMS applications [33, 52]. In this chapter we present the basics of SU-8 structure, properties, fabrication and modification prospects.

3.1 Structure

SU-8 is a negative photoresist, which monomer contains eight free epoxy groups (figure 9). It is based on multifunctional bisphenol A novolak epoxy resin (EPON® SU-8 resin, Shell Chemical) where the photoacid generator (PAG), a mixture of triarylsulfonium salts of hexafluoroantimonate (SbF_6^-) (CYRACURE® UVI, Union Carbide), is mixed in a concentration of 10 w-% [53]. The original solvent in SU-8 formulations was γ-butyrolactone (GBL), but for later products, it was replaced by cyclopentanone. The alteration offered improved coating quality, adhesion properties and faster processing times [53]. The resin-solvent ratio is one of the most important properties of SU-8 as it defines the material viscosity and obtainable layer depths [52-53].

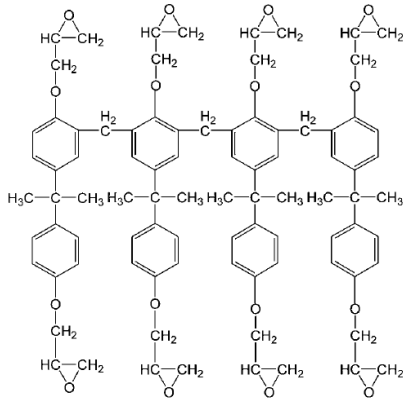

Figure 9. Molecular structure of SU-8 monomer. From ref. [30].

The high chemical and thermal resistance as well as good mechanical properties are based on the cross-linking of eight free epoxy groups. The cross-linking is initiated by UV-light exposure, which transforms the photoinitiator into hexafluoroantimonic acid. During post-exposure bake, formed strong acid catalyses the cationic ring-opening photo-polymerization reaction, which increases the molecular weight and diminishes the solubility of UV-exposed parts. This yields designed patterns in resist film upon development. [53-54]

SU-8 is commercially available from MicroChem Inc [55], which sells various blends of SU-8. The compositions of three different blends are illustrated in table 1. By diluting the commercially available blends, new formulations are obtained.

Table 1. The composition of SU-8 50, 100 and 2000 formulations. From ref. [56-57].

COMPONENT	**SU-8 50 (wt-%)**	**SU-8 100 (wt-%)**	**SU-8 2002 (wt-%)**
Resin	69	73	29
Solvent	30-35	20-30	65
SbF_6 (photoinitiator)	3,3	3,5	1,4
Viscosity (cSt)	12250	51500	7,5

3.2 Fabrication of SU-8 layer

SU-8 layer fabrication follows the five-step photolithographic process common for all negative photoresists: spin-coating, soft-bake (SB), exposure, post-exposure bake (PEB) and development steps (figure 10, table 2). The process results coatings with low surface roughness [58-59] and layer depths varying from 750 nm [52] up to 500 µm [60] depending on the blend viscosity. The exposure by UV limits the minimal feature size to submicron level, because feature size is dependent on the diffraction of the light. Process parameters are optimized for the equipment on the basis of the blend manufacture's reference values. According to a three-level L9 orthogonal-array based Taguchi method the most critical step is the soft bake, at least when good resolution and aspect ratio are desired [61]. The significance of development time as well as exposure dose, increase with the thicker layer depths.

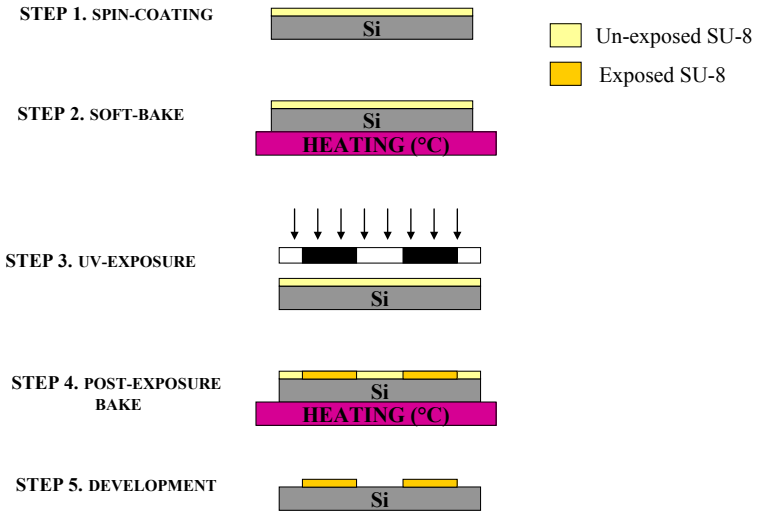

Figure 10. The process flow for a single-layer coating of negative photoresists SU-8.

Table 2. Experimental values for fabrication parameters of layer thicknesses of 20 and 50 µm.

FABRICATION PARAMETER	20 µm	50 µm
Spincoating	9000 rpm	3000 rpm
Soft bake (65°C + 95°C)	5 + 8 min	5 + 15 min
UV-exposure	12 s	16 s
Post-exposure bake (95°C)	8 min	15 min
Development	5-10 min	10+ min

SU-8 layer is fabricated most often on top of a dehydrated silicon (Si) substrate. The dehydration (for example a 40 min bake in 200°C oven [60]) removes the excess moisture bounded to silicon, which could cause bubbling and uneven film forming during the SB. Spin-coating is performed in a two-step process where first a low speed (500 rpm) step spreads the resists evenly to the whole wafer surface, while higher speeds (1000-9000 rpm) are used to adjust the thickness. The parameters (spin speed and time) are determined on the basis of material viscosity. The higher the viscosity is, the higher spin speeds and times are needed to obtain thinner layers as can be seen from the spin speed curve shown in figure 11. A specific problem of spin-coating is the edge bead effect, which is known as the accumulation of the

resist material on the edges of layers. This is emphasized especially with more viscous SU-8 blends [53].

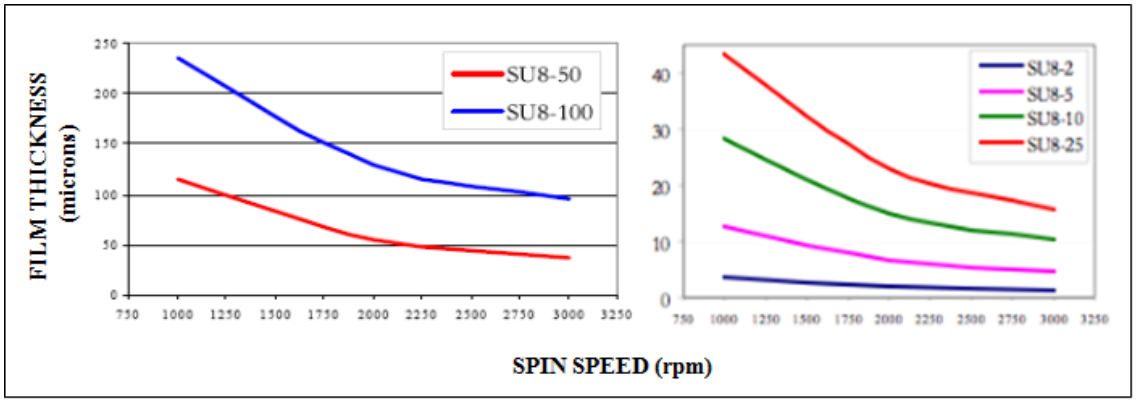

Figure 11. Spin speed curves for different SU-8 blends. The low viscosity material enables uniform coatings, defect and stress free layers as well as easy removal of unsolidified resin during development (e.g. SU-8 25). High viscosity is desirable when reduced lateral flow and the construction of stable and thick resist films are wanted (e.g. SU-8 100). [53] From ref. [55].

Soft bake is a diffusion-controlled process where excess solvent is evaporated away from the coated resist layer by baking the wafer on a flat-plane hotplate. Horizontal placement prevents the freshly spin-coated layer from flowing due to gravitation forces [62]. The hotplate is possible to replace with oven, but the ambient heat distribution ovens have, produces easily a skin-like layer to SU-8 surface hindering the pattern transfer later on [53]. The SB is performed using ramped temperature profiles to prevent the formation of residual stresses, which can cause cracking and wafer bowing [62]. Temperature is increased progressively from room temperature (RT) to close to 65°C and then up to 95°C. Baking times depend on the layer thickness. Higher temperatures than 95°C are not recommended as they increase the risk of crack formation [50]. In addition to solvent evaporation, the SB smoothens the edge bead effect and improves the adhesion of SU-8 to underlying Si [53]. Commercially available primers, OmniCoat and HMDS [53], can be used to enhance the adhesion.

After being cooled down to RT, the resist film is exposed to UV-light. Recommended wavelength is (mercury i-line) 365 nm [55]. Exposure time is optimized because too short times produce cracks [62] and too long times rounded edges [53]. If the resist layer is non-uniform either due to edge bead formation or uneven baking place, the diffraction effect, which is caused by Fresnell diffraction, takes place during the exposure step [53, 63] (figure 12). The

phenomenon is responsible for pattern enlargement especially near the edges of the photomask. The top parts of structures are exposed to higher dose of UV-light therefore leading to T-like profiles shown in figure 12. Diffraction error is especially emphasized with thicker films where thickness non-uniformity can be high. In a bad situation, the error in layer thickness can range from 30 to 100 µm when 0,1 to 1 mm coatings are made [63]. One solution is to use index match materials between the photomask and the film to compensate the air gap. With SU-8 no appreciable error was found when glycerol was used whereas the exposure without glycerol resulted in a pattern width error as high as 45 % [63].

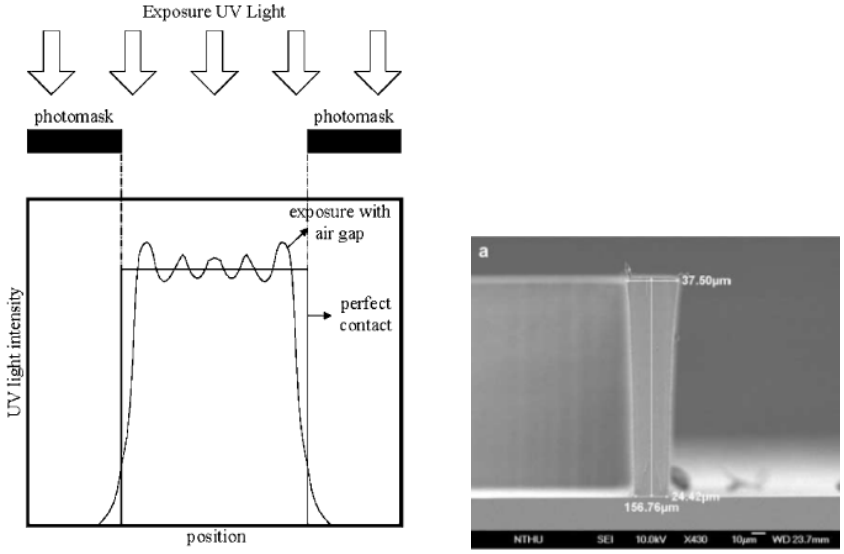

Figure 12. The effect of diffraction to the UV-light intensity profile in contact-based photolithography (on left). The T-like profiles in lithographically patterned structures are encountered due to thickness non-uniformity during the exposure step (on right). From ref. [63].

Post-exposure bake (PEB) takes place shortly after UV-exposure in order to limit the PAG diffusion from the polymer layer, which could hinder the cross-linking capability of the photopolymer [50]. In contrast to soft bake, no ramped profile is used which accelerate the cross-linking process [60]. Baking temperature is 95°C and baking time chosen by the layer thickness. The cross-linking process continues until the glass transition temperature (T_g) of the cross-linked SU-8 becomes close to the baking temperature [54].

After PEB, un-cross-linked areas are removed by developing the substrate at RT in propylene glycol methyl ether acetate (PGMEA) [53]. Agitation enhances the development but only gentle

approach should be used to prevent the destruction of fragile structures [62]. Development step might also cause minor pattern enlargement, because negative photoresists are prone to absorb organic solvents [63]. The development step also reveals fabrication induced residual stresses as a structural deformations and crack-like distortions, which lead to leakages in microfluidic systems as well as unwanted scattering and increased propagation loss in optical systems [50].

An extra step of a high temperature hard bake (HB) can be applied to diminish the amount of cracks. Besides reduction in the crack amount, HB at 200°C for 30 min improves the resistance of SU-8 towards most metal etches and solvents (e.g. nitric acid, sodium hydroxide (pH 13) at 90°C, ammonium fluoride-hydrofluoric acid and ferric chloride) [52].

Multi-layer coatings of SU-8 are obtained by repeating previously mentioned steps. The layers can be fabricated without separate PGMEA treatment [62]. Figure 13 presents a multi-layer SU-8 structure of six layers where only one development step is used. The lack of excess development steps accelerates the fabrication process, hinders the possibility of formation of unwanted cracks and reduces the probability of swelling due to PGMEA. Also the feature complexity and coating uniformity are enhanced. With multi-layer coatings thicknesses up to over 1 mm are obtained [51].

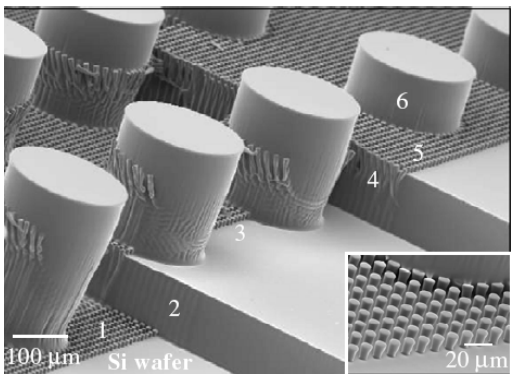

Figure 13. Up to six layers of SU-8 have been fabricated by using only a single development step at the end of the whole fabrication process. The numbers refer to fabrication order. Slight distortions are caused by the overlapping of various photomasks. From ref. [62].

3.3 Native SU-8 properties

Table 3 represents the material properties of SU-8. Given values are suggestive as properties are highly sensitive towards processing conditions [54] and selection of the solvent [64].

Table 3. Native properties of SU-8 50. Unless otherwise mentioned, the used solvent is GBL.

PROPERTY			**SU-8**	
MECHANICAL	Young's modulus, E (GPa)		3.2 ± 0.2	[65]
			4.95 ± 0.42	[66]
			5.9 ± 0.9	[65]
	Shear modulus, G (GPa)		0.3	[65]
			1.2 ± 0.4	[65]
	Max stress, σ_{tot} (MPa)		12	[54]
			34	[66]
	Friction coefficient, μ		0.19	[52]
	Poisson ratio, υ		0.29 ± 0.02	[65]
			0.33 ± 0.02	[65]
	Biaxial modulus of elasticity, E/(v-1), (GPa)		5.18 ± 0.89	[67]
	Elongation at break (%)		~ 7.5	[54]
	Bond strenght (MPa)	Silicon (Si)	18.5 ± 4.6 (cyclop.)	[64]
		Gold (Au)	4.8 ± 1.2 (cyclop.)	[64]
PHYSICAL	Glass transition temp. (un-cross-linked), T_g (°C)		49.5	[54]
	Glass transition temp. (cross-linked), T_g (°C)		max 238	[54]
	Decomposition temp., TD (°C)		> 340	[54]
	Thermal expansion coefficient, CTE (10^{-6}/°C)		52 ± 5.1	[67]
			102	[54]
			278 ± 31	[65]
	Thermal conductivity, κ (W/mK)		0.208 ± 0.035	[68]
	Viscosity, η (cSt)		12250	[56]
	Density, ρ (SU-8 50, kg/m^3)		1219	[56]
ELECTRICAL	Refractive index, n (600nm)		~ 1.595	[69]
	Dielectric constant (30 GHz), ε_r		3.25	[70]
	Dielectric loss (30 GHz)		0.027	[70]
OTHER	Contact angle, θ (°)		74	[58]
			90 (cyclop.)	[58]
	Surface energy, γ (mNm^{-1})		45.20	[58]
			26.48 (cyclop.)	[58]

Low Young's modulus combined with typical Poisson ratio for polymeric materials offer high compliance for micromechanical structures. Lithographically fabricated structures are mechanically stable and durable, and also inert towards various acids and bases often used in microfabrication [50]. Nowadays the aspect ratio (AR) around 20 is common [51-52, 61-63, 67], but careful optimization of fabrication process yields also higher ARs [61].

Relative high residual stresses (tensile stresses) on SU-8 coatings are built up during the fabrication and revealed during the development step as crack like distortions as already mentioned in the subchapter 3.2 [50]. Longer PEB times increase the stress (stress is 30 MPa with 5h PEB, but only 12 MPa with 30 min PEB) [54]. In addition, the environmental humidity has an effect on the stress of SU-8 layer, which is however reversible [54]. Besides the processing conditions, also the mismatch between thermal expansion coefficients (CTE) of silicon (2,6 x 10^{-6} /°C) [71, p.84] and SU-8 (52 x 10^{-6} /°C) induces tensile stress formation [51]. The large range of given CTE values for SU-8 (in table 3) originates from the assumption, which has been done, to make the measurement and calculations easier. Material is assumed to be isotropic to all directions even though the thickness and planar directions properties are not identical [54]. Therefore the measurements in out-of-plane direction give significantly higher CTE value for SU-8 [54]. Also the values for Young's modulus, shear modulus and Poisson ratio are affected [65].

Another problematic feature of SU-8 formulation as an organic material is the poor adhesion to most inorganic materials like glass, silicon dioxide (SiO_2) and gold [32, 64]. A better adhesion is observed with silicon nitride [32]. In addition to the solvent, various adhesion promoters and increase in exposure dosage, to a certain point, can improve the adhesion between SU-8 and the substrate [64]. SU-8 has high thermal stability compared to other thermosets like PEs [72]. It is an excellent electrical insulator and possible material for optical waveguides, due to relatively low refractive index [69]. In addition, SU-8 is optically transparent above 360 nm (figure 14).

Typical for polymeric materials, also SU-8 is known to be highly autofluorescent at least at emission wavelengths of FITC (fluorescein isothiocyanate) and Cy3 (red fluorescent dye of the cyanine dye family) [59]. Because fluorescence is the most used detection method among biological samples [3], this has to be taken into account while designing BioMEMS applications. The problem can be overcome by labelling the biomolecule under use e.g. with Alexa Fluor 647 - tag, which emits UV-light with higher emission wavelengths [30]. Other way to reduce the autofluorescence property is to decrease the layer depth. A 0.8 µm thick SU-8

layer has 20 % higher background fluorescence compared to standard glass plates while the value is 400 % with 12 μm thick layers [59].

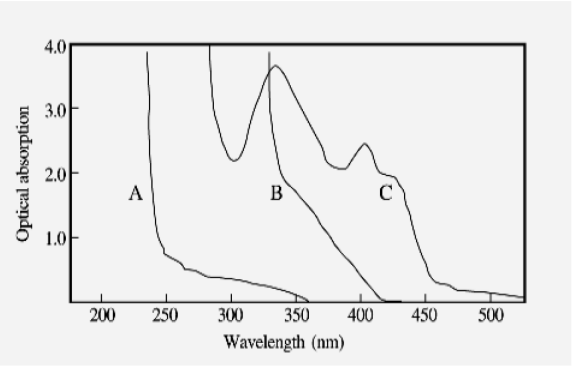

Figure 14. Absorption graph of photoresist materials: SU-8 (A), dry photoresist Riston® (B) and positive diazo resist (C). Compared to other photoresist materials, SU-8 absorbs significantly less UV-light. From ref. [73].

Post-exposure baked SU-8 layer is highly hydrophobic (contact angle around 75°) and has a low surface energy [58]. The contact angle is increased while different solvent is used in SU-8 formulation. The values are around 86-90° with cyclopentanone [74, 58].

SU-8 has sufficient biocompatibility and reduced biofouling properties, which enable its use in biomedical applications [29]. Nevertheless the observed mechanical delamination initiated especially at the corners of microfluidic devices might be a problem when using SU-8 in *in vivo / vitro* devices [29]. Problematic features are also the fairly poor hemocompatibility compared to polyurethane controls [75] and ability to not be able to support the growth of most eukaryotic cells [30]. At least with primary neuronal cultures, the reason for incapability was reported to be toxic leaching from the PAG (small amount of released antimony and fluorine detected) and improper ability to sustain neuronal adhesion [76]. Cytocompatibility can be increased by post-processing strategies, which include combinations of hard bake, isopropanol (IPA) sonication and oxygen plasma and parylene coatings [76].

3.4 Modification of SU-8

Native SU-8 surface is highly hydrophobic, which is not the ideal case with bio applications, because hydrophobic surface enhances biofouling, limits cell attachment and prevents the covalent biomolecule immobilization among other limitations [77]. Therefore most of the surface modification methods, both wet and dry methods, concentrate on enhancing the SU-8 surface hydrophilicity [60]. Bulk modification comprises usually boosting of electrical and magnetic properties of SU-8. Compared to the other polymeric materials common for microfluidics, e.g. PDMS, the modification of SU-8 has not had that much attention [78].

3.4.1 Wet surface modification

Most of the wet modification methods are based on the cleavage of the residual epoxy groups the surface has after curing process [31-33]. Cyclic epoxy groups are cleaved to reactive C-O bonds with different acid or alkali solutions. The formed C-O bond is highly reactive due to one extra free electron pair. It acts as a nucleophile in the following oxidation reaction donating the free electrons and converting into two hydroxyl groups. By treating the hydroxyl groups with suitable chemicals, in an adequate chemical environment, desired functional groups are possible to yield onto SU-8 surface.

In aminosilanization, the SU-8 surface is functionalized by amine groups ($-NH_2$). Residual epoxy groups are converted to hydroxyl groups by treating the surface with cerium ammonium nitrate (CAN) for 30 min [31] or with strong sulphocromic solution for 10 min [32]. By incubating aminopropyltriethoxysilane (APTES) for 1 h with former [31] and [3-(2-aminoethyl)aminopropyl]-trimethoxysilane (AEAPS) for 7 min [32] with the latter, the hydroxyl groups on the SU-8 surface react with silane groups, yielding free amine groups towards the solution phase (figure 15). Similarly, carboxyl acid groups (-COOH) are obtained on to the SU-8 surface after oxidation reaction with glycine or 11-mercapto undecanoic acid (MUA) for 2 h [33].

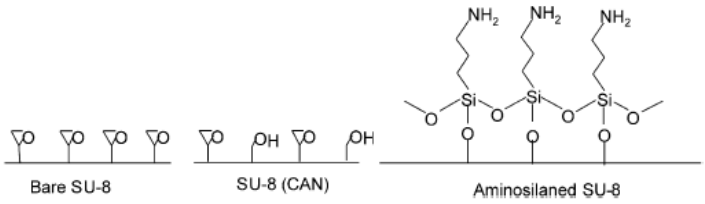

Figure 15. The CAN treatment converts the residual epoxy groups to more reactive hydroxyl groups in an oxidation reaction. The amine groups are formed by surface aminosilanization with APTES. From ref. [31].

Another common modification process is the graft polymerization with the help of UV light [77, 79]. Grafting process is based on the creation of reactive species like radicals on SU-8 surface, which can form covalent bonds between monomers. Grafted monomers serve as an initiation site for free radical polymerization reaction upon UV-light irradiation. One advantage of UV-mediated grafting is the possibility to pattern the grafted polymer with the help of photomask, just like the standard SU-8 patterning is done [77, 79]. Figure 16 presents the UV-mediated grafting process where SU-8 surface is covered with polymer.

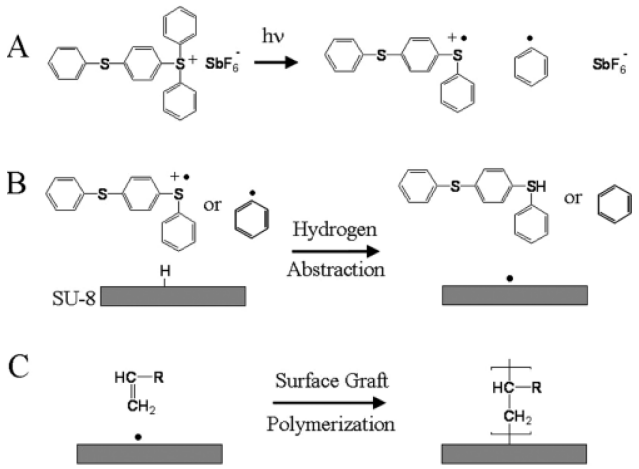

Figure 16. UV-mediated graft polymerization is composed of hydrogen abstraction step, where the free radical is produced to surface, and surface grafting step, where the monomer is bonded covalently to SU-8 surface via UV-light. From ref. [77].

Depending on the amount of residual photoacid generator, there are two approaches to grafting process. In the first scenario, the freshly fabricated SU-8 layer contains some residual photoacid generator, which can be used as initiator sites for the grafting process. UV-mediated grafting is executed by simply covering the SU-8 surface with wanted monomer solution and exposing to UV-light. For example, 10 wt-% acrylic acid solution forms grafted poly(acrylic acid) (PAA) on SU-8 surface after 10 min UV-exposure [77]. Surface coverage is directly proportional to the amount of photoacid generator on the surface. Also PEG and poly(acrylamide) (PAM) coatings are possible with the similar process [77].

If the fabrication process has decomposed most of the photoacid generator (the second scenario), additional photoiniator is bounded to the surface as initiator sites. By irradiating a photoinitiator covered surface with UV-light, free radicals are formed, which are capable of initiating the polymerization reaction. After this, the graft polymerization is performed as explained previously. For instance, hydrogels like 2-hydroxyethylmethacrylate-based (HEMA) hydrogels can be grafted on SU-8 using 1-hydroxycyclohexyl phenyl ketone (HCPK) as a surface-bound initiator [79].

Graft polymerization is also possible to perform without UV-exposure. Free radicals are produced by using catalyst containing solutions in cleaving and grafting steps. After the residual epoxy groups are oxidized to hydroxyl groups, catalyst, like cerium (IV) converts the hydroxyl groups to free radicals [30]. Free radicals react further with the solution yielding functional groups for grating. For instance, CAN + nitric acid or CAN + sulphuric acid solutions can be used to graft PAM or PAA polymers, respectively, on SU-8 surface.

With some bio applications, more hydrophobic SU-8 surface than native is beneficial. An example of this is the segmented flow operation microfluidic device, which is used to transfer small volume droplets in the channel without losing their droplet shape. This kind of approach is applicable e.g. to yeast suspension [74]. The walls of SU-8 channel yield contact angle close to 130° by using 10 min piranha solution (sulphuric acid hydrogen peroxide) treatment combined with 12 h octadecyltrichlorisilane solution (ODTS) soak [74].

3.4.2 Dry modification

Dry surface modification methods do not use harsh chemicals, which prevent the retention of toxic residues and the destruction of microstructures in the underlying substrate (e.g. SU-8). These processes are therefore considered better suited for biomolecule containing devices. [28]

Oxygen plasma treatment is a popular method to render all kinds of polymeric materials more hydrophilic [80]. The reduction in contact angle is adjusted by the plasma dose and treatment time. The higher the dose and the longer the time, the more notable change in hydrophilicity is obtained [80]. Treatment time can be in s or in min. For example, the 8 s treatment time (applied pressure: $2.7x10^{-4}$ bar, plasma power: 600 W) yields a contact angle of 25.6° [80] and a 2 min treatment (applied pressure: $2x10^{-4}$ bar, plasma power: 50 W, potential: 0.8 V and oxygen flow: 36 sccm) smaller than 5° contact angles [58]. The downside of oxygen plasma treatment is the quite fast hydrophobic recovery the contact angle experiences after storage. Recovery is dependent on the used plasma dose and time, longer times and higher doses yielding more stable surfaces [58]. Another problematic feature is the small amount of released antimony during the treatment [76, 80]. Because antimony is slightly toxic, this might be a problem while biological applications are under consideration.

Another well-known dry modification method is the pyrolytic dissociation of ammonia, which functionalizes SU-8 surface with amine groups [28]. First the hot wire chemical vapour deposition (HWCVD) decomposes thermally the ammonia gas to amine groups and highly energetic hydrogen species. Released hydrogen species cleave the residual epoxy groups with their energy making a bonding place for the amine groups on the SU-8 surface.

3.4.3 Bulk modification

By bulk modification, SU-8 is turned into a nanocomposite material, which shares the good processing capabilities of polymers with improvements in e.g. magnetism and conductivity obtained by the added inorganic phase [81]. Inorganic phase is composed of inorganic materials in a nanopowder format. It is added to SU-8 resist before the five step photolithographic fabrication process by simply mixing. Together these two materials form a suspension, which needs hours of mixing. Sometimes mixing is assisted with ultrasound sonication [81-83]. The amount of agglomerization is diminished by addition of a surfactant. This enhances the nanoparticles to distribute evenly in the SU-8 blend. To make SU-8 magnetic materials such as nickel (Ni) particles (approximately 100 nm in diameter) [84-85], ferromagnetic dopants [86], superparamagnetic magnetite nanoparticles [81, 83] or colloidal ferric oxide nanocrystals [82] have been added to SU-8 blend.

Similarly, improvement in electrical properties, like in conductivity, is obtained by dispersing silver (Ag) particles between 0.2 to 2.5 μm in size to SU-8 blend in a powder format [87]. 5-6

vol-% is enough to cause nanoparticle agglomeration, which acts as pathways for electrons leading to the increase in conductivity.

In addition to alter the native SU-8 properties by forming a composite suspension, another form of bulk modification is to make SU-8 porous by adjusting the solvent content in the resin material. Solvent amount controls the pore size during the UV-exposure and cross-linking steps. For example pore sizes between 6-10 nm are obtained with solvent contents 55-85 wt-% [88]. Porous SU-8 is used for filtering purposes. This porosity is capable of filtering smaller than 70 kDa molecules from a mixture of reagents [88].

3.5 SU-8 imprinting

Nanoimprint lithography (NIL) is a technique to fabricate nanosized structures onto the SU-8 surface by combination of mechanical deformation and UV-light. Usually low viscosity blends of the SU-8 family are used (e.g. SU-8 2000 [13, 89] and 3000 [90]). The mould is either hard (e.g. silicon [91] or nickel [90]) or elastic (e.g. PDMS [13]) depending on the applied technique.

As with standard photolithography, SU-8 is first spin-coated on a suitable substrate and soft baked. In conventional UV-NIL, the UV-exposure is applied through patterned quartz mould. The simultaneous UV-light and pressure transfer the patterns onto the SU-8 surface (figure 17). Patterns are finalized with the post-exposure bake. Another common UV-NIL version is the thermal assisted UV-NIL, where heating is incorporated into the imprint step (figure 17). The heating temperature should be above the T_g of un-cured SU-8, but below the soft-baking temperature in order to avoid the de-gassing effect [90]. UV-exposure is made either during [91] or after the imprint [13, 90]. In the latter case, an additional pre-UV-treatment is suggested to support the patterns from collapsing [90]. As was with the conventional UV-NIL, the patterns are finalized with baking. All the imprint parameters (temperature, pressure, exposure time etc.) depend greatly on the applied equipment and SU-8 layer depth. Therefore, only rough guidelines can be given for the parameter values. Egea et al. [13] fabricated nanoscale gratings onto the 800 nm thick SU-8 layer. Imprinting step (T = 90 °C, t = 2 min) with PDMS mould and the 30 s UV-exposure after demoulding yielded grooves of 225 nm in depth and 500 nm in width at a pitch of 1 μm. Thermal-assisted UV-NIL is also possible to do without commercial equipment [92]. The mould is simply placed by hand and pressed using extra weight at the end of the soft-bake step. The lack of vacuum in the mould placement caused bubbling, but it was not reported to have effect on the final structures.

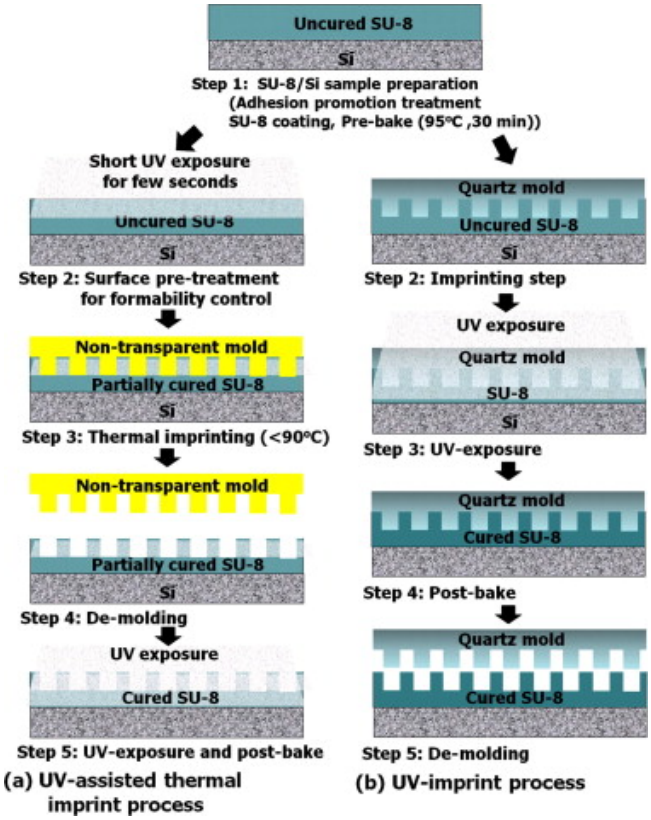

Figure 17. The process flow of the thermal-assisted (a) and conventional (b) UV-NIL processes for SU-8. In thermal-assisted UV-NIL (a), the SU-8 surface is UV-exposed before imprinting step in order to control the formability. From ref. [90].

Compared to the photolithography, NIL offers better resolution. Feature dimensions less than 10 nm are enabled [93]. The major drawback of the NIL process is the characteristic residual layer, which is formed during the imprint process. An additional processing step (e.g. RIE-treatment) is needed to remove the excess resist. The UV-NIL process offers many variations from which examples are reversal UV-imprinting (SU-8 is spin-coated to the mould instead of the substrate [94]), negative UV-NIL (NUV-NIL) (the imprinted features are used for the alignment of the UV lithography, which makes possible to fabricate both the micro and nano sized structures simultaneously [89]) and combined-nanoimprint-and-photolithography (CNP) with hybrid fused silica-nickel mould (technique enables patterns without residual layer and with higher aspect ratio than the structures have on the mould [93]).

4 Antibodies

Antibodies are a special group of glycoproteins called immunoglobulins (Ig), which are products of the B-lymphocyte cells of the mammalian immune system. They take part to a protective mechanism known as an adaptive part of humoral defense system by recognizing and destroying / neutralizing e.g. viral antigens noticed in the blood circulation. The system is mounted by white blood cells (both the B- and T-cell lymphocytes) and macrophages [95, p.1019-1020]. In human body, the antigen recognition and thereby the immunization process is actuated mainly by two immunoglobulin families: IgM and IgG [95, p.1022]. The primary immune response produces the low affinity IgM antibodies after infection. In the secondary phase, after the affinity maturation, the high affinity IgG antibodies are produced. Other immunoglobulin families have other functions in human body (summary in table 4).

Table 4. Immunoglobulin types and their functions in human body. Adapted from ref. [95, p.1022-1023].

CLASS	CONSTANT REGION STRUCTURE	ROLE IN HUMAN BODY	SERUM CONCENTRATION (mg/ml)	MASS (kD)	HEAVY CHAIN STRUCTURE
lgA	Dimer	First line of defense, external secretion	3	180-500	A
lgD	Homodimer	Task not known	0,1	175	Δ
lgE	Homodimer	Protection against parasites, responsible for allergic reactions	0,001	200	E
lgG	Homodimer	Secondary response	12	150	Γ
lgM	Pentamer	Primary response	1	950	M

The ability of antibodies to form highly sensitive and specific binding with antigen molecules, has yielded an important bioanalytical tool, immunoassay. Since its discovery, the immunoassay has been under widespread use in diagnostics. The later developments in fabrication of both the engineered antibodies and the antibody libraries have only broaden the application field. This chapter describes the antibody structure and the basic principle of immunoassay and introduces

the concept of recombinant antigen binding fragment (Fab) and its production prospects through bacteria expression using phage display libraries.

4.1 Antibody structure

The molecular structure of immunoglobulin G consists of three almost equally sized functional recognition compartments. All together they form a structure resembling closely the shape of letter Y (figure 18). Two of these compartments, forming the tips of Y, are called antigen binding - sites, Fabs (F=fragment, ab=antigen binding), where the antigen recognition takes place. The third compartment, known as Fc (c=crystallization) forms the tail of Y. It is not used in the antigen binding process, but is important in other immunological reactions called effector functions (e.g. phagocytosis, natural killer cell activation and activation of the classical complement pathway [96]).

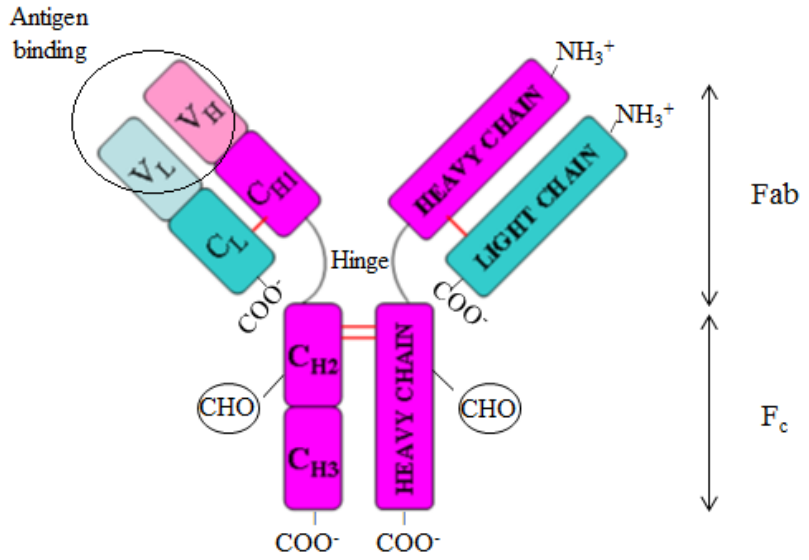

Figure 18. The structure of lgG. Bonds marked with red are disulfide bonds.

The tail and the tip are linked together by a hinge region, which is rich in proline (Pro), threonine (Thr) and serine (Ser) amino acids. Hinge region facilitates the movement of the different parts of the antibody molecule (flexibility is needed e.g. during the immunocomplex formation). It is highly prone to the proteolytic digestion of papain and pepsin molecules. These proteases digest the intact antibody into specific fragments: papain (pH 7.0) into two separate Fab fragments and a single Fc fragment and pepsin (pH 4.5) into a $F(ab)_2$ fragment and partially digested Fc region denoted as pFc. [96]

In structural domain level the immunoglobulin G consists of two identical polypeptide chains called heavy (H) chains and two also identical light (L) chains. The name light and heavy refers to the sizes of the chains. Heavy chain contains ca 450 (45 kDa) and light 250 amino acids (25 kDa), respectively [26]. Chains are linked together by disulfide bonds: two or more bonds between heavy chains and one bond between each heavy and light chain (marked as red in figure 18). Light chains have no physical connection between each other.

The both polypeptide chains can further be divided to immunoglobulin domains known as constant (C) and variable (V) domains. Heavy chain contains three homologous constant domains (C_{H1}, C_{H2} and C_{H3}) and one variable (V_H) domain. Light chain contains one constant (C_L) and one variable domain (V_L), respectively. The variable domains in both chains are called as amino(N)-terminal domains. They differ from one antibody to another and are responsible for the diversity of the specific antigen binding [26]. Compared to variable domains, constant domains are more similar between different antibodies belonging to the same family (listed in table 4).

The domain structure of antibody adopts tertiary structure known as immunoglobulin fold [26]. It is consisted of a pair of antiparallel β-sheets, which are linked together by a disulfide bond and hydrophobic interactions. At both variable domains (V_L and V_H) the fold comprises six hypervariable loops from which H_1, H_2, H_3 are found within the heavy chain variable domain and L_1, L_2, L_3 within the light chain, respectively. Together these six hypervariable loops form the antigen-binding site, which is also called as complementary determining region (CDR) [95, p.1024]. The CDR is surrounded by four framework regions (FRs), which form a scaffold to the antigen binding loops. Antibodies belonging to the IgG family are bivalent [96], because there are two antigen-binding sites per one antibody molecule.

Natural antibodies can be either monoclonal (MAbs) or polyclonal (PAbs) in nature depending on the amount of involved B-lymphocytes during the antibody production (after the recognition of viral antigen) [96]. PAbs are derived from multiple B-lymphocytes. They have multiple specificities and are therefore capable of binding to multiple different epitopes. This increases the immune protection. In contrast to PAbs, MAbs come from a single immune cell, thereby leading to always homogenous, well-defined and single epitope antibodies [96]. In addition, cultivated MAbs offer higher concentration and purity levels compared to the PAbs. A typical

concentration of a specific antibody in polyclonal sera is between 50 to 200 μg/mL whereas the MAbs offer 10-fold higher numbers in concentrations [96].

4.2 Antigen and antibody-antigen interactions

Antigens are a versatile group of molecules ranging from proteins to carbohydrates. They elicit the recognition process by a specific structure called epitope (or antigenic determinant), which is identified by the CDR loops of the antibody. Epitope is usually only four to ten amino acids in size. The small size enables the adoption of multiple epitopes in one antigen leading to a multivalent antigen molecule. Hapten is a special kind of antigen as it is a small organic compound used as a whole in the recognition process. It is not capable of immunogenic activity without covalent conjugation to a larger protein structure [97, p. 718].

The bonds between epitope and antigen-binding site are non-covalent in nature. Forces like hydrogen and electrostatic bonds, Van der Waals forces and hydrophobic interactions are formed, which result in reversible binding [97, p. 137]. Each of these interactions alone is respectively 100 to 1000 times weaker than a covalent bond and occurs only over short distance. Interactions are also easily disrupted by high salt concentrations, extremes of pH, detergents and by the competition with high concentrations of the pure epitope itself [97, p. 137]. The complementary shape of the antibody and the epitope strengthens the bond. Also structural changes, which sometimes occur during the binding process, strengthen the bond [26]. The binding strength between a single antigen-binding site and its antigen is called affinity [96]. It is measured by equilibrium binding affinity constant K_d (13)

$$Ab + Ag \underset{k_{off}}{\overset{k_{on}}{\leftrightarrow}} Ab\text{-}Ag$$

$$\xrightarrow{yields} K_d = \frac{k_{off}}{k_{on}} = \frac{[Ab][Ag]}{[Ab\text{-}Ag]} \tag{13}$$

where *Ab* is the concentration of the free antibody in the solution, *Ag* the concentration of the free antigen, *Ab-Ag* the concentration of antibody:antigen complex, k_{on} the formation rate constant and k_{off} the dissociation rate constant [26]. K_d is a thermodynamic property, which typically gets relatively low values of 10^{-5}-10^{-11} mol/l [26]. Another term related to the binding process is avidity. It is described as the combined synergistic strength of individual bond affinities with bi- and multivalent antibodies [97, p. 129]. Avidity is also assay specific [96].

4.3 Immunoassay

Immunoassay is a bioanalytical test to detect the concentrations of different substances from the solutions (e.g. saliva, blood, urine, lymph) by utilizing the specific binding capability the antibody and antigen have towards each other. There are two types of immunoassays: homogenous and heterogenous assays. In homogenous immunoassay, both the sample and the capture agent are in the same solution phase. All the reagents are placed simultaneously (one step assay) providing short analysis times, multiplexing capability as well as very fast electrophoretic separations. However, a separate pre-concentration step is often needed before electrophoresis. In heterogenous immunoassays, antibody is immobilized onto the substrate surface and the sample is in the solution phase. The immobilization step as a whole (immobilization surface, conditions and procedure) have an influence on the antibody, which makes it a very important step of the whole assay. The drawbacks of the heterogenous immunoassays are the several washing steps where unbounded reagents or analytes are rinsed as well as cognate mixing and separation steps which longer the performance time. [1, 3, 5]

The most common format of heterogenous immunoassay is the enzyme-linked immunosorbent assay (ELISA) [15], where one of the immunoreagents is immobilized onto the 96-well microtiter plate. One assay component is conjugated with the enzyme (biological label), which reacts with the color forming substrate. The reaction is detected by colorimetric system through which the target analyte binding is quantified.

The two most widely used ELISA assay formats are competitive and sandwich (also known as non-competitive) assay (figure 19). In competitive assays, the target analyte in the sample competes from the limited number of binding sites with the tracer (labeled, purified analytes). The amount of the analyte is inversely related to the detected tracers. Thereby the increase in the analyte concentration leads to reduction in the detection signal. The sandwich assay is based on two capture agents of which the first is immobilized and the other labeled. The labeled antibody is either added at same time or after the sample incubation. In contrast to the competitive assay, the proportion of the analyte is directly related to the amount of measured label. The specificity is high due to double recognition of the antigen molecule. However, the requirement of two different antibodies specific to one antigen set limitations to this assay format. [25]

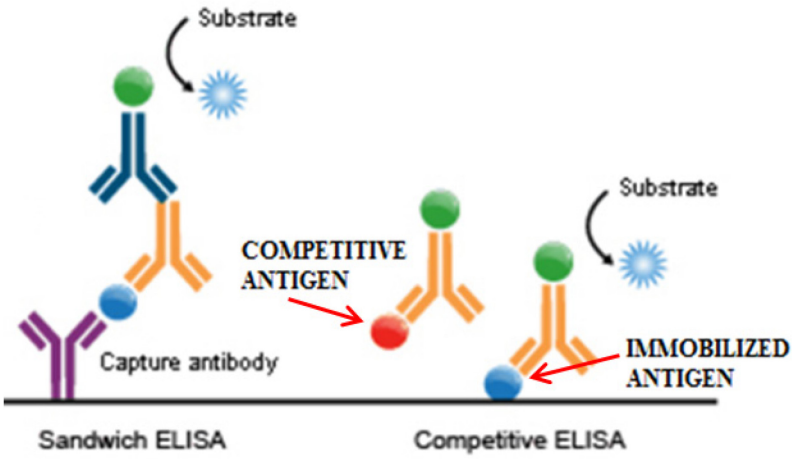

Figure 19. The variations of ELISA assay: direct, sandwich and competitive assay. The blue ball is antigen (Ag denotes antigen) and the green ball is the enzyme. Adapted from ref. [98].

Immunoassay demands moisture atmosphere and room temperature. In addition, an important point related to immunoassays, is the presence of a negative control. Control well does not contain the counterpart for the sample analyte, thereby no reaction should occur. Also several washes are performed to clean the wells from the unbound reagents. Usually physiological solutions, like thiobarbituric acid (TBA) and phosphate buffered saline (PBS), are used. The pH of these solutions is adjusted in order to avoid the disruption of the binding interaction. Adjustment is needed as the isoelectric point (pI) has an impact on the solubility of the molecule. The pI is the pH at which the net charge of a molecule is zero [97, p.730]. The blocking agent blocks the free space on the assay well to reduce the background binding caused by nonspecific adsorption of reagents and sample. A high level of nonspecific adsorption is seen in increase in the negative control signals and decrease in the specificity and sensitivity of the assay [5]. A well-known blocking agent is BSA [15].

Key features of the immunoassay are a high specificity and a wide detection limit, which range to picomolar (pM) or even femtomolar (fM) concentrations depending on the assay type. In addition, it usually does not involve the consumption of harmful reagents. However, the time-consuming and labor-intensive sample handling (incubation steps are measured in hours), long analysis times and expensive reagents (over 50-100 µl of each reagent [17]) are often referred to possible limitations of conventional immunoassays [1, 5]. Long analysis times originate from the inefficient mass transport of immunoreagents from solution phase to surface where the actual conjugation takes place [1]. Immunoreaction itself is a fast process.

4.3.1 Detection

The detection in immunoassays is based either on labeled or label-free methods from which the labeled methods are more common with biological samples [25]. Labeled methods include enzyme tracers and fluorescent dyes, which are detected with various optical and electrochemical detection methods. Common enzyme tracers are alkaline phosphatase (AP) and horseradish peroxidase (HP) [25]. The enzymes are conjugated to the antigen or to the detection antibody in sandwich assay and let to react with a substrate (e.g. 4-nitrophenyl phosphate disodium salt hexahydrate, (PNPP)). The reaction is detected by colorimetric means by measuring the absorption at a specific wavelength (e.g. 405 nm). Typical fluorescence dyes are Alexa Fluor - 647, Cy3 and FITC [5]. These labels are excited upon induction to fluorescence light. The drawback of labeled detection is the conjugation of the enzyme or fluorescent label to one of the immunoreagents. Modification may cause alterations in the functionality of the reagent and it also increases the process complexity [25].

Label-free methods concentrate on measuring the physical effects caused by biochemical binding, like change in the mass loading or thickness of the surface. The detection is done most often by acoustic and optical means [25]. These methods do not contain sample modification and are efficient, but require expensive machinery and people with skills [25]. They require only a single capture receptor but are prone to non-specific binding onto the sensor surface [2]. Optical methods include e.g. surface-plasmon resonance (SPR), which is a real-time detection method for binding and determination of the binding constants. The binding surface is covered with a thin layer, like gold (Au). The method is based on the change of the local index of refraction and resonance of surface plasmons in the metal. A light beam is reflected on the bottom of a thin metal layer and the angle and wavelength of the reflected light are detected. Vikholm-Lundin et al. [8] were able to detect the concentration of 1 ng/ml of CRP antibody Fab fragments from purified and 4 ng/ml of serum samples with SPR.

Another approach to label-free methods is the matrix-assisted laser desorption/ionization (MALDI) time-of-light (TOF) mass spectrometry (MS). In MALDI, the substrate containing the sample is covered with the light-absorbing matrix molecule (e.g. α-cyano-4-hydroxycinnamic acid (HCCA, alpha-matrix [36]). The drying of the matrix creates a crystalline matrix, which is vaporized and ionized in the gas phase process by nanosecond-duration laser pulses. The released ionized molecules from the sample are accelerated in the electrical field. Depending on the mass/charge ratio, the ionized molecules reach the detector at different times. MALDI is

liable to detect smaller than 700 Da molecules, but relatively high background and acidity of the matrix material are considered as the limitations of the method with antibody analysis [36].

4.4 Recombinant Fab fragments

Recombinant Fabs are antibody-binding fragments developed in the laboratory environment by means of genetic engineering. Laboratory enables the production of large quantities with ease and homogenous quality [99]. Recombinant Fabs constitute of four different domains: V_L and C_L forming an entire light chain and V_H and C_{H1} domains from heavy chain (called as Fd fragment, figure 18). One disulfide bond binds the heavy domains together (figure 18). Their structure and binding ability is equal to the intact IgG antibodies and the papain cleaved Fab fragments (see chapter 4.1) [26].

The overall production process of recombinant Fabs include five steps: creation of antibody gene library, display of the library on phage surface, affinity selection of antibodies, modification of selected antibodies and expression and production of selected antibodies in a chosen host system. Recombinant Fab fragments are typically produced with phage-display technique in bacteria like the gram-negative *Escherichia coli* (*E. coli*) [99]. Besides the bacteria, suitable host systems for expression are e.g. yeast (e.g. *Pichia pastoris* [100]), insect cells (e.g. *Drosophila S2* cells [101]) and plants (e.g. transgenic potato tubers, *Solanum tuberosum* cv. Désirée [102]), but the low price, well-known production process (due to known genome of *E. coli*) and fast growth (production takes only days rather than weeks) as well as high transformation rate favour the bacteria production [99]. The usage of bacteria is also supported by the fact no glycosylation is preferred in the Fab fragment production [99]. Obtainable yield depends on the chosen production method, but with bacteria expression, yields higher than 1-100 mg of purified material in litre are common [26]. Figure 20 illustrates the different stages of the production of the recombinant Fabs.

The production process, which is based on genetic engineering, enables to develop antibody fragments not present naturally in the mammalian body and also to tailor their properties. For instance, tailoring can be made by inserting short amino acid sequences called affinity tags to the end of the constant domain [99]. E.g. six histide (His6) has a strong affinity towards divalent metal ligands and is therefore important for the purification, immobilization and detection prospects [103].

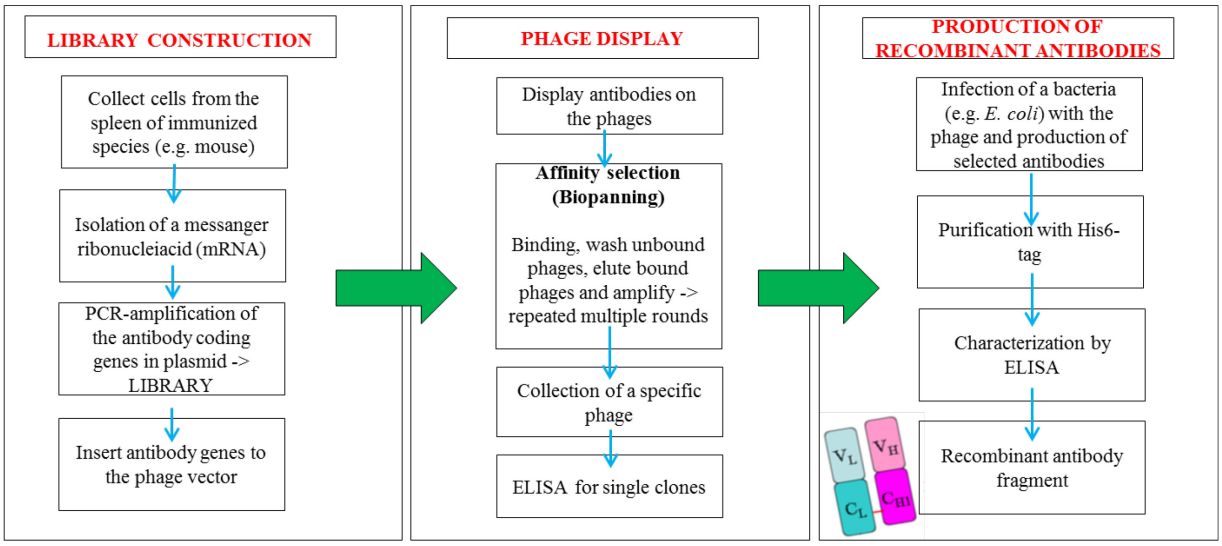

Figure 20. Schematic presentation of recombinant Fab production by phage display.

5 Heterogenic antibody immobilization on polymers

An essential step in the heterogenous immunoassay is the antibody immobilization, which can be performed via physical adsorption, covalent coupling or bio-specific immobilization [24-25]. Immobilization is defined as [104]:

"The attachment of molecules to a surface resulting in reduction or loss of mobility."

The suitable immobilization method is determined by the physicochemical and chemical properties of both the surface and the antibody [25]. Therefore there cannot be one generic solution for immobilization on polymer support, but the best possible method is chosen case-specific. The main target is to try to fulfill the requirements for the ideal antibody immobilization, which are categorized by Jung et al. [24] to proper and uniform orientation (figure 21), minimum antibody modification and soft incubation conditions. With microfluidic surfaces, the ideal antibody immobilization often includes some kind of a surface modification as this increases the control of interactions between antibody and the supporting polymer [1, 5]. Antibodies tend to adsorb onto hydrophobic surfaces. This chapter describes the common antibody immobilization methods onto polymer and explains the differences between recombinant Fab and intact antibody immobilizations. At the end of the chapter the current situation of the antibody immobilization onto SU-8 is reviewed.

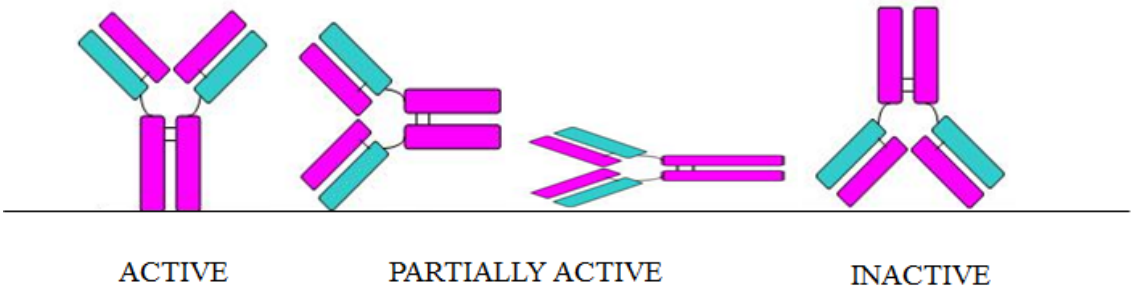

Figure 21. The functionality of immobilized antibody is based on the orientation of the antigen-binding site. The states are referred as (from left to right): end-on Fab up, side on, flat on and end-on Fab down.

5.1 Physical adsorption

Physical adsorption or simply non-covalent adsorption is by far the easiest, simplest and most cost-effective way to execute antibody immobilization, because there is no need for antibody modification or complicated coupling methods [24]. Antibodies are adsorbed to the solid support in a simple incubation procedure during which intermolecular forces like electrostatic forces, ionic -, hydrogen - and van der Waals bonds or hydrophobic interactions are formed [104]. The type of the interaction is based on the local dipoles the interacting molecules have between each other [25].

Antibodies are attached in a random orientation to the surface, which yields random placement of the active sites (figures 2 & 21). Some denaturation of the antibodies may occur. Also surface loadings can be very high, because the binding capacity is limited only by the geometric size of the immobilized antibody (e.g. antibody size is of the order of nm^2 in area). This causes steric hindrance, which occurs as a reduction in the binding efficiency, because antigens are not able to reach the antigen-binding site. Other related problems are relatively high background signal, leaching while buffers or other reagents normal to immunoassay are used and the need of highly purified samples in order to obtain good responses. [25, 104] Studies have shown that the usage of hydrophobic surfaces lead often to antibody denaturation [5].

By reason of all the previous, it is impossible to determine beforehand the fraction of antibodies that remain functional after physical adsorption. In the study of Butler et al. [105] for example, only 10 % of antibodies were active after immobilization.

5.2 Covalent coupling

In covalent coupling antibodies are attached to the surface via highly stable and strong covalent bonds [24]. Bond formation requires at least two functional groups, which are capable of interacting with each other. There are two types of covalent coupling methods: random and site-specific of which the behavior of the former resembles physical adsorption and the latter bio-specific immobilization discussed later [104]. Another clear distinction between these two is that the random covalent coupling does not require antibody modification [104].

5.2.1 Random covalent immobilization

Random covalent immobilization occurs between the support and the amino acid residues on the surface of the antibody. Most common bond former is lysine, which forms covalent bonds

through its amine groups [104]. Working as a nucleophile the primary e-amine group of lysine attacks towards the electrophile and forms the bond according to attractive and repulsive forces. Formed covalent bonds are more durable towards the processing conditions than the bonds in physical adsorption.

Because no antibody modification is involved in the random covalent immobilization the support needs to be chemically modified or contain by nature functional groups capable of bond formation. Epoxy -, aldehyde -, carboxyl - and carbodiimide groups -containing supports are commercially available and rather used [24-25] (commercially available supports, see [106]). In addition different soluble bifunctional linkers, like glutaraldehyde, are used while the direct attachment of support and lysine is not possible [104]. Linker molecules allow the antibodies to be farther away from the surface, which diminishes the steric hindrance.

Due to the abundance of lysine residues in the antibody structure (a standard intact antibody lgG contains at least 70 lysine molecules), the immobilization leads easily to random orientation and multipoint attachment [104]. The latter induces uncontrollable orientation and steric hindrance.

5.2.2 Site-specific covalent immobilization

Compared to random covalent immobilization, site-specific covalent immobilization requires antibody modification, but yields more homogenous surface loadings. Modification is directed either to carbohydrate moieties found in the Fc region or to thiol groups in the hinge region in proteolyted Fab fragments (see figure 20). Carbohydrate residues are treated with oxidation reaction. With sulfide bonds the coupling procedure is based on the reduction of disulphide bridges by cysteamine or mercaptoethanol treatments. This yields sulfhydryl groups. [24, 104]

Common characteristics to site-specific covalent immobilization are often better biomolecule activity, reduced non-specific adsorption, high surface coverage and better control of antibody positioning compared to physical adsorption [104]. From practical point of view this immobilization method is rather difficult to perform, because it demands antibody modification. Modification involves extra processing steps which add the processing time but may also affect the antibody structure leading to possible loss of antibody activity.

5.3 Bio-specific immobilization

Bio-specific immobilization reactions are based on the biochemical properties the antibodies have. Interactions are less stable than in covalent immobilization. The advantage of this method is the oriented and homogenous attachment, which is also reversible in nature and enables the repeated use of the same surface. These methods are also gentler due to no need of antibody modification. The most common bio-specific based methods comprise antibody-binding proteins, biotinylation and recombinant proteins with tags. [24-25]

5.3.1 Antibody-binding proteins

Antibody-binding proteins, like protein A, are capable of multivalent binding to different IgG from different species (humans, mouses etc). Protein A, which is a cell surface protein of *Staphylococcus aureus,* is a single polypeptide chain with molecular weight around 40-65 kDa [25]. This immobilization method enables the proper orientation of the antigen-binding site, because the antibody-binding proteins are affinity coupled to Fc part of the antibody whereas the antigen-binding site is left intact [24]. In addition no antibody modification is needed. The stability of the bond with antibody-binding proteins is lower compared to the covalent coupling [24].

Typically protein A is immobilized to the polymer surface either via electrostatic adsorption, amine-glutaraldehyde (GA) chemistry or tyrosinase (TR)-catalyzed reaction [20, 22]. Amine-GA chemistry is based on the covalent linking via amine groups in the protein A. Amine groups are present in abundance as there a total of 67-69 amine groups in the protein A structure. Therefore, both the adsorption and amine-GA chemistry yield random orientation of the protein A on the polymer surface [22]. TR, on the other hand, has a capability to convert tyrosine in the protein A into O-quinones, which are highly reactive towards primary amines. There are only 5-8 tyrosine residues on protein A and thereby, protein A immobilization based on TR-catalyzed reaction is said to be more site-selective [22]. TR-catalyzation results in better antibody activity compared to amine-GA chemistry immobilization. In the study of Yuan et al. [22], TR gave sevenfold and GA fourfold increase in antibody activity when compared to the PMMA surface where physical adsorption of the antibody was done. In all of the cases, the surface was first functionalized with plasma oxidation prior immobilization steps (300W, 30s, 20 sccm) (figure 22).

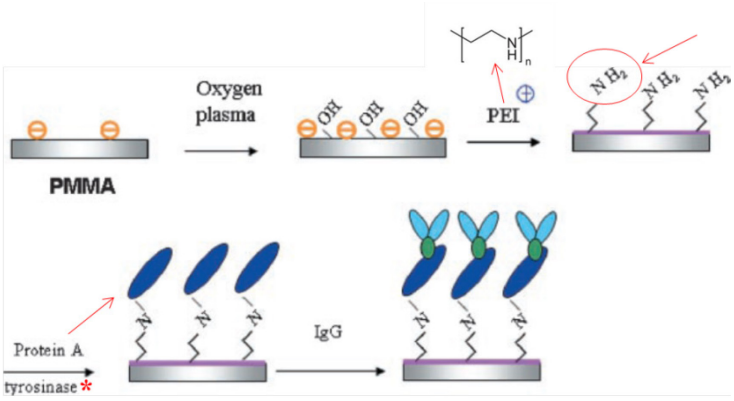

Figure 22. Schematic presentation of tyrosinase-catalyzed protein A based immobilization of antibodies. Before immobilization otherwise inert PMMA surface is treated with oxygen plasma and poly(ethyleneimine). Adapted from ref. [22].

5.3.2 Biotinylation

In biotinylation, the antibody is labeled with biotin, a vitamin H, which can act as an affinity tag. Biotin can form near irreversible bond with avidin, which is a glycosylated protein capable of binding up to four molecules of biotin. Similarly to avidin, streptavidin is capable to bind biotin. The biotin-avidin bond is one of the strongest known non-covalent bonds as the K_d value for it is as low as 10^{-15} [24, 104]. The avidin-biotin bonding enables harsh incubation conditions as the bond is unaffected by the pH, temperature, organic solvents, enzymatic proteolysis and other denaturing agents [22, 104].

Biotin is coupled to the antibody through e.g. carboxylic acid groups [24]. The carboxyl groups react with the lysine molecules on the antibody molecule. A more controlled coupling is done e.g. through disulphide groups [24]. In addition to labeling the antibody with biotin, this method also requires the avidin immobilization onto the substrate [104]. An example of this is the surface grafting by poly(ethylene glycol) (PEG), to which the avidin is coupled by covalent coupling [104]. The chemical and recombinant methods have been used to enhance the properties of avidin and streptavidin. This offers e.g. improved stability and more controlled biotin binding [25]. NeutrAvidin and NitrAvidin are examples of improved molecules.

5.3.3 Recombinant proteins with tags

Recombinant proteins are antibodies, which have been modified genetically. The fabrication method enables the attachment of a tag which was originally added for the purification purposes [27]. However, the tag also serves as an immobilization site as e.g. Hale et al. [34] have shown. During the cloning, the tag is attached to the C-terminal side of the antibody. Therefore, the tag is always on the opposite site of the antigen-binding site yielding optimal orientation of the antibody. The advantages of the recombinant proteins with affinity tags are the compatibility with organic solutions, low immunogenicity, reusability, efficient orientation capability and efficacy under native and denaturing conditions [104].

An example of the tag is a short amino acid chain, like histidine (His) – tag, which is made up of usually six consecutive histidine amino acids (figure 23). The antigen-binding ability of Fab fragment is not interfered with His-tag attachment even though multiple tags are attached [107]. The efficiency of His-tag is based on the affinity it has towards divalent transition metals (e.g. nickel (Ni^{2+}), zinc (Zn^{2+}) and cobalt (Co^{2+})) in aqueous solutions (figure 23) [103]. The imidazole rings on His-tag molecule have the chelating ability of IDA coordinated cobalt ions (figure 24). The formed coordination bonds are irreversible [103]. In addition to His-tags, cysteine (Cys) –tags are common [24].

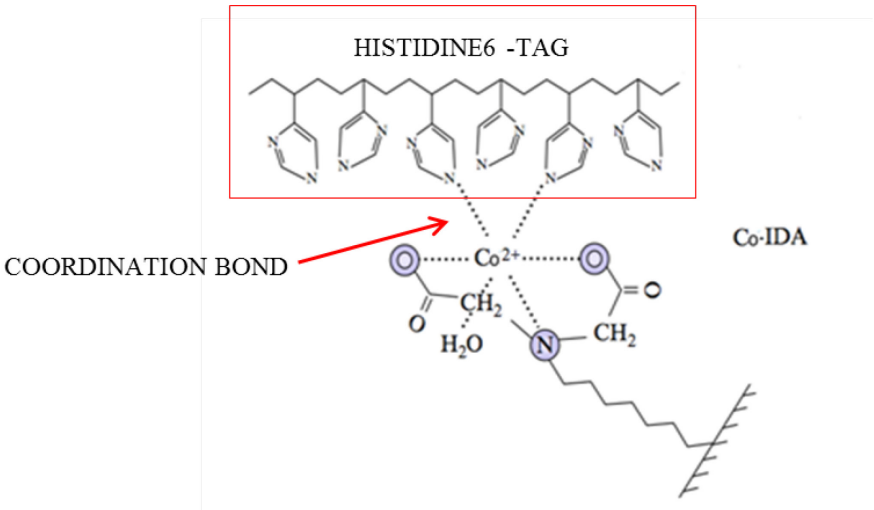

Figure 23. Histidine6-tag is affinity bonded to IDA-Co chelation system. His6-tag is marked with red box. Adapted from ref. [103].

Figure 24 summarizes the physical adsorption, covalent coupling and bio-specific immobilization and the parts of the antibody which enables the antibody immobilization. A good review about the antibody and protein immobilization in general is in [25, 104]. Table 5 presents the comparison between advantages and disadvantages of different immobilization methods.

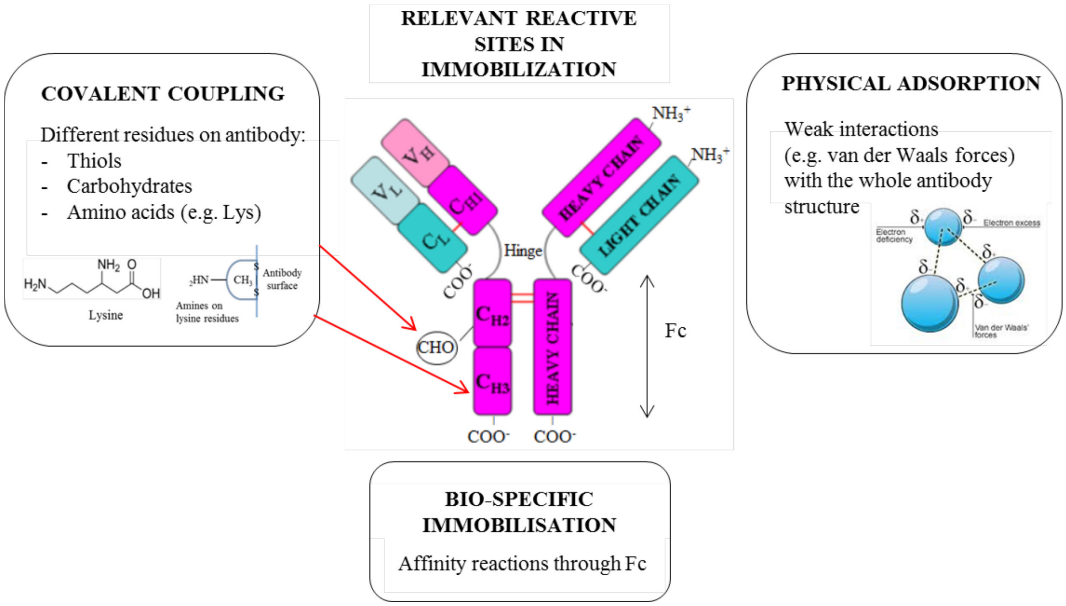

Figure 24. The antibody structures which enable different immobilization methods.

Table 5. Comparison of different immobilization methods (Ab denotes antibody). From refs. [24, 108].

IMMOBILIZATION METHOD		ADVANTAGES	DISADVANTAGES
Adsorption		Minimal manipulation, No Ab modification, Mostly high immobilization level	Random orientation, Ab denaturation, Nonspecific protein binding, Leakage of antibody from surface
Covalent coupling		Stable immobilization, Commercially available surfaces	Random orientation, Ab modification, Possible denaturation
Bio-specific immobilization	Antibody-binding proteins	Oriented immobilization, No Ab modification, Mild incubation	Surface stability, Not suitable for sandwich assays, Additional processing step for antibody-binding protein immobilization
	Biotinylation	Oriented immobilization, Mild incubation	Ab modification, Additional processing step for avidin immobilization
	Affinity tags	Oriented immobilization, Mild incubation, genetic Ab engineering	Surface stability

5.4 Fab immobilization and the differences to the immobilization of intact antibodies

The difference between intact antibody and truncated fragment immobilization is the size and the advantages it brings [27, 108]. The Fab fragments are much smaller (only one third of the whole antibody structure), which enables denser packing of molecules and thereby higher surface loadings on the substrate surface. This improves further the assay sensitivity. The smaller size of the fragment also provides faster assay kinetics. In the study of Brockmann et al. [27] the Fabs offered 3-folds higher binding capacity, faster kinetics and better detection limit of thyroid-stimulating hormone (TSH) compared to the whole monoclonal antibodies (0,09 mIU/L TSH and 0,26 mIU/L TSH, respectively). The Fab was 49 kDa in size whereas the monoclonal antibody 155 kDa, respectively.

5.5 Immobilization onto SU-8 substrate

There are only a few studies concerning the antibody immobilization onto SU-8 surface from which none presented immobilization of antibody fragments or recombinant antibodies. Two studies, where antigens were immobilized instead of antibodies were found [35, 109]. Table 6 summarizes the current situation of the antibody immobilization onto SU-8.

Table 6. Antibody immobilization onto SU-8.

ANTIBODY	ANTIGEN	SURFACE MOD.	IMMOB. METHOD	BLOCKING	OTHER	REF.
Human IgG	FITC-tagged goat anti-human IgG	-	Physical adsorption	BSA	Only weak and random fluorescence detected.	[32]
		Aminosilanization (H_2SO_4+ AEAPS + glutaraldehyde)	Covalent immobilization			
Mouse IgG	Cy3-conjugated antimouse-IgG	Aminosilanization (H_2SO_4 + APTES + glutaraldehyde)	Biospecific binding (protein A)	BSA	Antigen concentration of 1,5 ug/ml detected.	[110]
Alexa Fluor 647-labeled chicken anti-mouse IgG	-	-	Covalent immobilization	-	Not an immobilization study	[77]
Human IgG	FITC-tagged goat anti-HIgG	Carbodiimide chemistry (NaOH/HCl treatment + glycine)	Covalent immobilization	PBSTB	Glycine was the most effective, physical adsorption the worst.	[33]
		Succinimide chemistry (NaOH/HCl + 11-MUA)	Covalent immobilization			
		-	Physical adsorption			
Anti-CRP-cAb and anti-CRP-Cy5-dAb[1]	-	Aminosilanization (CAN + APTES + glutaraldehyde)	Covalent immobilization	BSA	Sandwich assay: LOD[2] of 300 ng/ml CRP	[31]
		CAN	Covalent immobilization		LOD[2] of 80 ng/ml CRP	
		-	Physical adsorption		LOD[2] of 30 ng/ml CRP	
Human IgG	FITC-tagged goat anti-human IgG	-	Physical adsorption	BSA	Only weak and random fluorescence detected	[28]
		HWCVD + glutaraldehyde	Covalent immobilization			

[1] *dAb = detector antibody, cAb = capture antibody*

[2] *LOD = limit of detection*

6 Materials and methods

6.1 Fabrication of the SU-8 substrates

The SU-8 layers were spin-coated on top of a RCA-1 and RCA-2 cleaned, single-side polished silicon wafers with a crystal orientation of <100>. The wafers were baked in a 120°C oven from 1 to 24 h prior the SU-8 layer fabrication. The fabrication process of all the SU-8 surfaces applied in the experimental part followed the five-step photolithographic process for negative photoresists presented in chapter 3.2: spin-coating (WPB Resist Coating, STANGL), soft bake, UV-exposure (MA6/BA6, Süss MicroTec) and post-exposure bake and development. The hotplate in the bakes was either programmable (UniTemp GmbH) or adjustable, leveled hotplate (Präzitherm).

6.1.1 Planar SU-8 surface

Planar SU-8 surfaces of 14.5 μm in thickness were fabricated using spin speed of 9000 rpm for 45 s. The layer was first soft baked at 65°C for 5 min and finalized at 95°C for 8 min. UV-exposure of 5 s was applied. The exposure step was done without the mask (flood-exposure) and no development step was needed, because the whole layer had been in contact with the UV-light. The layer was finalized with the 8 min PEB at 95°C. The wafer was cut into 1.5 cm x 1.5 cm pieces with a diamond pen.

6.1.2 Nanostructured SU-8 surface

SU-8 surface was structured with nanopillar features by using a composite stamp of PDMS / hard-PDMS (h-PDMS). The mask for the composite stamp was made of black silicon. The black silicon master was fabricated in a maskless Deep Reactive Ion Etching (DRIE) process. The features from the master were replicated to the composite PDMS stamp in an UV-embossing process. The black silicon mask fabrication and UV-embossing process are reported elsewhere, in [46] and [111], respectively.

The nanostructured SU-8 surface was 14.5 μm in thickness. Same spin-coating and bake parameters were used as with the planar surface (see chapter 6.1.1). The composite stamp was placed on top of a SU-8 layer during the soft bake, when the temperature was dropped from 95°C to 80°C. The stamp was gently pressed with tweezers to get rid of the air bubbles. The total time for the stamping process was 10 min. Upon UV-exposure, increased exposure time (60 s) was applied compared to the planar surface fabrication (5 s). The increase in exposure time both improved the adhesion of SU-8 to underlying silicon and ensured sufficient

crosslinking initiation to SU-8 (some of the UV-light is absorbed to the composite PDMS stamp). The stamp was removed after PEB, when the temperature reached the room temperature (RT). No development step was needed. The scanning electron microscope (SEM) image of the nanostructured surface is shown in figure 25. As was with planar surface, the wafer was cut into 1.5 cm x 1.5 cm pieces after finishing the fabrication process.

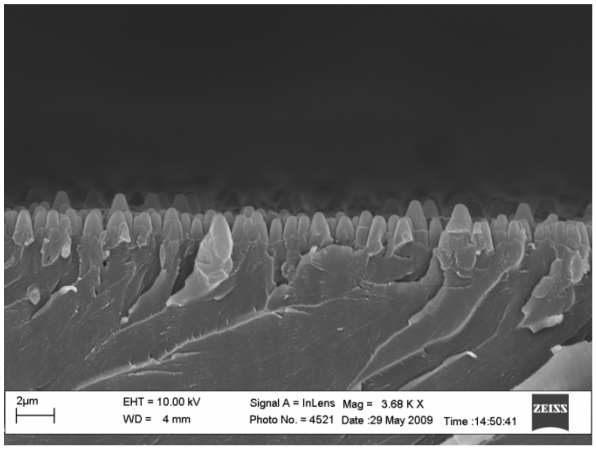

Figure 25. SEM-image of nanostructured SU-8 surface, which resembles grass or forest.

6.1.3 Immunochip design

Immunochip structure was designed on the basis of our previous research (see chapter 2.4) [37]. Triangle patterned microfluidic channels were found to be able to direct the water flow to a certain direction with a certain layer thickness and contact angle. The phenomenon is discovered when triangles are placed tips towards the proceeding meniscus. The chip contained two layers with equal depths. The base layer was planar and the second layer contained the channel design. Three different layer thicknesses were used: 14.5; 17.8 and 21.2 µm. Fabrication parameters for different layer thicknesses are presented in the table 7. At the end of the process, SU-8 structures were developed with PGMEA, which was followed by 2-propanol (IPA) rinsing and nitrogen dry.

The design of the chip is shown in figure 26. Fabricated channel chip was 1.5 cm in width and 3 cm in length. In addition to channel, the design consisted four square-shaped inlets from which three where positioned on the side and one at the beginning of the channel. The former were 0.5 cm x 0.5 cm and the latter was 0.7 cm x 0.7 cm in size. The inlets on the side were connected to channel by 1 cm long connection channel, also structured with squares.

Triangles inside the channel were 80 µm x 20 µm in size. They were placed in rows with 10 µm distance to the adjacent triangle as a total number of 150 triangles in a row. Three

different distances between consecutive rows where used: 17, 20 and 23 µm. Depending on the distance, there was a slight variation in the number of consecutive rows. All the inlets were structured with a square pattern. One square was 10 µm x 10 µm in size and the distance to every direction was 10 µm. In the places where inlets connected to channel, the square patterning was continued between triangle structures in order to facilitate the progression of the liquid.

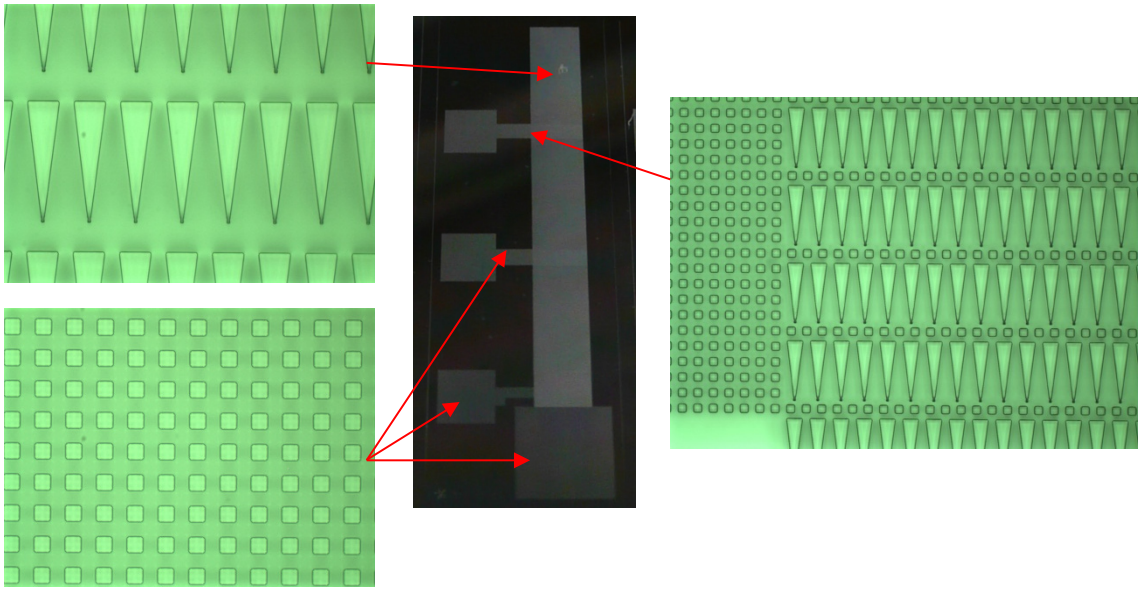

Figure 26. Fabricated immunochip structure made of SU-8. Detailed optical microscope pictures are presented: the triangle and square structures (magnification of 50) and the structure where the inlet connects to the channel structure (magnification of 20).

Table 7. Immunochip fabrication parameters and the channel details (exp. denotes exposure and dev. is development).

THICKNESS	SPIN SPEED AND TIME	SB	EXP.	PEB	DEV.
14.5 µm	9000 rpm, 45 s	in 65°C 5 min, in 95°C 8 min	5 s	in 95° 8 min	~ 5 min
17.8 µm	9000 rpm, 36 s	in 65°C 5 min, in 95°C 8 min	5 s	in 95° 8 min	~ 5 min
21.2 µm	9000 rpm, 30 s	in 65°C 5 min, in 95°C 8 min	5 s	in 95° 8 min	~ 5 min

6.2 Surface characterization

The SU-8 surface was characterized with Attenuated Total Reflection Fourier Transform Infrared (ATIR-FTIR) Spectroscopy measurement to ensure there are free epoxy groups, which are able to take part in the immobilization process.

Five different samples (denoted as sample1 to sample5) were fabricated. Sample1 was similar to planar SU-8 surface fabricated according to chapter 6.1.1. The samples 2 and 3 were fabricated otherwise as planar SU-8 surface but the exposure time was either diminished to 2.5 s (sample2) or increased to 20 s (sample3) from normal 5 s (sample1). The other two remaining samples (samples 4 and 5) were fabricated with either diminished PEB time of 4 min (sample4) or increased PEB time of 20 min (sample5). The longer exposure time is supposed to diminish the number of free epoxy groups, because of more effective cross-linking process [30]. With different PEB samples, no changes in the amount of free epoxy groups should take place as the change in PEB time within all of the samples is somewhat moderate. The amount of free epoxy groups per SU-8 monomer can be estimated by calculating the ratio of peak heights of wavelengths ~ 914 cm^{-1} and ~ 1608 cm^{-1} [30]. The former is the vibration of epoxy ring and the latter indicates the stretching of the benzene.

The measurements were done with Unicam MATTSON 3000 FTIR spectrometer and PIKE Technologies GladiATR® equipment with a diamond crystal, at Laboratory of Polymer Technology, in Otaniemi. The analysis program was EZ OMNIC. The samples were placed upside down, SU-8 coated side towards the diamond crystal.

6.3 Antibody-antigen model system

For the immobilization studies the anti-mycophenolic acid (α-MPA) antibody F5 in PBS buffer and its antigen mycophenolic acid (MPA) as an alkaline phosphatase (AP) conjugate were chosen. Antibody has a His6-tag at the opposite site to the antigen binding site, which enables the oriented immobilization. Antigen is composed of four MPA molecules conjugated to one AP enzyme. The conjugation degree has been checked with mass spectrometer. Negative controls were unconjugated AP enzymes. Both the antigen and antibody were provided by collaborates at VTT.

In the previous experiments this antigen-antibody pair has been shown to be suitable model system for various applications. Antibody has reasonable affinity for immobilization studies (100-200 nM) and the conjugation of the antigen to the detection enzyme (AP) directly makes possible the one step assay development and the signal is efficiently amplified.

6.4 System set-up for immobilization studies

Before starting the actual comparison tests with random and oriented immobilization studies, three different approaches for the immobilization step were designed: PDMS stamp, immersion of the SU-8 sample to the protein solution and droplet-based immobilization (figure 27). In PDMS stamp approach, the SU-8 surface was covered with 7 mm thick PDMS stamp with a hole in the middle (figure 29). PDMS (Sylgard® 184, Dow Corning) stamp was fabricated by mixing resin material and curing agent in a ratio of 10:1 in a Petri dish. A short vacuum treatment removed the air bubbles, which were formed during the mixing procedure. The stamp was finalized with 55°C oven treatment for overnight (o/n). The hole, 7 mm in diameter, was made by hulpiber. The purpose of the hole was to define the area under immobilization. PDMS stamp was removed before the detection step.

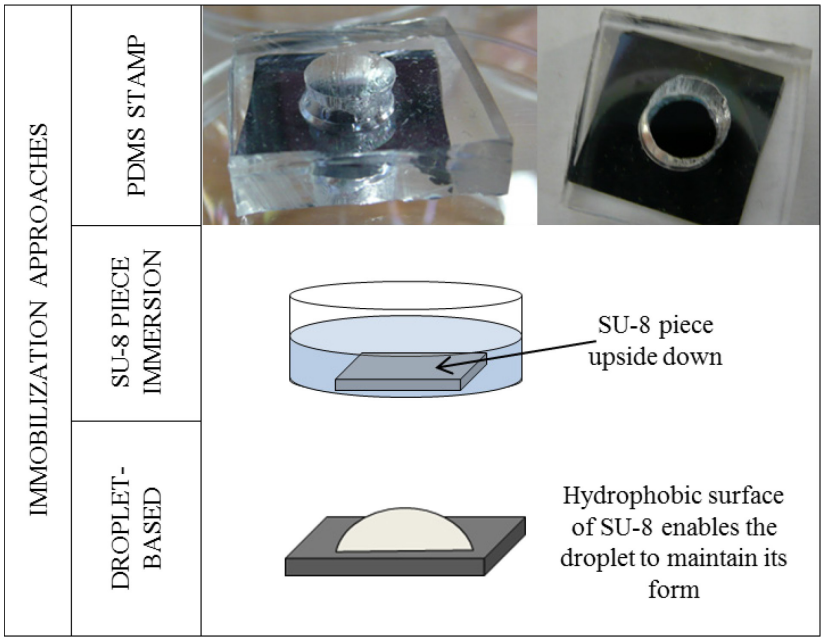

Figure 27. Different immobilization approaches utilized in the preliminary tests for SU-8: PDMS stamp, SU-8 piece immersion to protein solution and droplet-based immobilization.

The second approach comprised the immersion of the whole SU-8 piece to the protein solution. The whole area was therefore in contact with the protein solution. SU-8 pieces were turned upside down and sunk to the solution. As a highly hydrophobic surface the SU-8 pieces will float on the liquid without turning upside down. The few formed bubbles were removed by gently knocking the pieces with tweezers. In droplet-based approach, the protein solution was incubated onto SU-8 surface. The hydrophobic surface of SU-8 enables precise droplet formation.

6.5 α-MPA Fab F5 immobilization onto SU-8 surface

The immobilization studies both in random and oriented way were performed with 1.5 cm x 1.5 cm SU-8 pieces (area 2,3 cm^2), which were incubated in a lidded 6-well plate template having a wet paper in the lid. Assay conditions were adapted from routine immunoassay in microtiter plate for polystyrene. Between all the steps, the SU-8 pieces were rinsed three times in 2 ml of double-distilled water (DDIW). Rinsing was performed without incubation time.

6.5.1 Random immobilization

Random and covalent immobilization occurs between the lysine residue on the surface of the recombinant antibody fragment and the free epoxy group on SU-8 surface. The abundance of lysine residues leads to the random placement of the antigen-binding sites, which are either active, partly active or inactive as presented in figure 28.

40 µg of α-MPA Fab F5 in phosphate buffered saline (PBS) was manually spotted at a volume of 100 µl per drop onto pieces of SU-8. Droplet was placed in the middle of SU-8 piece and incubated o/n at room temperature (RT) in moisturized chamber. Free epoxy groups were blocked with blocking reagent, 1% bovine serum albumin (BSA, Sigma-Aldrich Co, USA) in 0,1 M sodium carbonate buffer (pH 9.6). SU-8 pieces were embedded in 2 ml of BSA blocking solution and incubated for two hours in RT with continuous shaking movement. 1.3 µg of MPA-AP in Tris-buffered saline (TBS) was spotted at a volume of 50 µl in the middle of the each SU-8 piece and incubated for one hour in RT. The principle of random immobilization is presented in figure 28.

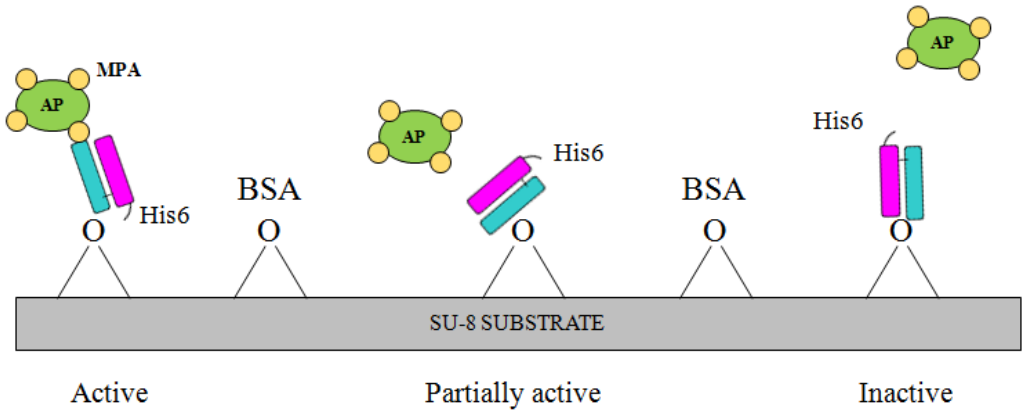

Figure 28. The principle of random immobilization in this thesis. The His6-tagged antibody fragments are immobilized via lysine residues onto the free epoxy groups at the SU-8 surface.

4-Nitrophenyl phosphate disodium salt hexahydrate (PNPP, Sigma-Aldrich, USA) substrate in Diethanolamine $MgMl_2$ – buffer (Reagena-buffer, Reagena, Finland) in a concentration of 2 mg/ml was applied for the detection. A droplet of 150 µl of aforementioned solution was placed in the middle of the SU-8 piece and was left to incubate for 51 min. A 100 µl of the incubated solution was transferred to the microtiter plate to measure the color change with absorbance using wavelength of 405 cm^{-1} (analysis program: Varioskan).

6.5.2 Oriented immobilization

In the oriented immobilization, the antibody is coupled to SU-8 surface through a chelation. Iminodiacetic acid (IDA) – cobalt (Co) system anchors the His6-tagged recombinant antibody fragments onto SU-8 surface by forming a bond between the Co-atom and histidines in the His6-tag. The system is chelated and made extremely stabile by increasing the oxidation state of cobalt from +II to +III in an oxidation step. This irreversible complex orients all the antigen-binding sites towards the liquid phase. Immobilization principle was based on the study of Hale et al. [34].

Oriented immobilization process started by fabrication of 1 M IDA solution. First, 100 nM sodium borate ($Na_2B_4O_7$) solution was made by mixing 3.8 g of $Na_2B_4O_7$ (Sigma-Aldrich, USA) to 100 ml of MilliQ-water (QPak, Millipore). Solution was stirred with magnetic stirrer in RT until all the sodium borate was dissolved. Next, 5.4 g of IDA (Sigma-Aldrich, USA) was stirred with 40 ml of 100 nM sodium borate solution. Before heating few milliliters of 5 M sodium hydroxide (NaOH) was pipetted to the solution. The temperature was adjusted to 50°C and stirring was continued until the solution cleared. The pH was measured (Knick pH-Meter 761 Calimatic) and adjusted to required 8.50 with 5 M NaOH.

Each SU-8 piece was embedded in 2 ml of IDA solution. The pieces were placed SU-8 surface downwards to avoid the floating caused by the hydrophobic SU-8 coating on top of the silicon. Possible air bubbles between the base of 6-well plate template and SU-8 surface were eliminated by gently knocking the SU-8 piece with tweezers. The pieces were incubated in 1 M IDA o/n with continuous shaking movement in RT.

Next the SU-8 surfaces were treated with cobalt. First, MilliQ-H_2O was filtered in a side-armed Erlenmeyer flask with a HVLP 0.45 µm membrane. The process was done in the vacuum by adjusting the compressed air flow on. After filtering the bottled water was treated with helium gas (He). The He-treatment of 250 ml of filtered water took 5 min. The water was treated with helium in order to maintain the oxidation state of cobalt during the antibody fragment immobilization. Next, cobalt(II)-chlorid-hexahydrat ($CoCl_2 \cdot 6\ H_2O$, Merck Oy,

Finland) was dissolved in degassed DDIW in a concentration of 100 mg/ml. Because $CoCl_2$ is poisonous, it was weighted in a hooded scale and dissolved to MilliQ-H_2O immediately after scaling. The piece was embedded and incubated in a 2 ml of cobalt solution in continuous shaking movement for one hour in RT. 40 µg of α-MPA Fab F5 in PBS was manually spotted at a volume of 100 µl per drop onto pieces of SU-8 and incubated o/n in RT.

After antibody immobilization cobalt was oxidized from oxidation state of +II to +III. 30 % hydrogen peroxide (H_2O_2, Sigma Aldrich, Finland) was diluted in DDIW in a ratio of 1:1000. A droplet of 150 µl of aforementioned solution was placed in the middle of the SU-8 piece and left to incubate for 1.5 h in RT. SU-8 pieces were embedded in 2 ml of BSA blocking solution and incubated for two hours in RT with continuous shaking movement. 1.3 µg of MPA-AP in TBS was spotted at a volume of 50 µl in the middle of each SU-8 piece and incubated for one hour in RT. Detection step was done as in random immobilization. The principle of oriented immobilization is illustrated in figure 29.

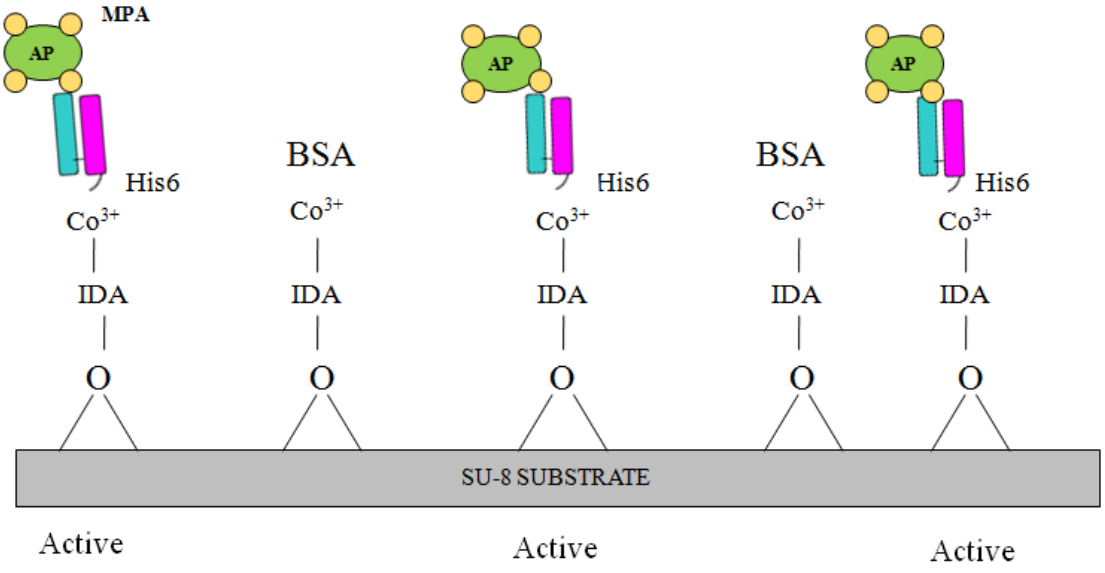

Figure 29. The principle of oriented immobilization in this thesis. The His6-tagged antibody fragments are immobilized via IDA-Co -system onto the free epoxy groups at the SU-8 surface.

6.6 Immobilization parameter studies

Immobilization procedures were optimized by means of antibody incubation time, antigen concentration, different incubation buffers in the antibody immobilization, pH (only for random immobilization), surface modification (both surface patterning and plasma oxidation treatment) and storing stability of the immobilized antibody as well as the substrate. All the

studies were performed with two or three parallel samples and the results were reported as a mean value of these separate results. Statistical analysis was performed to study the significance of the results. Significance was evaluated by Student's *t*-test, and the level of significance was set as $P < 0.05$.

6.6.1 Incubation time

The effect of the incubation time to the immobilization efficiency was studied in five different time points: 10 min, 30 min, 2 h, 4 h and o/n. Control sample was chosen to be o/n incubation as it is known to be sufficient time for the immobilization reaction if the immobilization is possible in general.

6.6.2 Amount of antigen

The sensitivity of SU-8 immobilization system was tested by diluting the antigen solution by 1x TBS. The starting point for the dilution series was 1:1 dilution (c = 0.025 mg/ml), which contained 1.27 µg of antigen on the SU-8 surface. The used dilutions were 1:1, 1:2, 1:5, 1:10, 1:20 and 1:100. Control sample was the dilution of 1:1.

6.6.3 Serum vs buffer

To demonstrate the feasibility of SU-8 surface for the analysis of pure biological samples, the antibody immobilizations were carried out with the human serum in addition to 1x PBS solution. Random and oriented immobilizations were done as mentioned in the chapter 6.5, but in addition to mixing the antibody to 100 µl in PBS, mixing with 100 µl in human serum was applied. Also the effect of incubation time was studied using o/n and 10 min time points. Control sample was buffer based immobilization with o/n incubation time.

6.6.4 pH in immobilization

The effect of pH was studied by using PBS solutions, which differed in pH, in random immobilization. The antibody immobilization pH in random immobilization is near pH 7 (pH of 1x PBS solution) whereas the pH in oriented immobilization is near pH 8.50 (IDA-Co chelation changes the surface pH). The adjustment of the pH was done with 5M NaOH solution. First a 300 ml of 1x PBS solution was prepared with measured pH of 7.24. By removing 100 ml of PBS solution of pH 7.24 and adding 3 droplets of 5M NaOH with a Pasteur – pipette the pH value was adjusted to 8.05. Again 100 ml of PBS solution was removed and additional 1 droplet of 5M NaOH added. The solution pH was 9.93. Antibody

was mixed to 100 µl in each of the prepared PBS solutions. Control sample was PBS solution with pH 7.24.

6.6.5 Surface modification of SU-8

The effect of surface wetting was studied by treating the SU-8 surface with oxygen plasma by Reactive Ion Etching (RIE) before taking the pieces out of the cleanroom environment. Oxygen plasma renders SU-8 surface more hydrophilic [80]. Etching conditions were chosen according to our earlier research (power 100, pressure 150) [37]. The SU-8 surface was RIE-treated for 5 s and 60 s. The contact angle was measured immediately after the RIE-treatment. Control sample was SU-8 surface, which was not treated with RIE.

The effect of surface structuring on immobilization efficiency was studied by applying nanostructured SU-8 surfaces which were fabricated according to chapter 6.1.2 as the immobilization support. Control sample was planar surface. Also the combined effect of RIE-treatment and nanostructuring on immobilization efficiency was studied. The RIE-treatment parameters were otherwise the same as mentioned above, but only the treatment time of 5 s was used. Control sample was planar SU-8 surface, which was not treated with RIE.

6.6.6 Storage stability of immobilized antibody

The storage stability of immobilized antibody in both wet and dry conditions was studied. The immobilization procedures were done according to the instructions in chapter 6.5 until the antigen incubation step. The wet storing was done by embedding the SU-8 samples in 2 ml of TBS and by keeping the wet paper in the lid of the 6-well plate template. The plate was sealed with paraffin in order to keep the well moisturized environment in the plate. The dry stored samples were in a lidded 6-well plate without TBS solution and wet paper. The immobilization procedures were continued normally after one day or one week storing time depending on the test.

6.6.7 Storage stability of SU-8

In substrate storage stability studies, the SU-8 coated wafers were fabricated as normal, but after finishing the process, they were stored in cleanroom conditions for 1, 2, 3 or 4 weeks. Control wafers were fabricated on the day the studies were started.

6.6.8 Simultaneous comparison of random and oriented immobilizations

The immobilization efficiency between random and oriented immobilizations was evaluated by comparing the immobilization results from previously described parameter studies (chapters 6.6.1 - 6.6.3 and 6.6.5 - 6.6.7). Only results from the studies, which were identical in terms of reagents (prepared at the same time) and SU-8 substrates (from the same wafer) for both immobilizations, were included in the analysis. Table 8 presents the included studies.

Table 8. Immobilization studies, which were included in the immobilization efficiency comparison studies between random and oriented immobilizations.

PARAMETER	**CHANGES**
Incubation time	10 min, 2h, o/n
Amount of antigen	Dilutions 1:1, 1:2, 1:5, 1:10, 1:20, 1:100
Serum vs buffer	Serum vs PBS; Serum vs PBS with incubation times of 10 min and o/n
Surface modification	Oxygen plasma treatment for 5 s or 60 s; Nanostucturing and oxygen plasma treatment for 5 s
Antibody stability over time	Wet and dry storing for 1 week
SU-8 stability over time	Storing at cleanroom for 1, 2, 3 and 4 weeks

The immobilizations were also compared by the remaining antibody - antigen stability after successful antibody immobilization study. After the substrate reaction, the SU-8 samples were again embedded in 2 ml of TBS for o/n in RT. A wet paper was kept in the lid of the 6-well plate template. Next day the SU-8 samples were transferred to a new well and a new substrate was placed on top of a SU-8 piece and the absorbance of the remaining antibody –antigen complex measured. The absorbance measurement was repeated. The substrate incubation in addition to absorbance was again repeated after a new antigen immobilization was made, but this time incubated with the BSA blocking solution.

6.7 SU-8 as a MALDI- base

The possibility to use SU-8 as a matrix-assisted laser desorption/ionization (MALDI) –base in mass spectrometer (MS) measurements was studied by using both planar and nanostructured SU-8 surfaces with and without RIE-treatment (time: 5 s, power: 100, pressure: 150; parameters from our previous study [37]) for which the antibody immobilization was done according to chapter 6.5. The correct functioning of immobilization was proven by extra sample for which the immobilization procedure was followed through (including also the substrate incubation, detection by eye). All the measurements were done at Biomedicum, in Helsinki.

The SU-8 samples were taped to metallic MALDI plate with conductive tape, after which the MALDI-matrix solution was pipetted in a volume of 1 µl on top of the samples. The solution consisted of a saturated solution of 3,5-dimethoxy-4-hydroxycinnamic acid also known as sinapinic acid which is commonly used with peptides, proteins and glycoproteins. The solvent was 40 % acetonitrile (ACN) and 0.1 % trifluoroasetic acid (TFA). Before loading the MALDI-base in the mass spectrometer equipment, the droplets were allowed to dry in a normal RT for about 10 min. Samples were shot 3000 times in a series of 250 shots. The results were therefore represented as sum spectra of 3000 shots. For comparison the standard spectra of pure samples of α-MPA F5 Fab and MPA-AP were also measured.

6.8 Immunochip – studies

The purpose of the immobilization parameter studies made with planar surfaces was to find out an optimal immobilization procedure for the immunochip design. In addition to immobilization parameters, the proper functioning of the chip structure requires the proper conditions in terms of contact angle, layer thickness and the distance between consecutive triangle rows.

6.8.1 Contact angle measurements

The contact angle between immunochip surface and α-MPA Fab F5 in PBS was measured by goniometer (KSV Cam 100). The antibody solution was placed onto SU-8 surface with volume of 1 µl and the contact angle was measured optically. Every contact angle was measured from three different spots and the results were reported as a mean value of these separate spots. In addition to standard contact angle measurements, measurements where done with decimal dilution series of PBST solution (0,05% Tween in PBS, Tween20®) and aforementioned solution mixed with α-MPA Fab F5 (20 µl in 100 µl PBST). Also the effect

of using different dilutions of PBST-solution in random immobilization as a buffer solution was studied. The immobilization was done as mentioned in chapter 6.5.1. Control sample was random immobilization with 1x PBS solution.

6.8.2 Directed capillary flow studies

The correct flow of the antibody solution in the immunochip structure was studied by flow tests. Immunochips were fabricated according to chapter 6.1.3 with all the mentioned thicknesses and triangle row distances. The surface contact angles (30° and 40°) and the RIE-treatment conditions (time: 5 s, power: 100, pressure: 150), which enabled the correct flow profile, were chosen according to our earlier research [37]. The adjustment of the contact angles was done by double RIE-treatment from which the first treatment was done immediately after finishing the SU-8 processing and the second after one or two days of cleanroom storing.

Flow studies were executed by manually pipetting a droplet of 1 µl in volume of α-MPA Fab F5 solution (2.1 mg/ml) or water to the middle inlet. Solution was allowed to flow freely from the inlet. Experiments were done in RT. Figure 30 presents the starting point of the flow studies.

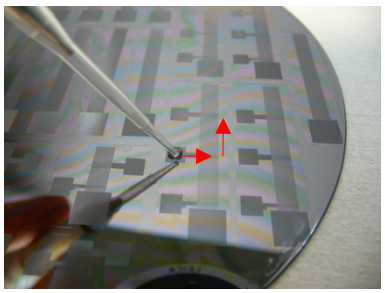

Figure 30. Directed capillary flow study on immunochip. The desired flow pattern is marked with red arrows.

6.8.3 Antibody immobilization on immunochip

The immobilization of α-MPA Fab F5 in PBS onto immunochip was studied with random immobilization. Compared to the immobilization principle presented in the chapter 6.5, the amounts of used reagents were scaled to correspond to the size of the chip structure. Because detection was done with fluorescence microscope (the substrate reaction is not sensitive enough), a fluorescence labeled MPA-AP antigen was used. Based on earlier studies [30], Alexa 647 –label was chosen. The used immobilization parameters are presented in the table 9.

Table 9. The random immobilization parameters in immunochip studies.

IMMOBILIZATION STEPS	INCUBATION TIME	AMOUNT
α-MPA Fab F5 in PBS	o/n	5 µl
Blocking with 1% BSA	1 h	3 ml
Alexa 647 -labeled MPA-AP	1 h	1 µl

7 Results and discussion

7.1 ATIR-FTIR -measurements of SU-8

ATIR-FTIR -measurement was applied to prove the existence of free epoxy groups as both random and oriented immobilizations developed here occur via the free epoxy groups on SU-8 surface. The spectrum of SU-8 surface, which was fabricated with the standard parameters (sample1), is presented in figure 31 (relevant peaks marked with functional groups). The spectra of the other samples (sample2 to sample5) and explanations of the relevant peaks in the spectra are presented in appendix A. The calculated values of the different samples (sample1 to sample5) are collected to table 10.

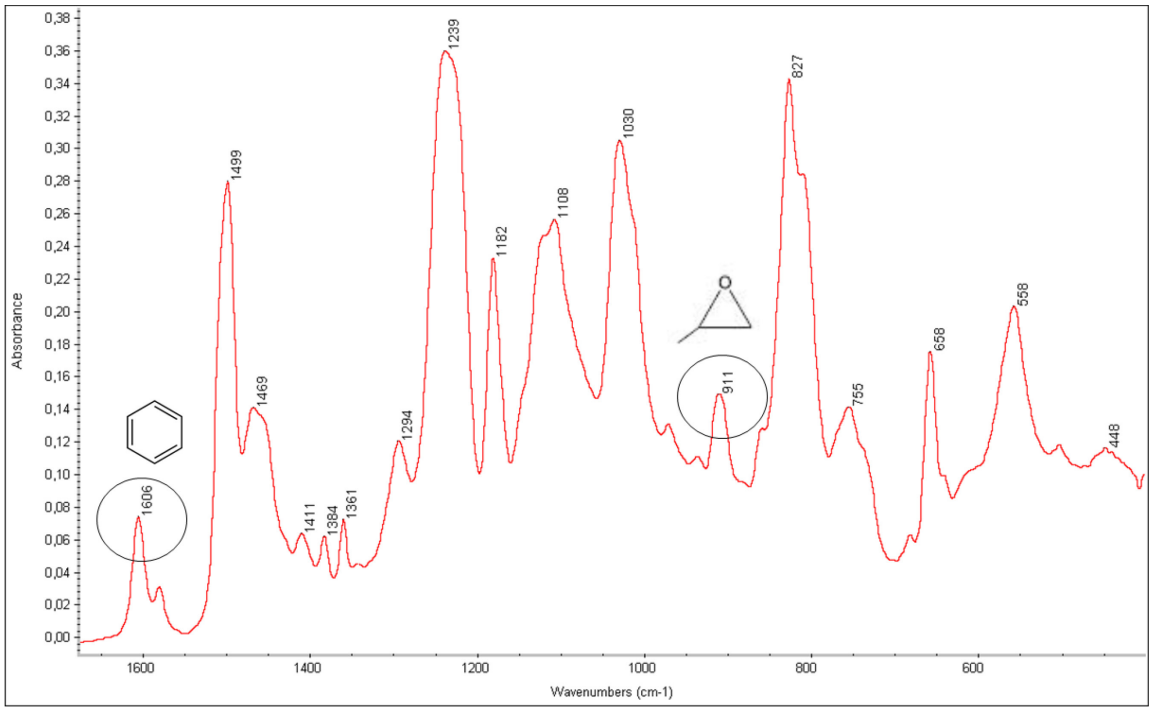

Figure 31. ATIR-FTIR spectrum of standard SU-8 surface (sample1: 5 s exposure and 8 min PEB). The peak close to 914 cm^{-1} denotes epoxy group and the peak around 1608 cm^{-1} benzene ring, respectively.

Table 10. Number of free epoxy groups per SU-8 monomer.

SAMPLE (exposure + PEB time)	PEAK HEIGHT AT 914 cm-1	PEAK HEIGHT AT 1608 cm-1	RATIO (I)	NUMBER OF FREE EPOXY GROUPS PER SU-8 MONOMER
SAMPLE1 (5s + 8 min)	8	11	0,73	1,5
SAMPLE2 (2.5s + 8min)	8	4	2,0	4
SAMPLE3 (20s + 8min)	4,5	6	0,75	1,5
SAMPLE4 (5s + 4min)	8	10	0,8	1,6
SAMPLE5 (5s + 20min)	6	6	1,0	2

ATIR-FTIR -results with the different exposure times (sample1: 5 s; sample2: 2.5 s; sample3: 20 s) were in accordance with the previous study [30]. The results indicate the shorter exposure time leaves greater amount of free epoxy groups onto SU-8 surface. Also the results obtained with the different PEB times (sample1: 8 min, sample4: 4 min, sample5: 20 min) were logical. The somewhat higher PEB time as was with sample5 is not long enough to eliminate the epoxy groups from the SU-8 surface. According to the previous study [30], the PEB time should have been around 2 h and the baking temperature close to 150ºC in order to PEB to eliminate the epoxy groups from the SU-8. As can be seen from the spectra (figure 31 and appendix A), all of our samples still have the peak for epoxy group, indicating all of them could serve as a reactive site for the covalent attachment of different molecules, e.g. antibodies.

7.2 System-setup study results

Three different approaches for immobilization step were evaluated before starting the actual study: PDMS stamp, immersion of the SU-8 sample to the protein solution and the droplet-based immobilization. The PDMS stamp was rejected due to weak adhesion between PDMS and SU-8. The weak adhesion allows the reagents to leak outside the defined area. This could lead to ineffective blocking or antibody / antigen immobilization, which would have been shown as a false positive result. PDMS is also known to have tendency to absorb proteins [78]. The amount of absorbed protein to stamp material is difficult to determine.

Also the immersion approach was rejected as it consumed high amounts of expensive reagents. The effective immersion demands at least 2 ml of reagent, which is 20 times higher

consumption compared to the droplet-based approach, where only 100 µl is needed. In addition, the immersion requires equal sized SU-8 pieces to have comparable immobilization area between parallel samples. Referring to the reasons explained above, the droplet-based approach was chosen for this preliminary immobilization study.

7.3 Immobilization tests

7.3.1 Incubation time

As can be concluded by the nature of oriented immobilization, it should not be or be only minimally affected by the diminishing incubation time. The results presented in figures 32-34 (four separate studies) confirm this trend. The IDA-Co chelation system has high affinity enough for His6-tagged Fab molecules to make the immobilization occur almost instantly after the contact with the antibody solution. The response in 10 min incubations was on average 0.82 ± 0.15 (mean and standard deviation from all of the studies) and in o/n incubations 0.86 ± 0.13, respectively. The responses in 10 min and o/n incubations did not differ either within (first study: t2 = -1.6, P = 0.243, second study: t2 = -0.3, P = 0.778, third study: t2 = 0.5, P = 0.674 and fourth study: t3 = 0.2, P = 0.881) or between the studies (t5 = -0.6, P = 0.567). T-test syntax and an example of the result output are presented in appendix B.

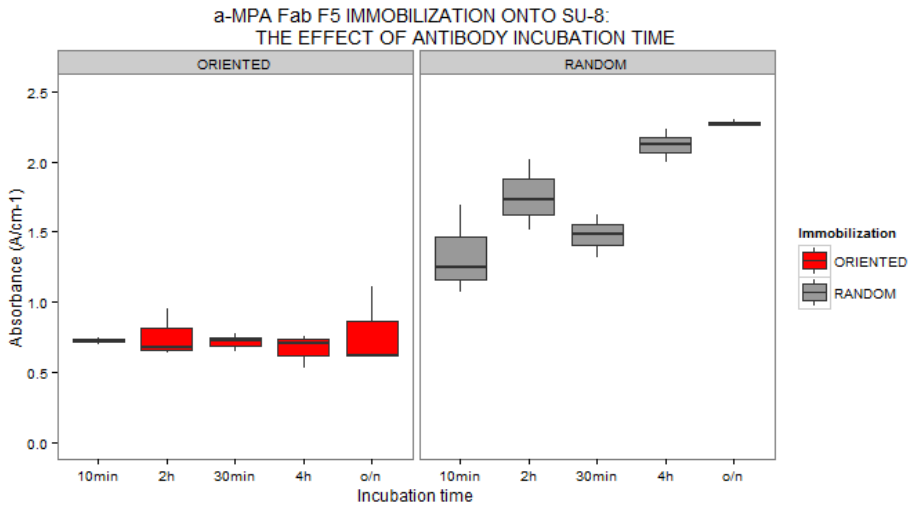

Figure 32. Decrease in incubation time had effect only on the immobilization efficiency in random immobilization. Boxplot: the edges of the box are upper and lower quartiles, whiskers are minimum and maximum values and the median is a line inside the box. (SU-8 pieces from different wafers).

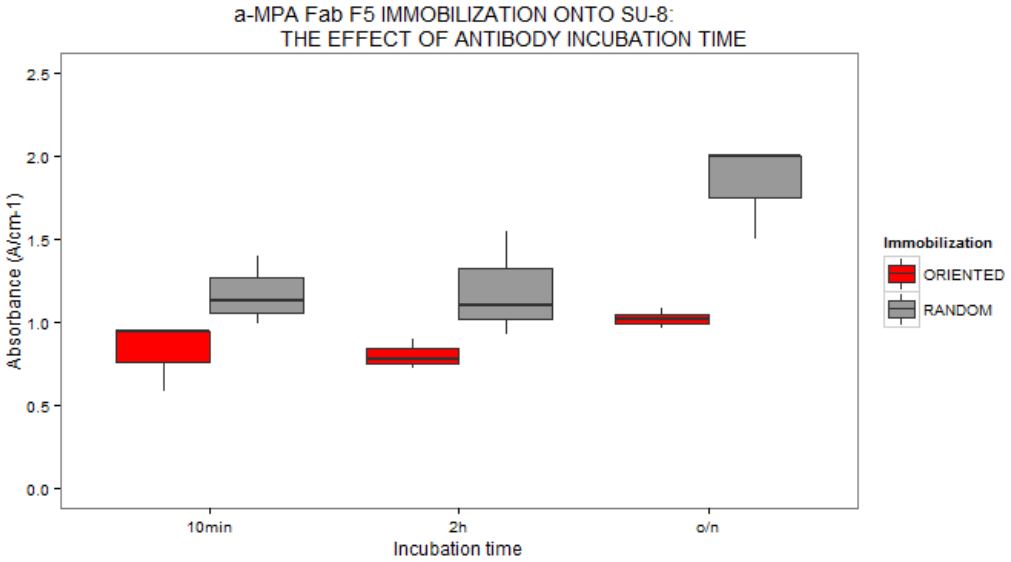

Figure 33. Immobilization efficiency in the random immobilization differed significantly between the longest and shortest incubation times whereas there was no difference in the oriented immobilization. (SU-8 pieces from the same wafer).

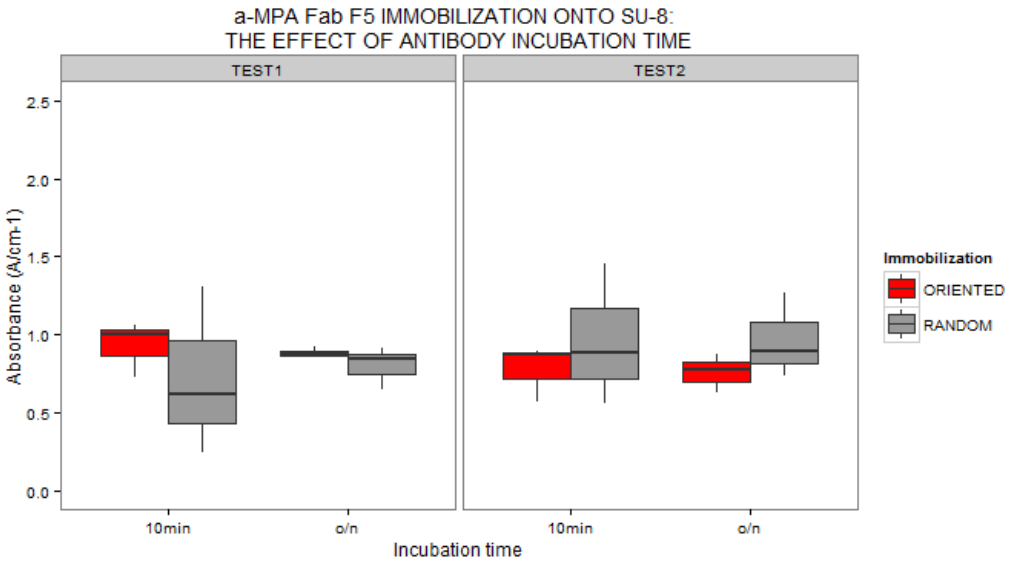

Figure 34. Repeated comparison tests between 10 min and o/n incubations in oriented immobilization were in line with the previous results. Instead in the random immobilization the 10 min incubation time should have given substantially lower responses compared to the o/n incubation. (SU-8 pieces from the same wafer).

In the first and second random immobilization studies (figures 32 and 33, respectively), the immobilization efficiency decreased by almost 40 %, when 10 min and o/n incubations were compared. In the first study, 10 min incubation response was 1.33 ± 0.30 and o/n response 2.27 ± 0.03, respectively. Similarly in the second study, the response in 10 min incubation was 1.17 ± 0.21 and in o/n 1.84 ± 0.29, respectively. In both studies, the difference between 10 min and o/n incubations was significant (first study: t2 = -5.1, P = 0.036, second study: t4 = -3.2, P = 0.038). However, in the last study set, where only 10 min and o/n incubations were compared to each other repeatedly (figure 34), no significant difference was observed. The response in the first repetition study for 10 min incubation was 0.72 ± 0.54 and for o/n 0.80 ± 0.13, respectively. Similarly in the second repeated study, the response in 10 min incubation was 0.97 ± 0.45 and in o/n 0.97 ± 0.27, respectively. Moreover, the variation in the responses in random immobilization both between and within the different studies was considerable. Variation was especially high within the 10 min incubations. Furthermore, the responses in 10 min incubations were surprisingly high in random immobilization.

7.3.2 Amount of antigen

The minimum usable concentration of antigen was determined by diluting the originally used antigen / TBS solution (c = 0.025 mg/ml). The first study set (figure 35) was made with dilutions 1:1, 1:10 and 1:100 and the second set (figure 36) with dilutions 1:1, 1:2, 1:5, 1:10 and 1:20. As can be seen from the figure 35, the chosen dilutions in the first set were too dilute and only low responses were obtained. Also with the second set similar characteristics were seen. There was a notable change in the slope of the dilution series curve already with dilution 1:2. Therefore, regarding the preliminary testing phase, the antigen concentration should not be changed from 0.025 mg/ml.

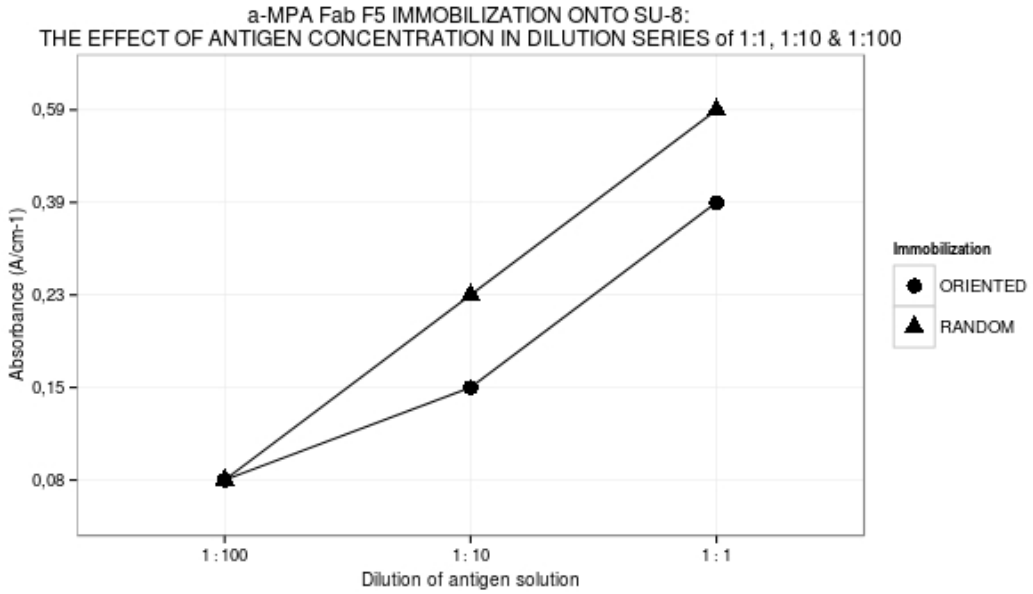

Figure 35. First dilution series offered a too fast decrease in the immobilization efficiency. (SU-8 pieces from the same wafer).

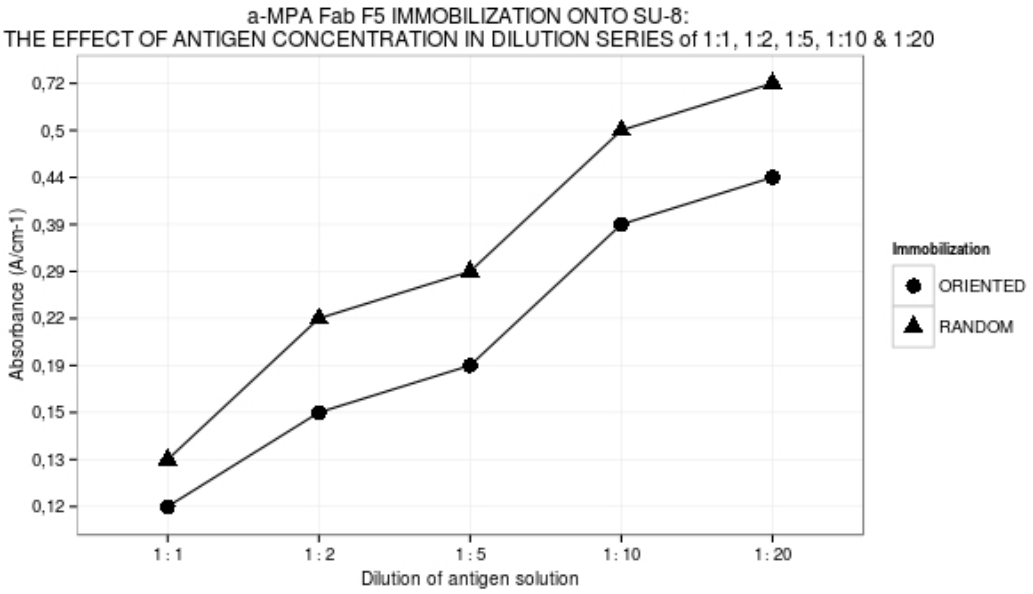

Figure 36. Already dilution 1:2 caused a notable change in the slope of dilution curve. (SU-8 pieces from the same wafer).

7.3.3 Serum vs buffer

Serum is a biological liquid, which contains lots of different molecules, like electrolytes and proteins, which can interfere the random immobilization whereas the oriented immobilization as a high affinity reaction should not be disturbed by the serum molecules. As can be seen from figure 37, the results in both immobilizations were as expected. In oriented immobilization, the response in buffer incubation was 0.68 ± 0.09 and in serum 0.60 ± 0.25, respectively, and no statistically significant difference was observed ($t2 = 0.5$, $P = 0.655$). In contrast, in random immobilization, the response within the serum incubation was almost 50 % smaller compared to the buffer incubation response (buffer: 1.10 ± 0.18, serum: 0.59 ± 0.10) causing statistically significant difference ($t3 = 4.4$, $P = 0.019$).

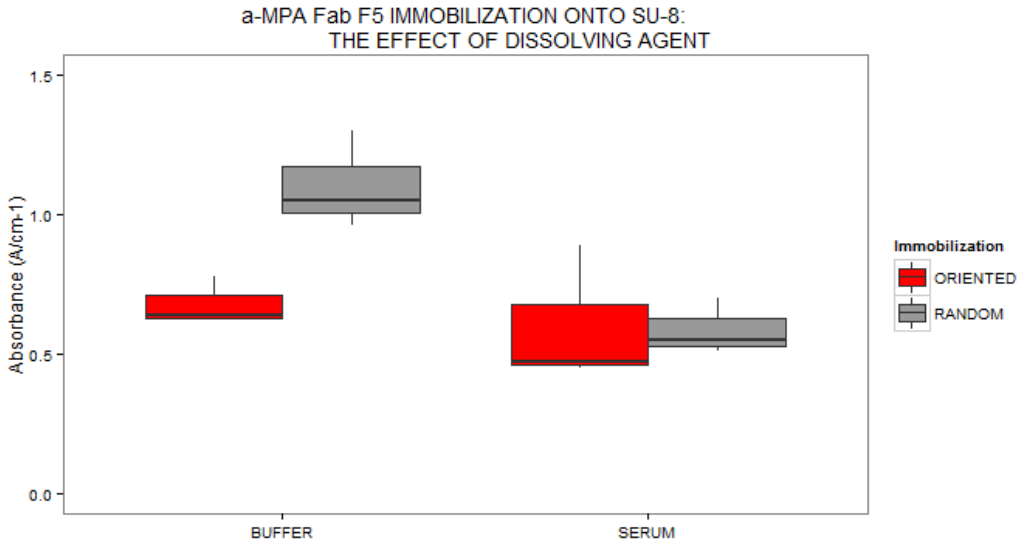

Figure 37. Choice of dissolving agent had significant effect on the random immobilization whereas the oriented immobilization was not affected. (SU-8 pieces from the same wafer).

In order to confirm the result, the buffer and serum immobilization study was repeated by applying 10 min and o/n antibody incubation times (study conducted twice). Again, the oriented immobilization should not be affected whereas the random immobilization should give lower responses in serum immobilization and when using shorter incubation time. As can be seen from the figure 38, the previously obtained result from the oriented immobilization was able to be repeated. In the first study, the responses in oriented immobilization did not differ either in 10 min (buffer: 0.93 ± 0.18 and serum 0.66 ± 0.28; $t3 = 1.4$, $P = 0.243$) or in o/n incubations

(buffer 0.88 ± 0.04 and serum 0.83 ± 0.02; t2 = 2.4, P = 0.109). A similar result was observed from the second study (10 min incubation in buffer: 0.78 ± 0.18 and in serum: 0.66 ± 0.28; t3 = 0.6, P = 0.576; o/n incubation in buffer: 0.76 ± 0.12 and in serum: 0.83 ± 0.02; t2 = -1.0, P = 0.421). These results suggest that the choice of dissolving agent do not have an effect on the oriented immobilization even though the incubation time is diminished from o/n to 10 min.

On contrary, in random immobilization, the combined study of incubation time and the choice of buffer did not confirm the previously obtained result. According to figure 38 (right panel, test2), it seems, that the shorter incubation time and serum as a dissolving agent would be more efficient compared to the o/n incubation and buffer as a dissolving agent. The result is not logical and more studies are needed. In the first study (test1), the response in 10 min incubation in buffer was 0.72 ± 0.54 and in serum 0.48 ± 0.16. The response in o/n incubation in buffer was 0.80 ± 0.13 and in serum: 0.73 ± 0.04. Similarly in the second study (test2), the response in 10 min incubation in buffer was 0.97 ± 0.46 and in serum 1.03 ± 0.21. The response in o/n incubation in buffer was 0.97 ± 0.27 and in serum: 0.63 ± 0.16. In both studies, the difference between buffer and serum was not statistically significant (first study (test1): 10 min incubation t2 = 0.8, P = 0.518 and o/n incubation t2 = 0.9, P = 0.466; second study (test2): 10 min incubation t2 = -0.2, P = 0.851 and o/n incubation t3 = 1.8, P = 0.160).

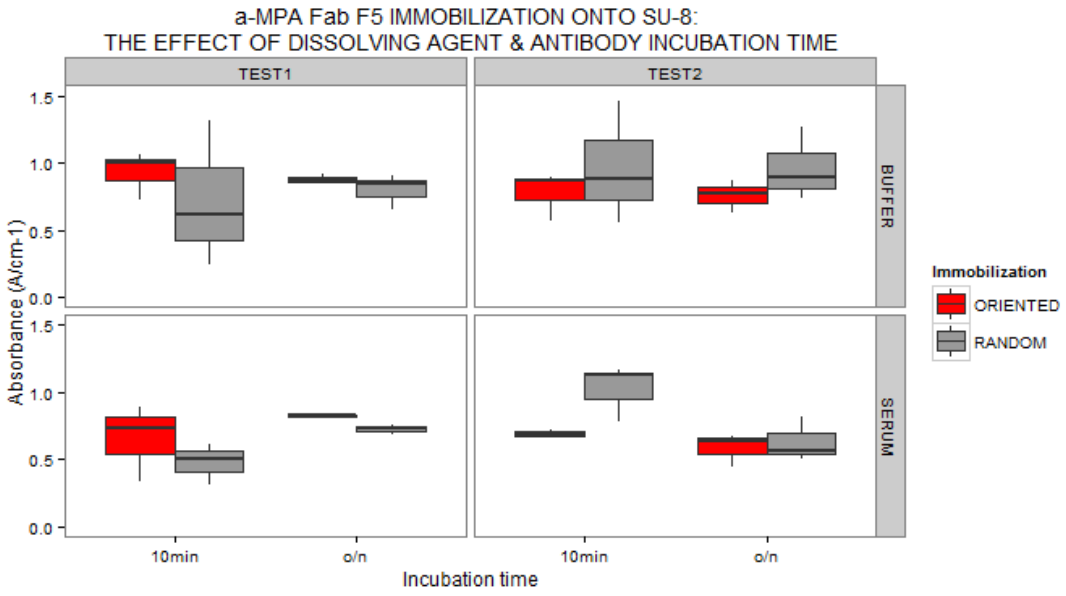

Figure 38. Decrease in incubation time or the choice of the dissolving agent did not have an effect on the oriented immobilization whereas the results obtained with the random immobilization were not logical as the serum and shorter incubation time seemed to give better responses. (Both between and within the studies: SU-8 pieces from the same wafer).

7.3.4 The effect of pH

The effect of immobilization pH was studied as the random immobilization was executed in a lower pH than oriented immobilization. The IDA-Co –treatment in oriented immobilization increased the surface pH to near 8.50 whereas the pH in random immobilization was the physiological pH (PBS as the immobilization buffer). The results shown in figure 39 indicate that the buffer pH had only a minimal effect on the immobilization responses in random immobilization (pH 7.24: 0.69 ± 0.12, pH 8.05: 0.72 ± 0.15 and pH 9.93: 0.71 ± 0.14). The results in oriented and random immobilizations are therefore comparable at least by the immobilization pH.

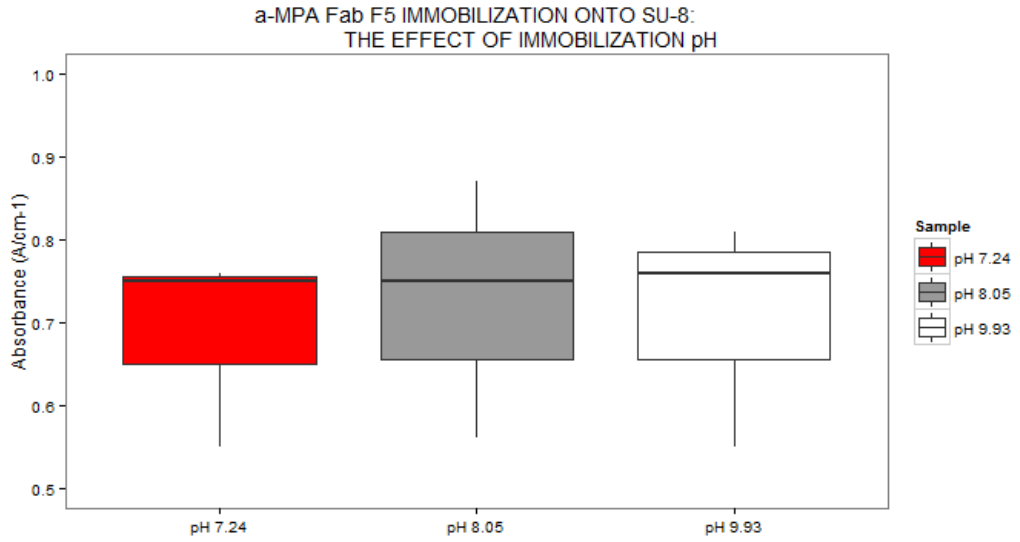

Figure 39. Buffer pH did not have an effect on the immobilization efficiency in random immobilization.

7.3.5 Surface modification: nanostructuring and plasma oxidation

The oxygen plasma treatment of the immobilization substrate by RIE is known to increase the immobilization efficiency due to higher surface roughness and activation of functional groups [22]. Similar tendency is presupposed to happen with SU-8 surface. Figure 40 presents the results.

In the oriented immobilization, the response in 5 s RIE-treatment was 1.0 ± 0.06, in 60 s RIE 0.84 ± 0.23 and in control sample 0.67 ± 0.35, respectively. The difference between 5 s RIE-

treatment and control sample was not significant (t1 = 1.3, P = 0.413), however, this is mainly explained by the high variation between the separate samples in the control group (absorbance in separate samples were 0.92 and 0.42). In random immobilization, the response in 5 s RIE-treatment was 1.48 ± 0.10, in 60 s RIE 1.4 ± 0.06 and in control sample 0.88 ± 0.07, respectively. The 5 s RIE-treated surface gave almost 45 % higher response compared to the surface where no modification was applied. This yielded a significant difference (t1 = 7.0, P = 0.026). In both immobilizations, the longer RIE-treatment did not improve the immobilization efficiency, but instead decreased the responses. Thereby a shorter treatment time should be used. When considering these results, it needs to be remembered that the effective immobilization area was not similar between RIE-treated and control samples as the RIE-treatment lowers the contact angle. Therefore the droplet spread to a larger surface area within the RIE-treated samples.

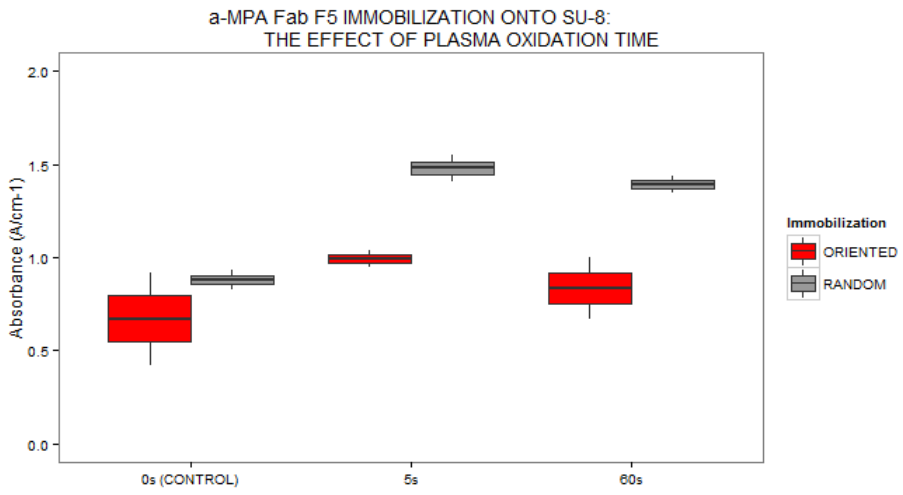

Figure 40. Plasma oxidation treatment improved the immobilization efficiency in both the random and oriented immobilizations, even though the difference was significant only in the random immobilization. The shorter treatment time of 5 s influenced the results more. (RIE denotes reactive ion etching; SU-8 pieces from the same wafer).

The result from the nanostructure modification study is shown in figure 41. As could be expected, the higher surface area offered more immobilization sites and therefore more efficient immobilization in both immobilizations. The response in oriented immobilization for nanostructured SU-8 surface was 0.97 ± 0.13 and for planar surface 0.39 ± 0.06, respectively.

Similarly in random immobilization the result for nanostructured SU-8 surface was 1.34 ± 0.04 and for planar surface 0.73 ± 0.32, respectively. The immobilization with nanostructured SU-8 was 59 % higher in oriented and 45 % in random immobilization compared to the planar SU-8. The difference was significant in both immobilizations (oriented immobilization: t2 = 7.2, P = 0.007, random immobilization: t2 = 3.2, P = 0.082).

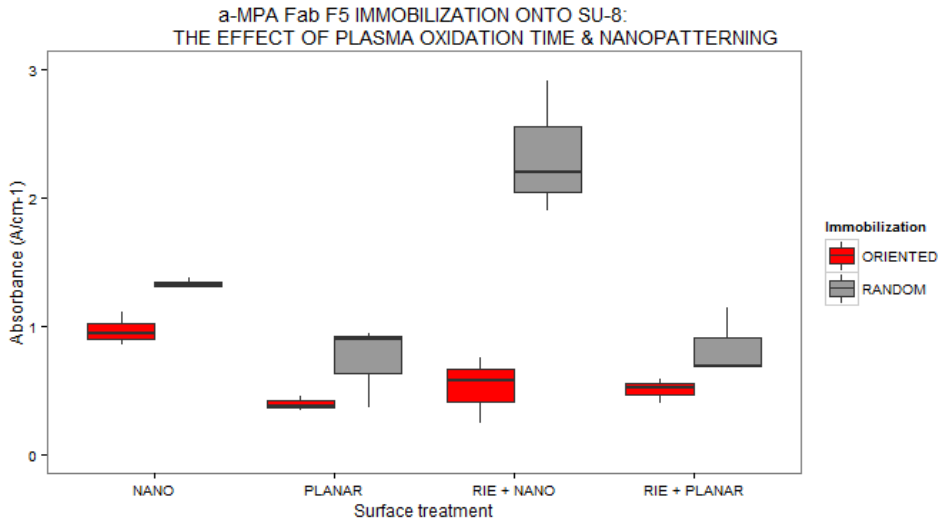

Figure 41. Surface modification either through plasma oxidation or nanostructuring caused improvements in the immobilization efficiency, but only in nanostructuring, in both immobilizations and in plasma oxidation, in random immobilization the differences were significant compared to their controls. (SU-8 pieces from the same wafer).

To obtain similar efficient immobilization area in both the nanostructured and the planar surfaces, an additional RIE-treatment was applied. The hydrophobicity of the SU-8 surface is higher within the nanostructured SU-8 surface compared to the planar SU-8. Therefore, the droplet spreads to a much smaller area within the nanostructured surface compared to the planar surface. Results from this study are presented in figure 41.

In oriented immobilization, the response in nanostructured and RIE-treated incubation was 0.52 ± 0.26 and in simple RIE-treated 0.50 ± 0.10, which did not give a significant difference between results (t2 = 0.1, P = 0.910). In contrast, in random immobilization the response within the combined surface modification incubation was almost 64 % higher compared to the sample without nanostructures (nanostructured and RIE-treated: 2.34 ± 0.52, simple RIE-treated: 0.84 ±

0.26) causing statistically significant difference (t3 = 4.4, P = 0.022). Surprisingly, the difference between planar SU-8 and simple RIE-treated SU-8, was not observed in neither of the immobilizations (in oriented immobilization in planar: 0.39 ± 0.06 and in RIE-treated: 0.50 ± 0.10 and in random immobilization in planar: 0.73 ± 0.32 and RIE-treated: 0.84 ± 0.26). This is not in line with the above presented results for RIE-treatment.

7.3.6 Storage stability of immobilized antibody

The results from the one week storage stability study indicate that the efficiency of the antibody is preserved regardless of the storing conditions (wet or dry, figure 42). Storing in dry conditions reduced the responses only by 7 % in oriented and by 17 % in random immobilization compared to the wet conditions (in oriented immobilization, dry condition: 0.60 ± 0.13 and wet condition: 0.56 ± 0.17 and in random immobilization, dry condition: 0.67 ± 0.12 and wet condition: 0.81 ± 0.09). The difference was not significant in either of the immobilizations (in oriented immobilization: t3 = 0.3, P = 0.799 and in random immobilization: t3 = -1.6, P = 0.181). Thus, the efficiency of immobilized antibody is maintained in dry conditions at least when storing is within the one week period. The results from the o/n storing study (dry and wet conditions) were excluded from this thesis due to technical difficulties in maintaining the dry conditions. The wet paper was forgotten to be taken away from the lid of the microtiter plate.

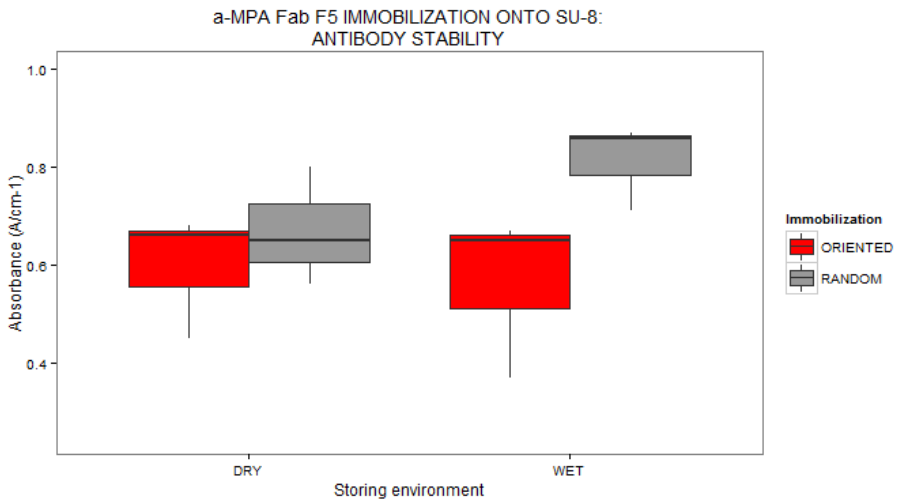

Figure 42. Immobilized antibody maintained its efficiency both in wet and dry storing conditions when one week storing was applied. (SU-8 pieces from the same wafer).

7.3.7 Storage stability of SU-8

In order to find out whether or not the SU-8 surface is able to maintain its storage stability after fabrication and thereby the immobilization efficiency, if no surface treatments are applied and the storing is made in a normal cleanroom conditions, two sets of storage stability studies were executed. The first set included 1 and 2 weeks, and the second set 3 and 4 weeks storing times in addition of a freshly fabricated control surface. The results from SU-8 stability studies are presented in figure 43.

In oriented immobilization, the response in 1 week storing was 0.78 ± 0.02, in 2 weeks 0.58 ± 0.18 and in control sample 0.67 ± 0.36, respectively. Similarly, the response in 3 weeks storing was 0.99 ± 0.27, in 4 weeks 0.78 ± 0.06 and in their control sample 0.75 ± 0.04, respectively. Neither of the storing times differed significantly from their control samples (in 1 and 2 week study, 1 week storing time: t1 = -0.4, P = 0.738 and 2 weeks storing time: t1 = 0.3, P = 0.783; in 3 and 4 week study, 3 weeks storing time: t1 = -1.3 , P = 0.418 and 4 weeks storing time: t1 = -0.7 , P =0.584).

In random immobilization, the response in 1 week storing was 1.43 ± 0.23, in 2 weeks 1.39 ± 0.48 and in control sample 0.88 ± 0.07, respectively. Similarly, the response in 3 weeks storing was 1.02 ± 0.26, in 4 weeks 1.44 ± 0.10 and in their control sample 1.28 ± 0.17, respectively. As was with oriented immobilization, also in random immobilization the different storing times did not give significant difference compared to their control samples (in 1 and 2 week study, 1 week storing time: t1 = -3.2, P = 0.164 and 2 weeks storing time: t1 = -1.5, P = 0.369; in 3 and 4 week study, 3 weeks storing time: t1 = 1.2, P = 0.375 and 4 weeks storing time: t1 = -1.2, P = 0.371).

Even though no statistical significance was observed between the different storing times, the slight variation in the mean values of the results would suggest that the immobilization studies at this preliminary stage should only be done onto the freshly fabricated SU-8 surface in order to be sure the difference in results is caused by the parameter under observation and not by the SU-8 surface.

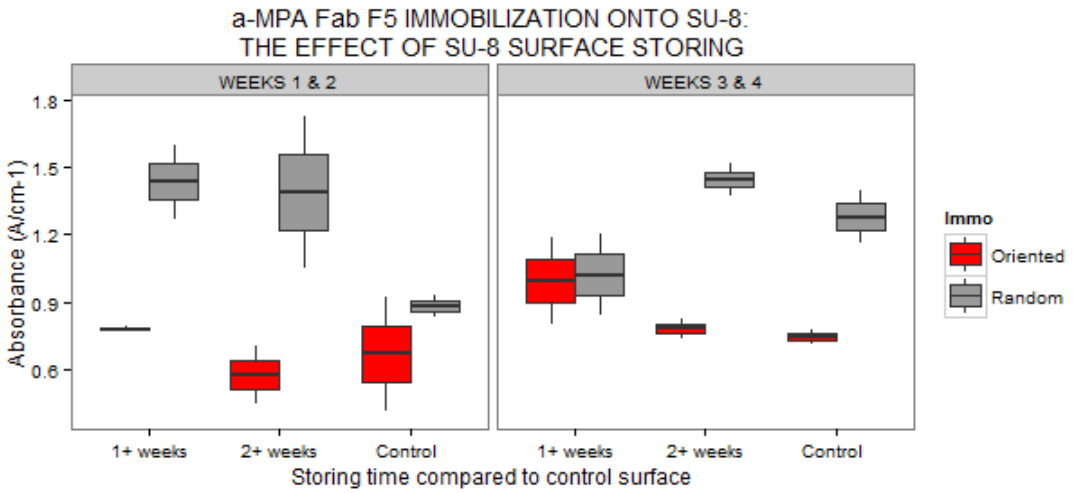

Figure 43. Storing of SU-8 surface did not cause a significant difference between the immobilization results at least during four weeks period. (Within the study: SU-8 pieces from the same wafer and between the studies: SU-8 pieces from different wafers).

7.4 Comparison of random and oriented immobilizations

A total of 13 comparison studies of random and oriented immobilization studies were included in this thesis. The immobilizations were compared if the SU-8 pieces were from the same wafer and all the reagents were made at the same time. In 84.6 % of comparison studies, random immobilization gave higher responses compared to the oriented immobilization. Interestingly, in 53.8 % of those, the random immobilization was over 30 % better than the oriented immobilization. The result is quite unexpected as the random, covalent immobilization is affected by many more variables compared to the oriented immobilization. Results are presented in appendix C.

However, during the oriented immobilization studies, IDA solution was not prepared for purpose but beforehand to speed up the testing. A comparison test of fresh and aged (72 days old) IDA solution showed that there is a clear impact on the immobilization efficiency as the old solution gave almost 40 % smaller responses compared to the fresh solution. The average response for the fresh IDA solution was 0.79 ± 0.18 and for the old IDA solution 0.48 ± 0.09, respectively. Due to this difference, a correction factor was calculated for all of the studies were old IDA solution was used. The correction coefficient was calculated according to equation (14)

$$d = \frac{\frac{1\text{-}MEAN_{old}}{MEAN_{new}}}{72} = 0{,}0054 \quad (14)$$

where $MEAN_{old}$ was the mean value for the old IDA solution and $MEAN_{new}$ for the new IDA solution. As the obsolescence process can be considered to be a linear process, the correction coefficient was multiplied by the number of days the IDA solution was older than the freshly made (therefore a maximum value for multiplying is 72). Despite the correction, only in one case the situation changed in favor of the oriented immobilization (results not shown).

Secondly, the proper functioning of IDA-cobalt chelation system was tested. If the chelation does not take place, all the oriented immobilizations on SU-8 surface would be random immobilizations. To verify the proper functioning, a study with an additional blocking step was conducted. In oriented immobilization, the additional blocking step was made after the cobalt incubation and in random immobilization before the antibody incubation. In oriented immobilization, this excess blocking step should not have any effect on the responses whereas in random immobilization a notable decrease should take place, because there is no functional group for the antibody to couple with. Control samples were normal oriented and random immobilizations described in the chapter 6.5 and samples with excess BSA-blocking, but with wrong antigen (AP).

As can be seen from figure 44, the excess blocking step does not have an effect on the response obtained in the oriented immobilization (normal oriented immobilization: 0.58 ± 0.05, immobilization with two BSA-blockings: 0.54 ± 0.05), which indicates that the IDA-cobalt chelation system is working correctly. On contrary, in random immobilization, there is a 55 % decrease in immobilization efficiency if the excess blocking step takes place (normal random immobilization: 1.59 ± 0.11, immobilization with two BSA-blockings: 0.72 ± 0.14). In both immobilizations, the negative controls are working correctly and have only background absorbance from the SU-8 surface (oriented immobilization: 0.08 ± 0.00, random immobilization: 0.09 ± 0.00). Therefore, neither of the two potential reasons presented here explains the superiority of the random immobilization.

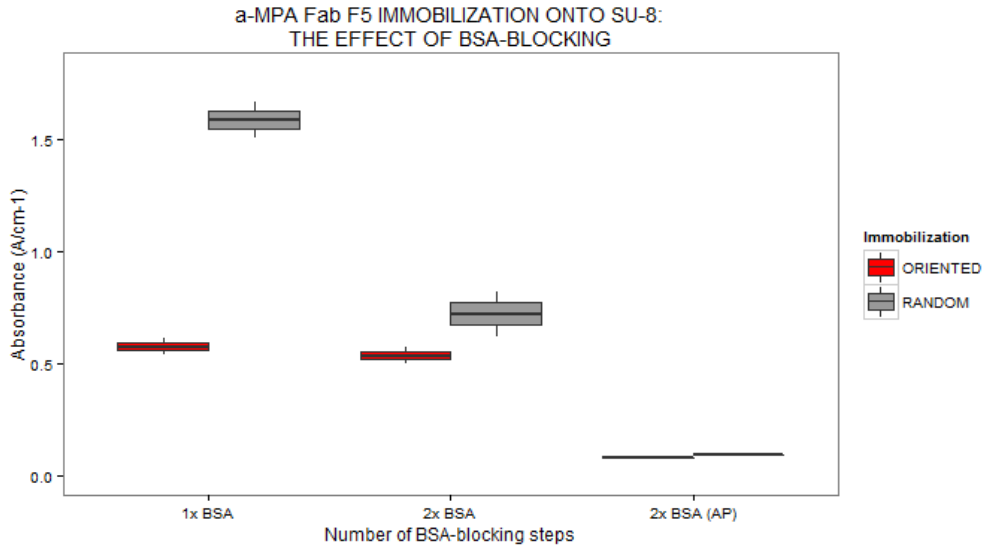

Figure 44. Number of BSA blocking steps had effect only on random immobilization, which suggests both the blocking and IDA-Co chelation steps are working correctly within the immobilizations presented in this thesis.

In addition to comparing the responses obtained from the different studies, the immobilization methods were also compared in terms of remaining antibody –antigen complex stability after o/n TBS-treatment. The few conducted studies are presented in appendix D. According to the results, it seems, the o/n TBS treatment has equally impaired the antibody-antigen stability in both immobilizations when a new substrate was placed. In random immobilization, only on average 39.7 % of the obtained absorbance was remained after o/n TBS treatment. In oriented immobilization, the same was 37.2 %, respectively. Addition of a new antigen followed by a new substrate did not improve the responses. The incubated antigen did not have free sites for binding. These results suggest that the interaction of the chosen antibody-antigen model system has not high affinity enough for the immobilization studies. This could also be explanation to some of the unexpected results obtained in the immobilization parameter studies. The appendix D also presents results from the two studies where only random immobilization was studied in terms of remaining antibody-antigen complex stability. The obtained results were in line with the comparison study results presented above.

7.5 MALDI-measurements

The MALDI-measurement spectra for planar and nanostructured SU-8 are presented in appendix E (a selection of successful experiments). Despite the efforts antigen detection on planar surfaces was not possible. This is not explained by the failure in antibody immobilization as a control sample (detection with substrate) gave a response (detection by eye). One potential explanation for the failure is the inadequate immobilization density in the planar surfaces for MALDI. This fact is supported by the better results obtained with the nanostructured surfaces both in random and oriented immobilizations.

A total of five MALDI-experiments were done, from which two times only planar surfaces were experimented. During those two times, no signal was observed. Nanostructured surfaces were studied three times (two times random and once the oriented immobilization surfaces), from which two studies gave responses (shown in appendix E). These preliminary studies showed that the choice of immobilization method did not have an influence on the result. The most interpretable results were obtained when the surface was treated both with nanostructures and oxygen plasma.

As can be seen from the spectra (appendix E), the peaks with SU-8 base are a bit shifted to the right compared to the spectra of the pure samples. This shifting might be caused by the higher position of the SU-8 surface compared to the actual metallic MALDI-base (SU-8 piece is glued to the MALDI-base). Another notable fact is that the peaks of α-MPA Fab F5 and MPA-AP are very close to each other in the spectra. Some kind of inner calibration should be done before the measurement, to be sure which one of them (antibody or antigen) causes the peak in MALDI-spectrum. One solution could be to use another antigen, like MPA- human serum albumin (HSA), which has a clear difference compared to the spectrum of α-MPA Fab F5. But its spectrum resembles closely the spectrum of the applied blocking agent BSA, which would again lead to the misinterpretation of the peaks. Therefore, at least at this point, the sensitivity of MALDI is not enough to verify the suitability of the SU-8 as a MALDI-base. Careful testing and potential change in the immobilization procedure (e.g. in terms of antibody, antigen, blocking agent etc.) have to be considered.

7.6 Immunochip

7.6.1 Contact angle tests

Capillary-driven flow is enabled if the contact angle between SU-8 surface and the solution is near 40° as stated in our own study [37]. The measured contact angle between freshly fabricated SU-8 surface and α-MPA Fab F5 in PBS solution was around 75° (dashed line in figure 48). Thus, no capillary-driven flow is possible to be obtained in channel structures (figure 26), if no modification is done to the setup. A known solution would have been to choose the oxygen plasma treatment, because it makes the SU-8 surface more hydrophilic [80]. However, the fast hydrophobic recovery, discussed in chapter 3.4.2, makes it not an optimal choice. Therefore, other methods to decrease the contact angle between SU-8 and the antibody solution were tried to find.

Tween, a well-known surfactant, was mixed to PBS and the contact angle of this PBST solution in different dilutions measured with SU-8 surface. The change in contact angle is presented in figure 45. The contact angle between pure PBS and SU-8 is shown as a dashed line. The contact angle was measured four times in a 2 min period from the same droplet. As the results show, the contact angle decreased significantly with the original PBST solution and its first dilution. The decrease in contact angle with these solutions would offer sufficient conditions for the capillary-driven flow. The same PBST solution in different dilutions were placed in 50 µl droplets on SU-8 surface and photographed after 10 min incubation (figure 46).

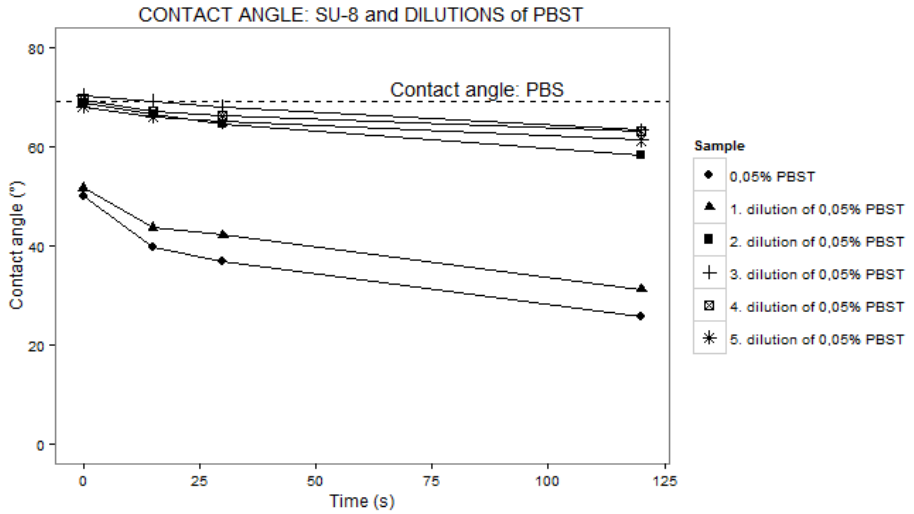

Figure 45. Change in contact angle during a 2 min period between different dilutions of PBST and SU-8 surface. The dashed line indicates the contact angle between PBS and SU-8.

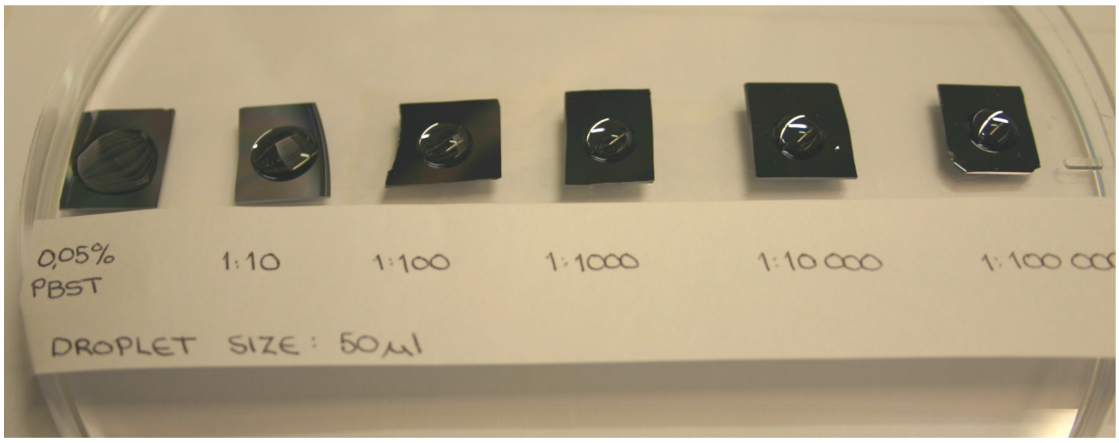

Figure 46. Different dilutions of PBST solution on SU-8 surface after 10 min incubation.

Next, the same dilutions of PBST were fabricated, but this time also antibody was included to the solution and the contact angle measured with SU-8 surface. On basis of the first contact angle study (figure 45), the fourth and fifth dilutions of PBST were excluded due to incapability to lower the contact angle. The change in contact angle is presented in figure 47. The contact angle between SU-8 and α-MPA Fab F5 in PBS solution is shown as a violet dashed line. The study showed that the only solution capable to produce the correct angle was the original PBST solution (0.05% PBST + F5). Even though the adjustment of the contact angle was correct with the original PBST solution, the use of it was prevented due to significant drop in the immobilization responses as shown in figure 48. The responses with both the original PBST-solution and its first dilution were 51 % and 45 % lower, respectively, compared to the control sample, which included antibody in normal PBS (PBST: 0.54 ± 0.05, 1. dilution of PBST: 0.61 ± 0.16 and control: 1.11 ± 0.13). Therefore, oxygen plasma treatment was chosen to be the method to lower the contact angle on SU-8 surface.

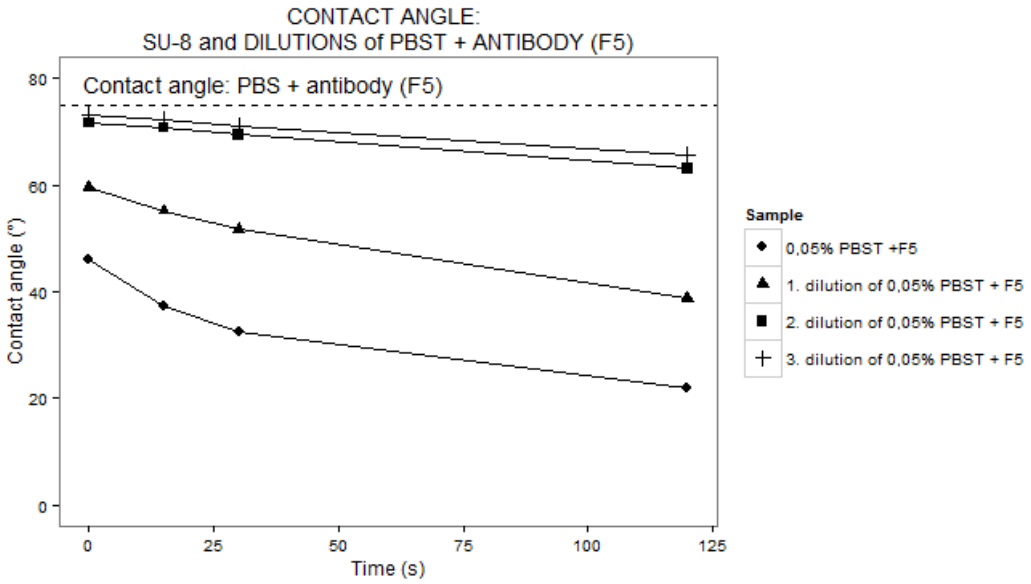

Figure 47. Change in contact angle during a 2 min period between different dilutions of antibody - PBST solution and SU-8 surface. The dashed line indicates the contact angle between antibody - PBST solution and SU-8.

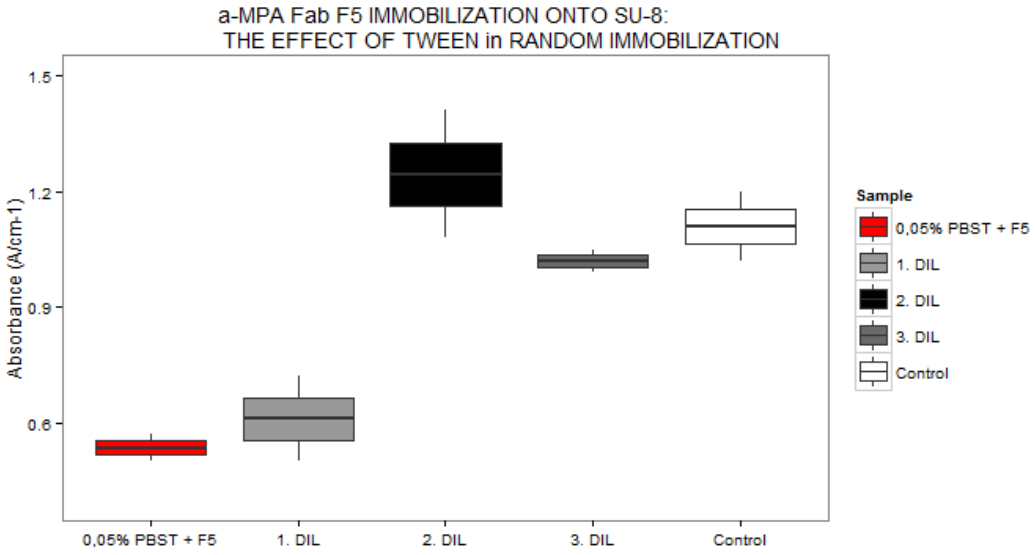

Figure 48. Tween should not be used in the antibody immobilization as the immobilization efficiency of antibody is decreased significantly in random immobilization when higher concentrations of Tween are used.

7.6.2 Liquid flow studies

The correct layer depth and distance between consecutive rows (see table 7) for the immunochip design was decided by the liquid flow studies. The test was executed with water and antibody solution. The tested contact angles were 30º and 42 º.

The flow studies were not successful with contact angle of 30° with any of layer thicknesses. The wrong contact angle allowed the liquid to flow in both directions (upwards and downwards after the inlet whereas the desired path was only upwards). The studies indicated that the correct flow profile was obtained when the contact angle was around 42°. This result was repeated both with the water and the antibody solution. In addition to contact angle, also the layer thickness and the consecutive row distance of the structures were defined. The correct flow profile was obtained with 14.8 µm thick SU-8 layer, where the row distance was 23 µm (figure 49). Also this was able to be repeated with both the water and the antibody solution. Appendix F presents the incorrect flow profiles in the most common problem situations and a more detailed photo series of the correct flow profile (made with water).

During the flow studies, we noticed that in addition to proper contact angle and the SU-8 structure parameters, the flow profile is as dependent on the humidity of the surroundings. If the surroundings are not humid enough, the liquid flows correctly at first, but due to evaporation of the PBS (in antibody solution), after a 20 s period, the flow is also directed downwards (see appendix F). The studies showed that the droplet dries in about 1 min. Therefore, some kind of a box with a cover is needed when using the immunochips.

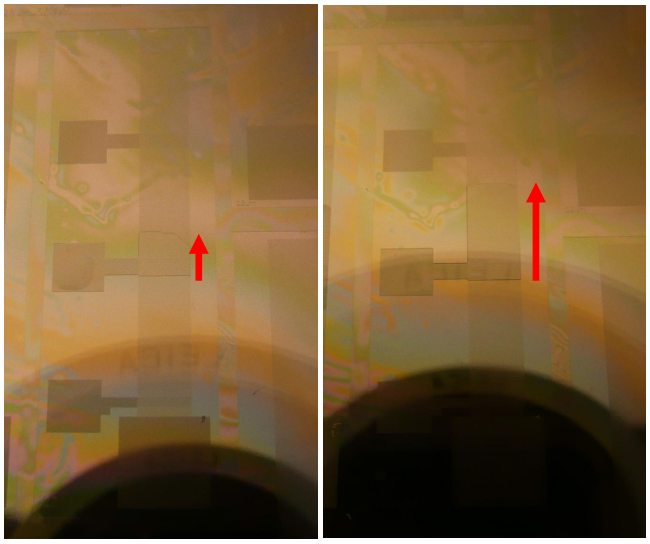

Figure 49. The correct flow profile with antibody solution was obtained when the chip was sealed inside a covered Petri dish (contact angle: 42°). The progress of the solution is marked with red arrow.

7.6.3 Immobilization tests using immunochip structures

We did over 30 different immobilization studies with immunochip structures according to random immobilization shown in table 9. On the basis of the previous studies made within this thesis, the correct contact angle and structure parameters (see chapter 7.6.2) as well as the requirement for humid conditions were implemented to the studies. The correct flow profile was obtained couple of times and one of the most promising samples was taken to the fluorescence detection. The results (figure not shown) indicated that some kind of immobilization had taken place. The fluorescence was the most efficient on the tips of the triangles as the illustrative figure 50 presents. In order to be sure, that the fluorescence was caused by the correct immobilization and not e.g. by the evaporation of the buffer, more repetitions are needed.

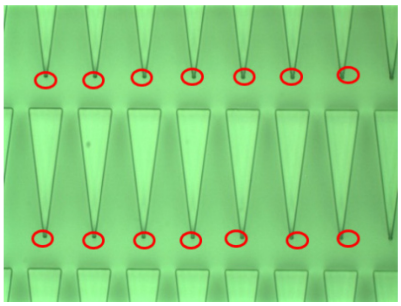

Figure 50. An illustrative presentation of the fluorescence microscope detection obtained from the immunochip study. The red circles present the places where the fluorescence was highest.

8 Conclusion

This thesis studied the His6-tagged α-MPA Fab F5 immobilization onto SU-8 surface by random covalent and IDA-Co chelation immobilizations. The scope was to compare these two immobilization methods in terms of various immobilization parameters. In addition, the aim was to observe wheatear or not SU-8 is a feasible base material for MALDI-MS. Also the determination of the optimal conditions as well as the fabrication parameters for the immunochip structure was the scope of this thesis.

The results obtained in this thesis indicate that the antibody immobilization is possible with both immobilization methods. Moreover, in both immobilizations neither the SU-8 surface storing stability nor the dry storing conditions distract the immobilization significantly, which are desired results by thinking the potential applications. The results in oriented and random immobilization were promising, but still more repetitions are needed. In comparison studies the random immobilization was better in antibody immobilization efficiency. But even though the responses in random immobilization were notably higher throughout the studies, the higher variation between parallel samples and therefore poorer repeatability would suggest that the oriented immobilization is more desired in the applications.

In addition to antibody immobilization, we were able to show that SU-8 is potentially applicable to be used as a MALDI-base, if further considerations regarding the surface modification by oxygen plasma and nanostructuring are taken into account. We also presented the fabrication parameters and surface modification prospects to the correct operation of the innovative immunochip structure.

In the future, the immobilization should be done with smaller SU-8 pieces, which would enable the immersion based immobilization or in a microtiter plate, which would have been fabricated entirely of SU-8. In addition, a new antibody-antigen model system, which would have higher affinity, should be used. The change in antibody-antigen pair would also be beneficial regarding the MALDI-measurements as in the current immobilization the BSA blocking solution, antibody as well as the antigen are very close to each other in the spectra. It is difficult to determine which of them caused the change in the spectrum.

At least to our knowledge there are no previous studies showing the recombinant antibody fragment immobilization onto SU-8 surface. Overall the number of studies regarding the antibody immobilization onto SU-8 is scarce despite the fact SU-8 is known to be sufficiently

biocompatible and that there are also plenty of different surface modification methods developed, which are able to activate the existent residual epoxy groups and to pose new functional groups on SU-8. Therefore, this thesis contributes to the current understanding of how the antibody immobilization is done onto SU-8 surface. In addition, this thesis serves as a guideline to follow-up studies and further development steps as well as a comprehensive review on SU-8 both in properties, fabrication methods and surface modification prospects.

9 References

[1] Lin, C.-C., Wang, J.-H., Wu, H.-W. and Lee, G.-B. Microfluidic immunoassays. *Journal of laboratory automation*, 15:253-274, 2010.

[2] Gervais, L., de Rooij, N. and Delamarche, E. Microfluidic chips for point-of-care immunodiagnostics. *Advanced Materials*, 23:H151-H176, 2011.

[3] Bange, A., Halsall, H.B. and Heineman, W.R. Microfluidic immunosensor systems. *Biosensors and Bioelectronics*, 20:2488-2503, 2005.

[4] Hosokowa, K., Omata, M., Sato, K. and Maeda, M.. Power-free sequential injection for microchip immunoassay toward point-of-care testing. *Lab on a Chip*, 6:236-241, 2006.

[5] Henares, T.G., Mizutani, F. and Hisamoto, H.. Current development in microfluidic immunosensing chip. *Analytica chimica acta*, 611:17-30, 2008.

[6] Goluch, E.D., Nam, J.-M., Georanopoulou, D.G., Chiesl, T.N., Shaikh, K.A., Ryu, K.S., Barron, A.E., Mirkin, C.A. and Liu, C. A bio-barcode assay for on-chip attomolar-sensitivity protein detection. *Lab on a Chip*, 6:1293-1299, 2006.

[7] Li, P., Sherry, A.J., Cortes, J.A., Anagnostopoulos, C. and Faghri, M. A blocking-free microfluidic fluorescence heterogenous immunoassay for point-of-care diagnostics. *Biomedical Microdevices*, 13:475-483, 2011.

[8] Vikholm-Lundin, I. and Albers, W.M.. Site-directed immobilization of antibody fragments for detection of C-reactive protein. *Biosensors and Bioelectronics*, 21:1141-1148, 2006.

[9] Obeid, P.J. and Christopoulos, T.K. Continuous-flow DNA and RNA amplification chip combined with laser-induced fluorescence detection. *Analytica Chimica Acta*, 494:1-9, 2003.

[10] Becker, H. and Gärtner, C. Polymer microfabrication technologies for microfluidic systems. *Analytical and Bioanalytical Chemistry*, 390:89–111, 2008.

[11] Liu, C. Recent developments in polymer MEMS. *Advanced Materials*, 19:3783-3790, 2007.

[12] Wang, H., Meng, S., Guo, K., Liu, Y., Yang, P., Zhong, W. and Liu, B. Microfluidic immunosensor based on stable antibody-patterned surface in PMMA microchip. *Electrochemistry Communications*, 10:447-450, 2008.

[13] Egea, A.M.C. and Vieu, C. Microcontact printing of biomolecular gratings from SU-8 masters duplicated by Thermal Soft UV NIL. *Microelectronic Engineering*, 88:1935-1938, 2011.

[14] Gervais, L. and Delamarche, E. Towards one-step point-of-care immunodiagnostics using capillary-driven microfluidics and PDMS substrates. *Lab on a Chip*, 9:3330-3337, 2009.

[15] Bernard, A., Michel, B. and Delamarche, E. Micromosaic immunoassays. *Analytical Chemistry*, 73:8-12, 2001.

[16] Heyries, K.A., Loughran, M.G., Hoffmann, D., Homsy, A., Blum, L.J. and Marquette, C.A. Microfluidic biochip for chemiluminescent detection of allergen-specific antibodies. *Biosensors and Bioelectronic*s, 23:1812-1818, 2008.

[17] Gao, Y., Lin, F.Y.H., Hu, G., Sherman, P. and Li, D. Development of a novel electrokinetically driven microfluidic immunoassay for the detection of Helicobacter pylori. *Analytica Chimica Acta*, 543:109-116, 2005.

[18] Darain, F., Gan, K.L. and Tjin, S.C. Antibody immobilization on to polystyrene substrate - on chip immunoassay for horse IgG based on fluorescence. *Biomedical Microdevices*, 11:653-661, 2009.

[19] Sung, D., Shin, D.H. and Jon, S. Toward immunoassay chips: Facile immobilization of antibodies on cyclic olefin copolymer substrates through pre-activated polymer adlayers. *Biosensors and Bioelectronics*, 26:3967-3972, 2011.

[20] Wen, X., He, H. and Lee, L.J. Spesific antibody immobilization with biotin-poly(L-lysine)-g-poly(ethylene glycol) and protein A on microfluidic chips. *Journal of Immunological Methods*, 350:97-105, 2009.

[21] Rucker, V.C., Havenstrite, K.L., Simmons, B.A., Sickafoose, S.M., Herr, A.E. and Shediac, R. Functional antibody immobilization on 3-dimensional polymeric surfaces generated by reactive ion ething. *Langmuir*, 21:7621-7625, 2005.

[22] Yuan, Y., He, H. and Lee, L.J. Protein A-based antibody immobilization onto polymeric microdevices for enhanced sensitivity of enzyme-linked immunosorbent assay. *Biotechnology and Bioengineering*, 102: 891-901, 2009.

[23] Hashimoto, M., Kaji, H., Kemppinen, M.E. and Nishizawa, M. Localized immobilization of proteins onto microstructures within a preassembled microfluidic device. *Sensors and Actuators B*, 128:545-551, 2008.

[24] Jung, Y., Jeong, J.Y. and Chung, B.H. Recent advances in immobilization methods of antibodies on solid supports. *The analyst*, 133:697-701, 2008.

[25] Bilitewski, U. Review: Protein-sensing assay formats and devices. *Analytica Chimica Acta*, 568:232-247, 2006.

[26] Maynard, J. and Georgiou, G. Antibody Engineering. *Annual Review of Biomedical Engineering*, 2:339-376, 2000.

[27] Brockmann, E.-C., Vehniäinen, M. and Pettersson, K. Use of high-capacity surface with oriented recombinant antibody fragments in a 5-min immunoassay or thyroid-stimulating hormone. *Analytical Biochemistry*, 396:242-249, 2010.

[28] Joshi, M., Kale, N., Lal, R., Rao, V.R. and Mukherji, S. A novel dry method for surface modification of SU-8 for immobilization of biomolecules in Bio-MEMS. *Biosensors and Bioelectronics*, 22:2429-2435, 2007.

[29] Voskerician, G., Shive, M.S., Shawgo, R.S., von Recum, H., Anderson, J.M., Cima, M.J. and Langer, R. Biocompatibility and bioufouling of MEMS drug delivery devices. *Biomaterials*, 24:1959-1967, 2003.

[30] Wang, Y., Pai, J.H., Lai, H.-H., Sims, C.E., Bachman, M., Li, G.P. and Allbritton, N.L. Surface graft polymerization of SU-8 for bio-MEMS applications. *Journal of Micromechanics and Microengineering*, 17:1371-1380, 2007.

[31] Blagoi, G., Keller, S., Johansson, A., Boisen, A. and Dufva, M. Functionalization of SU-8 photoresist surfaces with lgG proteins. *Applied Surface Science*, 255:2896-2902, 2008.

[32] Joshi, M., Pinto, R., Rao, V.R. and Mukherji, S.. Silanization and antibody immobilization on SU-8. *Applied Surface Science*, 253:3127-3132. 2007.

[33] Deepu, A., Sai, V.V.R. and Mukherji, S. Simple surface modification techniques for immobilization of biomolecules on SU-8. *Journal of Materials Science: Materials in Medicine*, 20:S25-S34, 2009.

[34] Hale, J.E. Irreversible, oriented immobilization of antibodies to cobalt-iminodiacetate resin for use as immunoaffinity media. *Analytical Biochemistry*, 231:46-49, 1995.

[35] Holdago, M., Barrios, C.A., Ortega, F.J., Sanza, F.J., Casquel, R., Laguna, M.F., Bañuls, M.J., López-Romero, D., Puchades, R. and Maquieira, A. Label-free biosensing by means of periodic lattices of high aspect ratio SU-8 nano-pillars. *Biosensors and Bioelectronics*. 25: 2553-2558, 2010.

[36] Hua, L., Low, T.Y., Meng, W., Chan-Park, M.B. and Sze, S.K.. Novel polymer composite to eliminate background matrix ions in matrix assisted laser desorption /ionization-mass spectrometry. *Analyst*, 132:1223-1230, 2007.

[37] Jokinen, V., Leinikka, M. and Franssila, S. Microstructured surfaces for directional wetting. *Advanced Materials*, 21: 4835-4838, 2009.

[38] Simple English Wikipedia. Webpage. Cited on 16.5.2014. Retrieved from http://simple.wikipedia.org/wiki/Microtiter_plate.

[39] Manz, A., Harrison, D.J., Verpoorte, E.M.J., Fettinger, J.C., Paulus, A., Lüdi, H. and Widmer, M. Planar chips technology for miniaturization and integration of separation techniques into monitoring systems: Capillary electrophoresis on a chip. *Journal of Chromatography A*, 593:253-258, 1992.

[40] Sikanen, T., Tuomikoski, S., Ketola, R.A., Kostiainen, R., Franssila, S. and Kotiaho, T. Characterization of SU-8 for electrokinetic microfluidic applications. *Lab on a chip*, 5:888-896, 2005.

[41] Garstecki, P., Fuerstman, M.J., Stone, H.A. and Whitesides, G.M. Formation of droplets and bubbles in a microfluidic T-junction – scaling and mechanism of break-up. *Lab on a Chip*, 6:437-446, 2006.

[42] Butt, H.-J., Graf, K. and Kappl, M. *Physics and Chemistry of Interfaces*. 2.ed., Weinheim, Wiley-VCH, 2006.

[43] Caputo, G., Cortese, B., Nobile, C., Salerno, M., Cingolani, R., Gigli, G., Cozzoli, P.D. and Athanassiou, A. Reversibly light-switchable wettability of hydrid organic/inorganic surfaces with dual micro-/nanoscale roughness. *Advanced Functional Materials*, 19:1149-1157, 2009.

[44] Ramé-hart instrument co. Webpage. Cited on 14.5.2014. Retrieved from http://www.ramehart.com/contactangle.htm.

[45] Jung, Y.C. and Bhushan, B. Contact angle, adhesion and friction properties of micro- and nanopatterned polymers for superhydrophobicity. *Nanotechnology*, 17:4970-4980, 2006.

[46] Jokinen, V., Sainiemi, L. and Franssila, S. Complex droplets on chemically modified silicon nanograss. *Advanced Materials*, 20:3453-3456, 2008.

[47] Lee, S-M. and Kwon, T.H. Effects of intrinsic hydrophobicity on wettability of polymer replicas of a superhydrophobic lotus leaf. *Journal of Micromechanics and Microengineering*, 17:687-692, 2007.

[48] Chen, T.-H., Chuang, Y.-J., Chieng, C.-C. and Tseng, F.-G. A wettability switchable surface by microscale surface morphology change. *Journal of Micromechanics and Microengineering*, 17: 489-495, 2007.

[49] Novo, P., Volpetti, F., Chu, V. and Conde, J.P. Control of sequential fluid delivery in a fully autonomous capillary microfluidic device. *Lab on a Chip*, 13:641-645, 2013.

[50] Anjoh, T.A., Jorgensen, A.M., Zauner, D.A. and Hübner, J. The effect of soft bake temperature on the polymerization of SU-8 photoresist. *Journal of Micromechanics and Microengineering*, 16:1819-1824, 2006.

[51] Lorenz, H., Despont, M., Fahrni, N., Brugger, J., Vettiger, P. and Renaud, P. High-aspect ratio, ultrathick, negative-tone near-UV photoresist and its applications for MEMS. *Sensors and Actuators A*, 64:33-39, 1998.

[52] Lorenz, H., Despont, M., Fahrni, N., LaBianca, N., Renaud, P. and Vettiger, P. SU-8: a low-cost negative resist for MEMS. *Journal of Micromechanics and Microengineering*, 7:121-124, 1997.

[53] del Campo, A. and Greiner, C. Topical review, SU-8: a photoresist for high-aspect-ratio and 3D submicron lithography. *Journal of Micromechanics and Microengineering,* 17:R81-R95, 2007.

[54] Feng, R. and Farris, R.J. Influence of processing conditions on the thermal and mechanical properties of SU-8 negative photoresist coatings. *Journal of Micromechanics and Microengineering*, 13:80-88, 2003.

[55] MicroChem homepages. Webpage. Cited on 03.06.2013. Retrieved from http://www.microchem.com/index.htm.

[56] MicroChem homepages: Material data sheet of SU-8 photoresist. Webpage. Cited on 21.5.2014. Retrieved from http://www.microchem.com/pdf/SU8_50-100.pdf.

[57] MicroChem homepages: Material data sheet of SU-8 2000 series resists. Webpage. Cited on 21.5.2014. Retrieved from http://coewww.rutgers.edu/www4/biomems/docs/SU8_2002-2025.pdf.

[58] Walther, F., Davydovskaya, P., Zürcher, S., Kaiser, M., Herberg, H., Gigler, A.M. and Stark, R.W.. Stability of the hydrophilic behavior of oxygen plasma activated SU-8. *Journal of Micromechanics and Microengineering*, 17:524-531, 2007.

[59] Marie, R., Schmid, S., Johansson, A., Ejsing, L., Nordström, M., Häfliger, D., Christensen, C.B.V., Boisen, A. and Dufva, M. Immobilization of DNA to polymerised SU-8 photoresist. *Biosensors and Bioelectronics*, 21:1327-1332, 2006.

[60] Koukherenko, E., Kraft, M., Ensell, G.J. and Hollinshead, N. A comparative study of different thick photoresists for MEMS applications. *Journal of Materials Science: Materials in Electronics*, 16:741-747, 2005.

[61] Zhang, J., Tan, K.L., Hong, G.D., Yang, L.J. and Gong, H.Q. Polymerization optimization of SU-8 photoresist and its applications in microfluidic systems and MEMS. *Journal of Micromechanics and Microengineering,* 11:20-26, 2001.

[62] Mata, A., Fleischman, A.J. and Roy, S. Fabrication of multi-layer SU-8 microstructures. *Journal of Micromechanics and Microengineering,*16:276-284, 2006.

[63] Chuang, Y.J., Tseng, F.-G. and Lin, W.-K. Reduction of diffraction effect of UV exposure on SU-8 negative thick photoresist by air gap elimination. *Microsystem Technologies*, 8:308-313, 2002.

[64] Nordström, M., Johansson, A., Noguerón, E.S., Clausen, B., Calleja, M. and Boisen, A. Investigation of the bond strenght between the photo-sensitive polymer SU-8 and gold. *Microelectronic Engineering*, 78-79:152-157, 2005.

[65] Feng, R. and Farris, J. The characterization of thermal and elastic constants for an epoxy photoresist SU-8 coating. *Journal of Material Science*, 37:4793-4799, 2002.

[66] Dellmann, L., Roth, S., Beuret, C., Racine, G.-A., Lorenz, H., Despont, M., Renaud, P., Vettiger, P. and de Rooij, N.F. 1997, 'Fabrication process of high aspect ratio elastic structures for piezoelectric motor applications'. *Transducers '97*.

[67] Lorenz, H., Laudon, M. and Renaud, P. Mechanical Characterization of a new high-aspect-ratio near UV-photoresist. *Microelectronic Engineering*, 41/42:371-374, 1998.

[68] Glatz, W., Muntwyler, S. and Hierold, C.. Flexible polymer based microthermogenerator. Online article. Available: http://www.micro.mavt.ethz.ch/publications/Glatz2005_CP.

[69] Borreman, A., Musa, S., Kok, A.A.M., Diemeer, M.B.J. and Driessen, 2002, 'A. Fabrication of polymeric multimode waveguides and devices in Su-8 photoresist using selective polymerization'. *Proceedings Symposium IEEE/LEOS Benelux Chapter*.

[70] Mbairi, F.D. and Hesselbom, H. High frequency design and characterization of SU-8 based conductor backed coplanar waveguide transmission lines.

[71] Franssila, S. *Introduction to microfabrication*. 1.ed., England, John Wiley & Sons Ltd, 2005.

[72] Becker, H. and Gärtner, C. Review: Polymer microfbrication methods for microfluidic analytical application. *Electrophoresis*, 21:12-26, 2000.

[73] Fu, C., Hung, C. and Huang, H. A novel and simple fabrication method of embedded SU-8 micro channels by direct UV lithography. *Journal of Physics: Conference Series*, 34:330-335, 2006.

[74] Shumacher, J.T., Grodrian, A., Kremin, C., Hoffman, M. and Metze, J.. Hydrophobic coating of microfluidic chips structured by SU-8 polymer for segmented flow operation. *J. Micromech. Microeng.*, 18:1-6, 2008.

[75] Weisenberg, B.A. and Mooradian, D.L. Hemocompatibility of materials used in microelectromechanical systems: Platelet adhesion and morphology *in vitro*. *Journal of Biomedical Materials Research*, 60:283-291, 2002.

[76] Vernekar, V.N., Cullen, D.K., Fogleman, N., Choi, Y., Carcía, A.J., Allen, M.G., Brewer, G.J. and LaPlaca, M.C. SU-8 2000 rendered cytocompatible for neuronal bioMEMS applications. *Journal of Biomedical Materials Research Part A*, 89A:138-151, 2009.

[77] Wang, Y., Bachman, M., Sims, C., Li, G.P. and Allbritton, N.L. Simple photografting method to chemically modify and micropattern the surface of SU-8 photoresist. *Langmuir*, 22:2719-2725, 2006.

[78] Makamba, H., Kim, J.H., Lim, K., Park, N. and Hahn, J.H. Surface modification of poly(dimethylsiloxane) microchannels. *Electrophoresis*, 24:3607-3619, 2003.

[79] Gao, Z., Henthorn, D.B. and Kim, C.-S. Enhanced wettability of an SU-8 photoresist through a photografting procedure for bioanalytical device applications. *Journal of Micromechanics and Microengineering*, 18:045013 (7pp), 2008.

[80] Chung, C.K. and Hong, Y.Z. Surface modification of Su-8 photoresist for shrinkage improvement in a monolithic MEMS microstructure. *Journal of Micromechanics and Microengineering,* 17:207-212, 2007.

[81] Gach, P.C., Sims, C.E. and Allbritton, N.L.. Transparent magnetic photoresists for bioanalytical applications. *Biomaterials*, 31: 8810-8817, 2010.

[82] Ingrosso, C., Martin, C., Llobera, A., Murano, F.P., Innocenti, C., Sangregorio, A., Voigt, A., Gruetzner, G., Brugger, J., Striccoli, M., Agostiano, A., Curri, M.L. 2009, 'Magnetic nanocrystals modified epoxy photoresist for microfabrication of AFM probes'. *Proceedings of the Eurosensors XXIII conference*, p. 580-584.

[83] Suter, M., Ergeneman, O., Zürcher, J., Moitzi, C., Pané, S., Rudin, T., Pratsinis, S.E., Nelson, B.J. and Hierold, C. A photopatternable superparamagnetic nanocomposite: Material characterization and fabrication of microstructures. *Sensors and actuators B: Chemical*, 156:433-443, 2011.

[84] Tsai, K.L., Ziaei-Moayyed, M., Candler, R.N., Hu, W., Brand, V., Klejwa, N., Wang, S.X. and Howe, R.T. Magnetic, mechanical, and optical characterization of a magnetic nanoparticle-embedded polymer for microactuation. *Journal of Microelectromechanical systems*, 20:65-72, 2011.

[85] Damean, N., Parviz, B.A., Lee, J.N., Odom, T. and Whitesides, G.M. Composite ferromagnetic photoresist for the fabrication of microelectromechanical systems. *Journal of Micromechanics and Microengineering*, 15:29-34, 2005.

[86] Hartley, A.C., Miles, R.E., Corda, J. and Dimitrakopoulas, N. Large throw magnetic microactuator. *Mechatronics*, 18: 459-465, 2008.

[87] Jiguet, S., Bertsch, A., Hofmann, H. and Renaud, P. Conductive SU8 photoresist for microfabrication. *Advanced Functional Materials*, 15:1511-1516, 2005.

[88] Chang, C.-J., Yang, C.-S., Chuang, Y.-J., Khoo, H.-S. and Tseng, F.-G.. Micro-patternable nanoporous polymer integrated with microstructures for molecular filtration. *Nanotechnology*, 19:365301 (8pp), 2008.

[89] Skjolding, L.H.D., Teixidor, G.T., Emnéus, J. and Montelius, L. Negative UV-NIL (NUV-NIL) - A-mix-and-match NIL and UV strategy for realisation of nano- and micrometre structures. *Microelectronic Engineering*, 86:654-656, 2009.

[90] Youn, S.-W., Ueno, A., Takahashi, M. and Maeda, R. Microstructuring of SU-8 photoresist by UV-assisted thermal imprinting with non-transparent mold. *Microelectronic Engineering*, 85:1924-1931, 2008.

[91] Wang, X., Liao, Y., Liu, B., Ge, L., Li, G., Fu, S., Chen, Y. and Cui, Z. Free-standing SU-8 subwavelength gratings fabricated by UV curing imprint. *Microelectronic Engineering*, 85:910-913, 2008.

[92] Nordström, M., Hübner, J. and Boisen, A. Sloped side walls in SU-8 structures with 'Step-and-Flash' processing. *Microelectronic Engineering*, 83:1269-1272, 2006.

[93] Cheng, X. and Guo, L.J. A combined-nanoimprint-and-photolithography patterning technique. *Microelectronic Engineering*, 71:277-282, 2004.

[94] Hu, W., Yang, B., Peng, C. and Pang, W. Three-dimensional SU-8 structures by reversal UV imprint. *Journal of Vacuum Science & Technology B*, 24:2225-2229, 2006.

[95] Berg, J.M., Tymoczko, J.L. and Stryer, L. *Biochemistry*, 7.ed., England, W.H. Freeman and Company, 2012.

[96] Lipman, N.S., Jackson, L.R., Trudel, L.J. and Weis-Garcia, F. Monoclonal versus polyclonal antibodies: Distinguishing Characteristics, Applications and Information sources. *ILAR Journal*, 46:258-268, 2005.

[97] Murphy, K., Travers, P. and Walport, M. *Janeway's Immunobiology*. 7.ed., USA, T&F informa, 2008.

[98] Abnova Newsletter ELISA Kit Collection homepages. Cited on 14.5.2014. Retrieved from . http://www.abnova.com/newspaper/1001213/index.html.

[99] Plückthun, A. Biotechnological Aspects of antibody production in E. coli. *Acta Biotechnologica*, 11:449-456, 1991.

[100] Zakharov, A.V., Smirnovm, I.V., Serebryakova, M.V., Dronina, M.A., Kaznacheeva, A.V., Kurkova, I.N., Belogurov, A.A., Friboulet, A., Ponomarenko, N.A., Gabibov, A.G. and Bobik, T.V. Expression of catalytic antibodies in eukaryotic systems. *Molecular Biology*, 45:74-81, 2011.

[101] Backovic, M., Johansson, D.X., Klupp, B.G., Mettenleiter, T.C., Persson, M.A.A., Rey, F.A. Efficient method for production of high yields of Fab fragments in Drosophila S2 cells. *Proteins Engineering*, 2010, p. 1-6.

[102] De Wilde, C., Peeters, K., Jacobs, A., Peck, I. and Depicker, A. Expression of antibodies and Fab fragments in transgenic potato plants: a case study for bulk production in crop plants. *Molecular Breeding*, 9:271-282, 2002.

[103] Block, H., Maertens, B., Spriestersbach, A., Brinker, N., Kubicek, J., Fabis, R., Labahn, J. and Schäfer, F. Immobilized-metal affinity chromatography (IMAC): a review. *Methods in Enzymology*: 463:439-473, 2009.

[104] Rusmini, F., Zhong, Z. and Feijin, J. Protein immobilization strategies fro protein biochips. *Biomacromolecules*, 8:1775-1789, 2007.

[105] Butler, J.E., Li, N., Brown, W.R., Joshi, K.S., Chang, J., Rosenberg, B. and Voss Jr, E.W. The immunochemistry of sandwich elisas –VI. Greater than 90% of monoclonal and 75% of polyclonal anti-fluorescyl capture antibodies (Cabs) are denaturated by passive adsorption. *Molecular Immunology*, 30:1165-1175, 1993.

[106] Biacor homepages. Cited on 14.5.2014. Retrieved from www.biacore.com.

[107] Garcia-Suarez, M.D.M., Villaverde, R., Gonzalez-Rodriguez, I., Vazquez, F. and Mendez, F.J. Oriented immobilization of anti-pneumolysin tagged recombinant antibody fragments. *Current Microbiology*, 59:81-87, 2009.

[108] Saerens, D., Huang, L., Bonroy, K., Muyldermans, S., Review; antibody fragments as Probe in biosensor development. *Sensors* (2008), 8, p. 4669-4686.

[109] Shew, B.Y., Cheng, Y.C. and Tsai, Y.H. Monolithic SU-8 micro-interferometer for biochemical detections. *Sensors and Actuators A: Physical*, 141:299-306, 2008.

[110] Jiang, L., Gerhardt, K.P., Myer, B., Zohar, Y. and Pau, S. Evanescent-Wave Spectroscopy Using an SU-8 Waveguide for Rapid Quantitative Detection of Biomolecules. *Journal of Microelectromechanical systems*, 17:1495-1500, 2008.

[111] Aura, S., Jokinen, V., Sainiemi, L., Baumann, M. and Franssila, S. UV-embossed inorganic-organic hybrid nanopillars for bioapplications. *Journal Nanoscience and Nanotechnology*, 11: 6710-6715, 2009.

[112] Jokinen, V. and Franssila, S. 2013, 'Microfluidics via controlled imbibition'. *MRS Proceedings*.

Appendix A. ATIR-FTIR results of different SU-8 samples

Table 1. The relevant peaks in the SU-8 ATIR-FTIR spectrum.

WAVENUMBER (cm^{-1})	CHARACTERISTIC VIBRATION
861	C–O stretching of *cis* substituted epoxy rings
910	C–O stretching of *trans* substituted epoxy ring
1000–1230	C–O–C stretching in ethers
1000–1290	C–O stretching in phenols and secondary alcohols
1500	Aromatic C–C stretching (in-ring)
1700–1750	C=O stretching cyclopentanone (solvent)

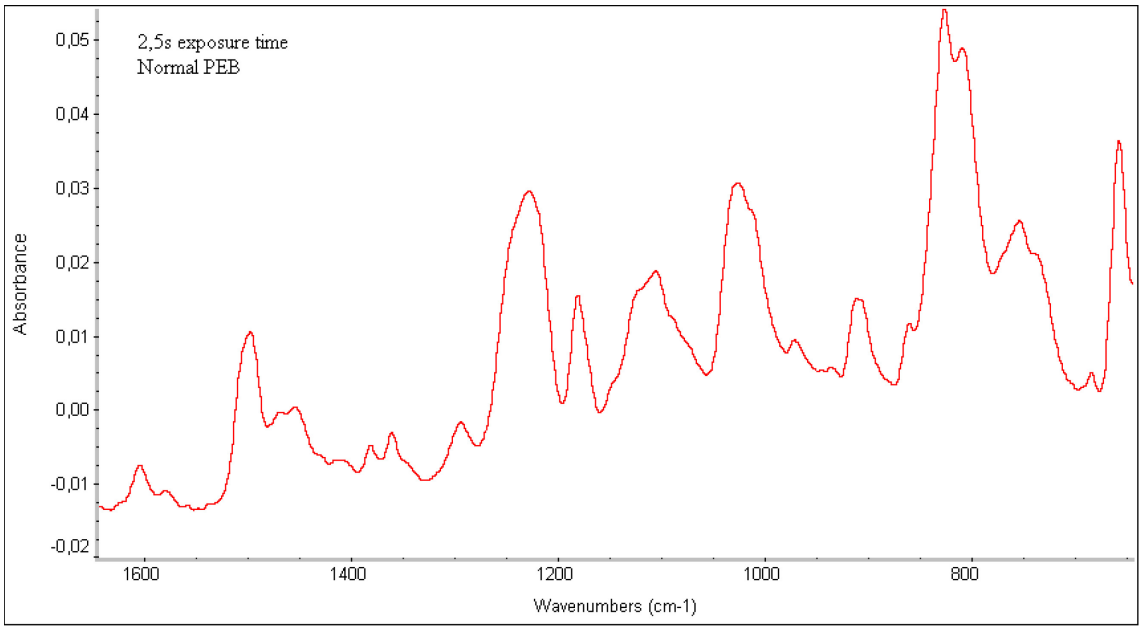

Figure 1. ATIR-FTIR spectrum of sample2.

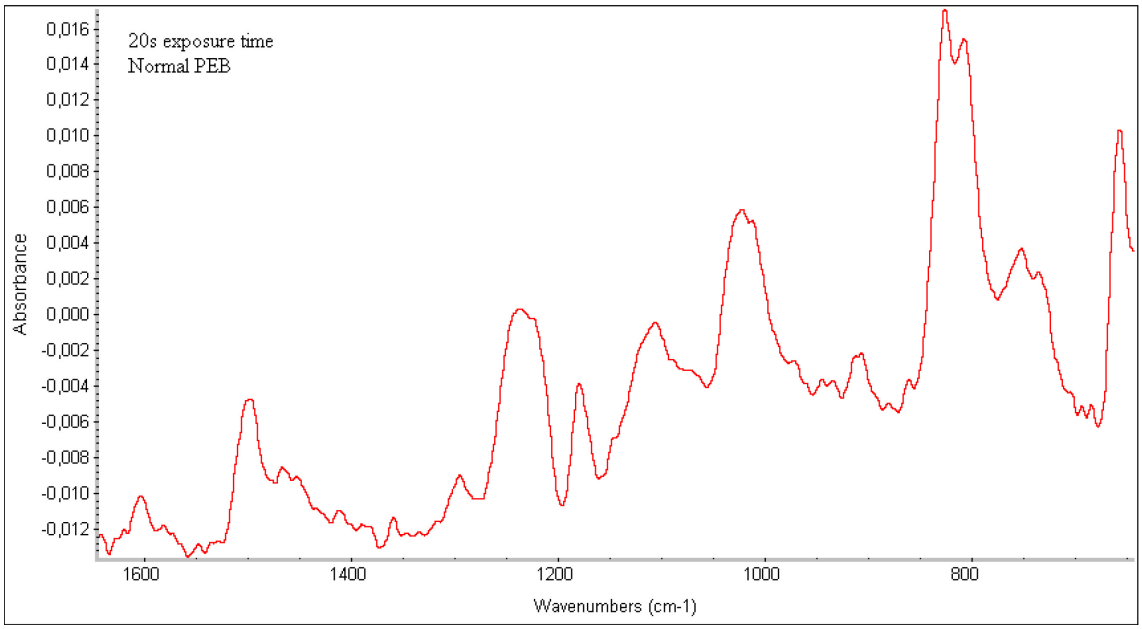

Figure 2. ATIR-FTIR spectrum of sample3.

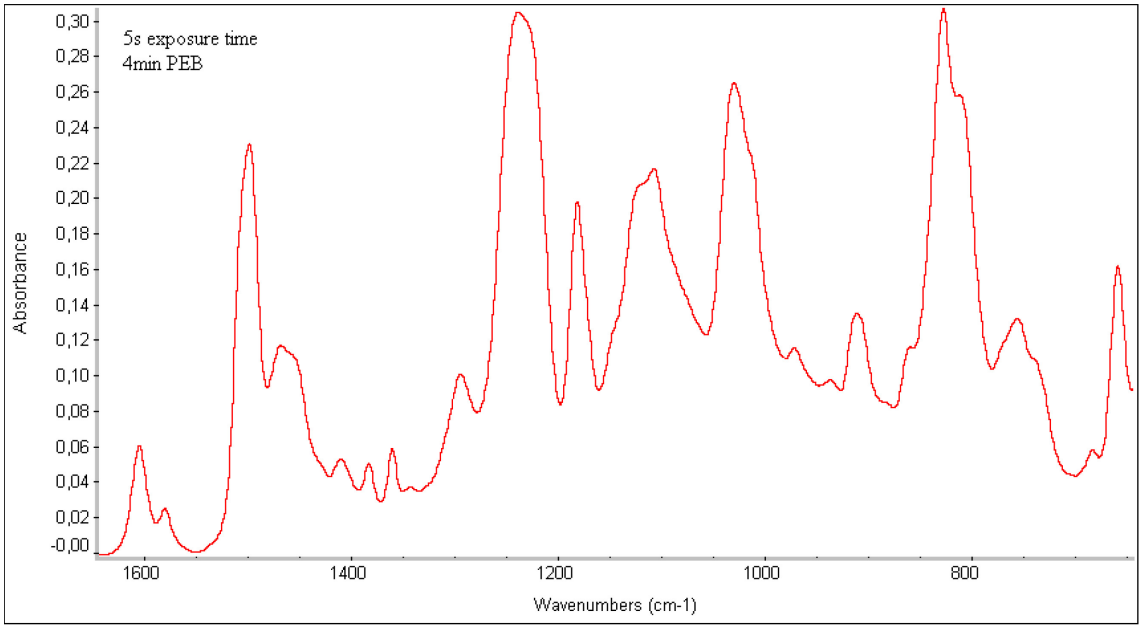

Figure 3. ATIR-FTIR spectrum of sample4.

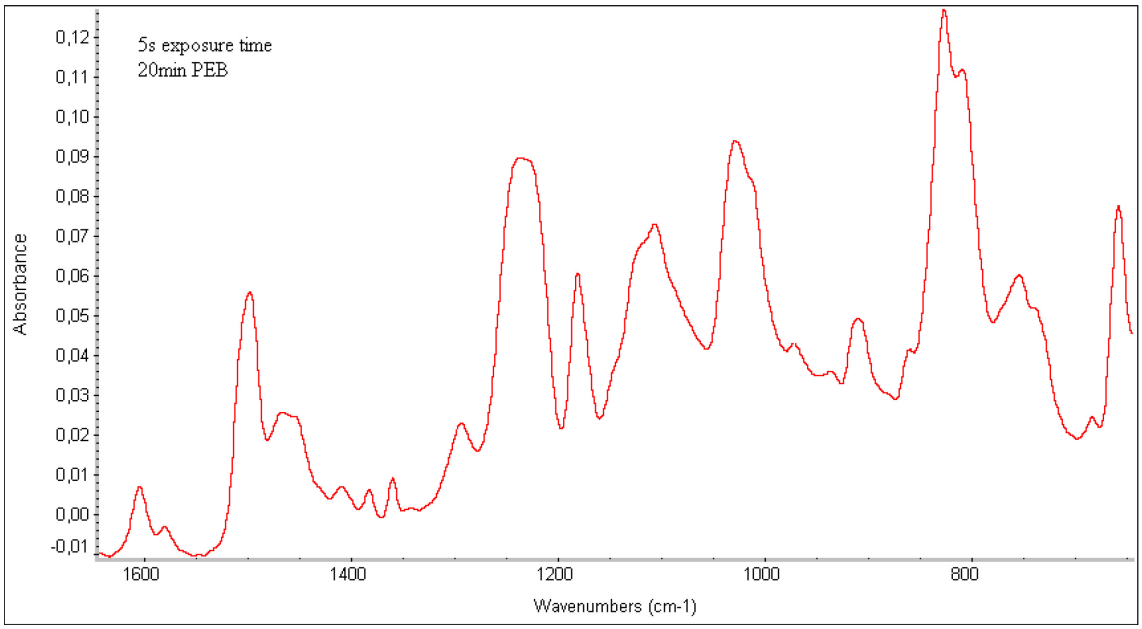

Figure 4. ATIR-FTIR spectrum of sample5.

Appendix B.Statistical testing by Student t-test: R syntax and output

9.1.1 R syntax for Student's t.test

```
t.test(x, ...)

## Default S3 method:
t.test(x, y = NULL,
       alternative = c("two.sided", "less", "greater"),
       mu = 0, paired = FALSE, var.equal = FALSE,
       conf.level = 0.95, ...)
```

Parameter definition:

a <- c(0.95, 0.94, 0.58)

b <- c(1.08, 0.96, 1.02)

t.test(a, b)

Result output:

Welch Two Sample t-test

data: a and b

t = -1.5542, df = 2.322, p-value = 0.2433

alternative hypothesis: true difference in means is not equal to 0

95 percent confidence interval:

-0.6747898 0.2814565

sample estimates:

mean of x mean of y

0.8233333 1.0200000

Appendix C. Comparison study results: random and oriented immobilization

Table 1. Comparison tests results (same SU-8 wafer and reagents fabricated same time).

STUDY	SAMPLE	IMMOBILIZATION TYPE	ABSORBANCE (mean ± sd)	BETTER IN RESPONSE
Incubation time	10 min	random	1.17 ± 0.21	random
		oriented	0.83 ± 0.21	
	2 h	random	1.19 ± 0.32	random
		oriented	0.80 ± 0.09	
	o/n	random	1.84 ± 0.29	random
		oriented	1.02 ± 0.06	
Incubation time	10 min	random	0.72 ± 0.54	oriented
		oriented	0.93 ± 0.18	
	o/n	random	0.80 ± 0.13	oriented
		oriented	0.88 ± 0.04	
Incubation time	10 min	random	0.97 ± 0.45	random
		oriented	0.77 ± 0.18	
	o/n	random	0.97 ± 0.27	random
		oriented	0.75 ± 0.12	
Amount of antigen	1:1	random	0.59 ± 0.20	random
		oriented	0.39 ± 0.10	
	1:10	random	0.23 ± 0.05	random
		oriented	0.15 ± 0.03	
	1:100	random	0.08 ± 0.01	-
		oriented	0.08 ± 0.00	

STUDY	SAMPLE	IMMOBILIZATION TYPE	ABSORBANCE (mean ± sd)	BETTER IN RESPONSE
Amount of antigen	1:1	random	0.72 ± 0.21	random
		oriented	0.44 ± 0.09	
	1:2	random	0.50 ± 0.13	random
		oriented	0.39 ± 0.13	
	1:5	random	0.29 ± 0.05	random
		oriented	0.19 ± 0.06	
	1:10	random	0.22 ± 0.02	random
		oriented	0.15 ± 0.01	
	1:20	random	0.13 ± 0.01	random
		oriented	0.12 ± 0.01	
Serum vs. buffer incubation	Buffer	random	1.10 ± 0.18	random
		oriented	0.68 ± 0.09	
	Serum	random	0.59 ± 0.10	oriented
		oriented	0.61 ± 0.25	
Serum vs. buffer incubation & incubation time	Buffer 10 min	random	0.72 ± 0.54	oriented
		oriented	0.93 ± 0.18	
	Buffer o/n	random	0.80 ± 0.13	oriented
		oriented	0.88 ± 0.04	
	Serum 10 min	random	0.48 ± 0.16	oriented
		oriented	0.66 ± 0.29	
	Serum o/n	random	0.73 ± 0.04	oriented
		oriented	0.83 ± 0.02	

STUDY	SAMPLE	IMMOBILIZATION TYPE	ABSORBANCE (mean ± sd)	BETTER IN RESPONSE
Serum vs. buffer incubation & incubation time	Buffer 10 min	random	0.97 ± 0.45	random
		oriented	0.77 ± 0.18	
	Buffer o/n	random	0.97 ± 0.27	random
		oriented	0.75 ± 0.12	
	Serum 10 min	random	1.03 ± 0.22	random
		oriented	0.69 ± 0.03	
	Serum o/n	random	0.63 ± 0.17	random
		oriented	0.59 ± 0.12	
Surface modification by nanostructuring and RIE	Nano	random	1.35 ± 0.04	random
		oriented	0.97 ± 0.13	
	Planar	random	0.73 ± 0.32	random
		oriented	0.39 ± 0.05	
	RIE	random	0.83 ± 0.26	random
		oriented	0.50 ± 0.09	
	Nano + RIE	random	2.34 ± 0.53	random
		oriented	0.52 ± 0.26	
Surface modification by RIE	Control	random	0.88 ± 0.07	random
		oriented	0.36 ± 0.36	
	5 s RIE	random	1.48 ± 0.10	random
		oriented	1.00 ± 0.06	
	60 s RIE	random	1.39 ± 0.06	random
		oriented	0.83 ± 0.23	

STUDY	SAMPLE	IMMOBILIZATION TYPE	ABSORBANCE (mean ± sd)	BETTER IN RESPONSE
Immobilized antibody stability	Wet	random	0.81 ± 0.09	random
		oriented	0.56 ± 0.17	
	Dry	random	0.67 ± 0.12	random
		oriented	0.60 ± 0.13	
Storage stability of SU-8 surface	1 weeks	random	1.43 ± 0.23	random
		oriented	0.78 ± 0.02	
	2 week	random	1.39 ± 0.48	random
		oriented	0.58 ± 0.18	
	Control	random	0.88 ± 0.07	random
		oriented	0.67 ± 0.36	
Storage stability of SU-8 surface	3 weeks	random	1.02 ± 0.26	random
		oriented	0.99 ± 0.27	
	4 weeks	random	1.44 ± 0.10	random
		oriented	0.78 ± 0.06	
	Control	random	1.28 ± 0.17	random
		oriented	0.75 ± 0.04	

Appendix D. Comparison study results: Antibody-antigen complex stability in o/n TBS treatment

Table 1. Remaining activity of the antibody-antigen complex after o/n TBS treatment.

STUDY	SAMPLE	IMMOBILIZATION TYPE	REMAINING IMMOBILIZATION EFFICIENCY (%: mean ± sd)	
			NEW SUBSTRATE	NEW ANTIGEN & SUBSTRATE
Antibody incubation time	10 min	random	16.4 ± 1.5	Not measured
		oriented	37.6 ± 10.5	
	2 h	random	21.4 ± 6.0	
		oriented	31.7 ± 3.2	
	o/n	random	20.2 ± 3.5	
		oriented	29.4 ± 11.7	
Amount of antigen	1:1	random	40.8 ± 5.0	27.0 ± 5.0
		oriented	32.1 ± 4.4	27.8 ± 5.3
	1:2	random	40.3 ± 7.4	30.6 ± 9.9
		oriented	29.8 ± 7.7	30.8 ± 7.0
	1:5	random	42.6 ± 4.0	37.0 ± 5.9
		oriented	51.5 ± 14.9	49.8 ± 14.1
	1:10	random	50.1 ± 6.8	49.8 ±7.6
		oriented	56.0 ± 3.5	59.6 ± 2.3
	1:20	random	67.1 ± 5.9	64.9 ± 7.4
		oriented	71.7 ± 10.6	69.6 ± 7.6

STUDY	SAMPLE	IMMOBILIZATION TYPE	REMAINING IMMOBILIZATION EFFICIENCY (%: mean ± sd)	
			NEW SUBSTRATE	NEW ANTIGEN & SUBSTRATE
Serum vs. buffer	Buffer 10 min	random	33.9 ± 4.0	Not measured
		oriented	25.8 ± 3.0	
	Buffer o/n	random	45.2 ± 4.4	
		oriented	28.2 ± 2.6	
	Serum 10 min	random	52.9 ± 35.6	
		oriented	34.5 ± 6.2	
	Serum o/n	random	68.8 ± 21.7	
		oriented	43.4 ± 7.8	
Serum vs. buffer	Buffer 10 min	random	34.2 ± 11.8	Not measured
		oriented	22.9 ± 2.2	
	Buffer o/n	random	28.6 ± 4.2	
		oriented	27.0 ± 2.4	
	Serum 10 min	random	39.3 ± 7.7	
		oriented	40.4 ± 18.7	
	Serum o/n	random	33.5 ±7.1	
		oriented	32.7 ± 3.4	
Buffer pH	pH 7.24	random	42.2 ± 5.1	29.2 ± 5.7
	pH 8.05		37.7 ± 7.9	30.7 ± 4.4
	pH 9.93		47.5 ± 9.4	34.7 ± 9.5
Surface modification	Nano	random	15.7 ± 2.0	14.1 ± 1.3
	Planar		20.4 ± 8.5	17.1 ± 9.8
	RIE		21.9 ± 6.0	17.5 ± 4.0
	Nano + RIE		17.2 ± 8.6	12.7 ± 6.5

Appendix E. MALDI spectra.

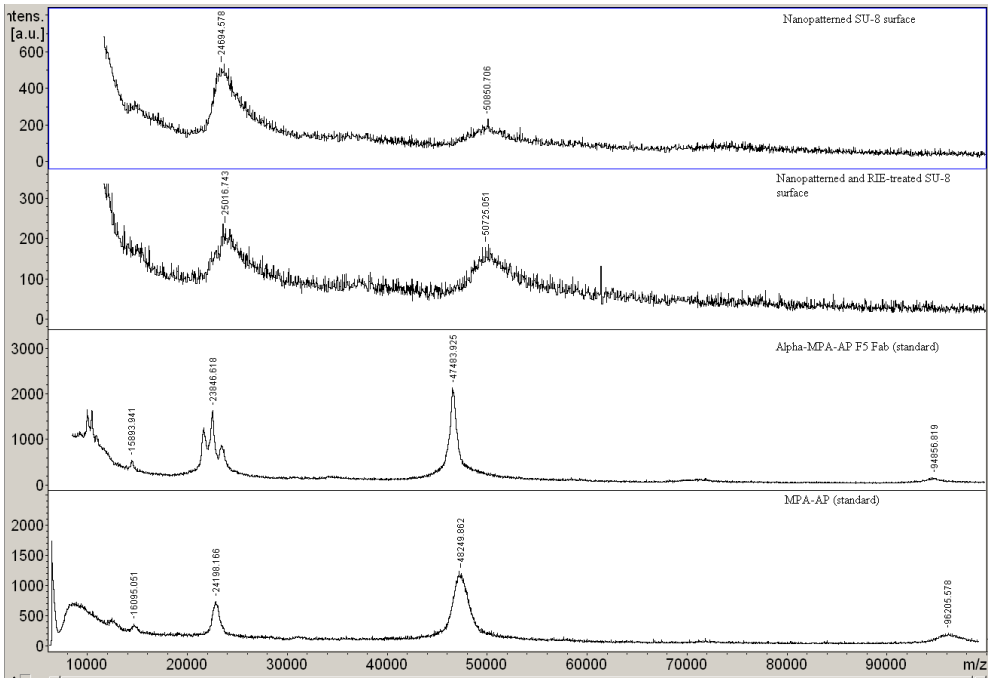

Figure 1. MALDI spectra of SU-8 surfaces with random immobilization and reference spectrum for antibody and antigen.

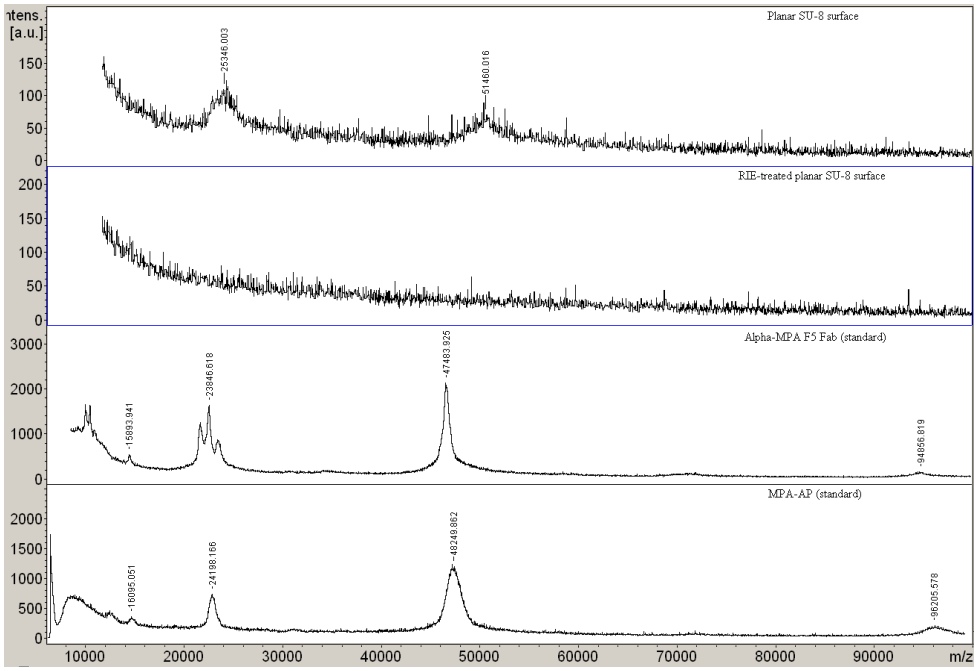

Figure 2. MALDI spectra of SU-8 surfaces with oriented immobilization and reference spectrum for antibody and antigen

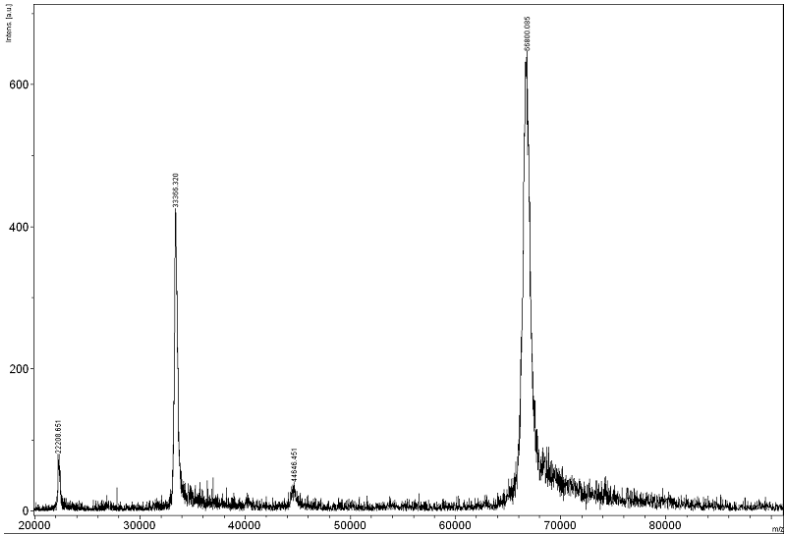

Figure 3. BSA reference spectrum on SU-8 (500 shots).

Appendix F. Liquid flow studies

- **Incorrect behavior,** because of wrong contact angle: the liquid flows up- and downwards from the inlet.

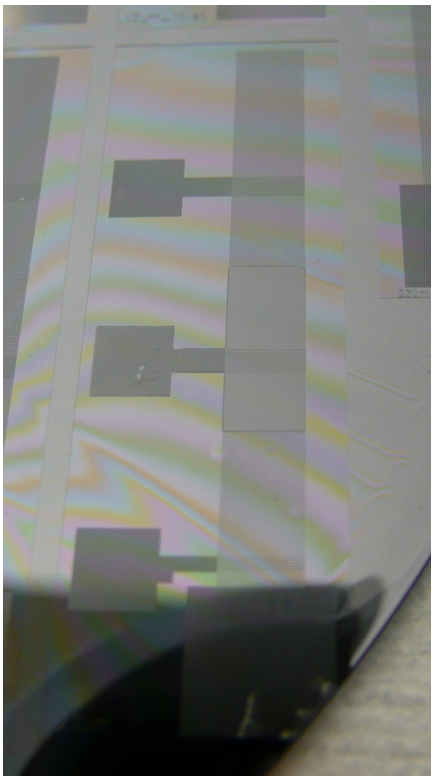

Figure 1. Due to too low contact angle, the liquid flows up- and downwards from the inlet. SU-8 layer is 17.8 µm thick and the contact angle is 26.5°.

- **Incorrect behavior**, because of the PBS evaporation: the liquid flows correctly at first, but after a while the liquid flows also downwards.

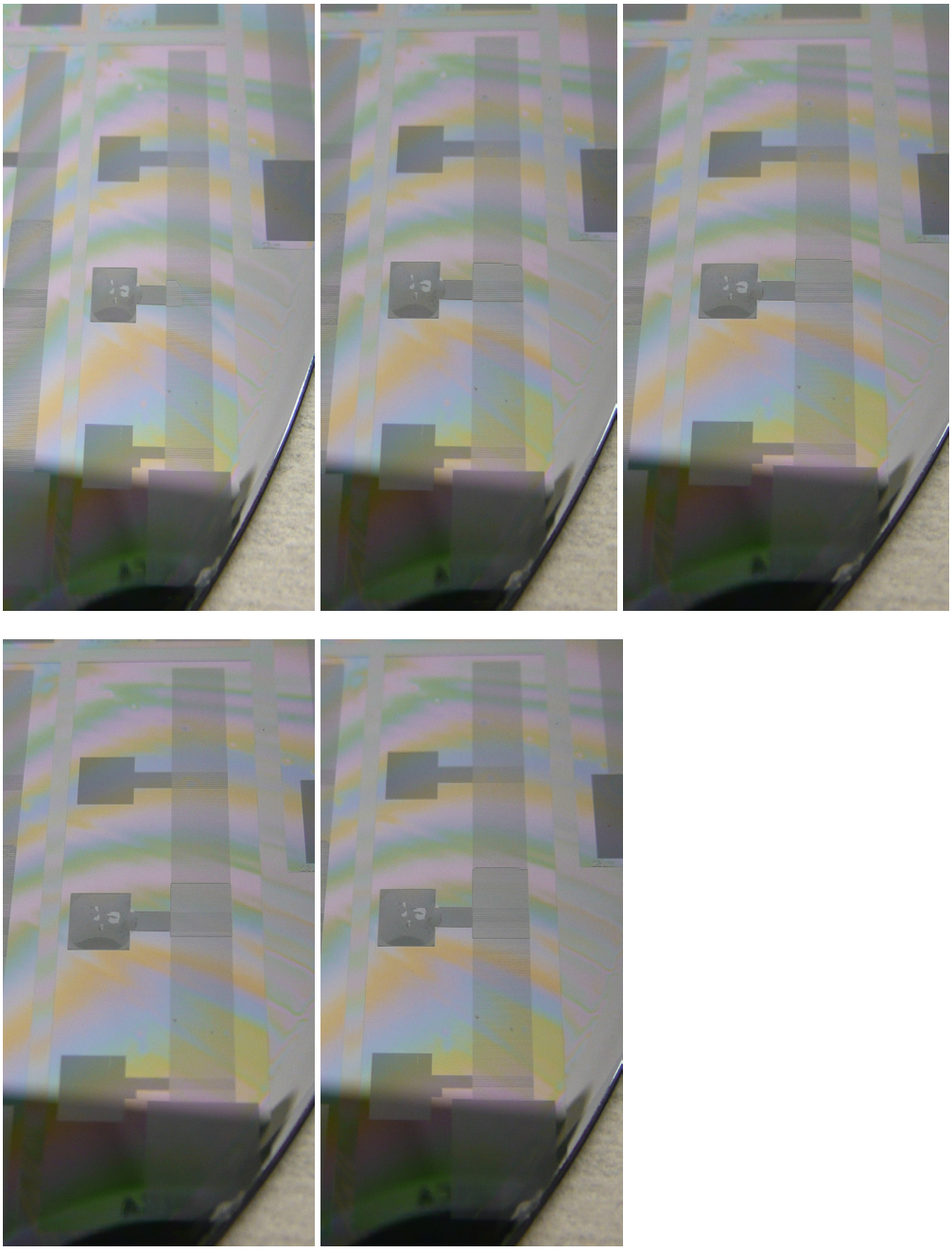

Figure 2. The liquid flow in 14.8 µm thick SU-8 chip when contact angle is 42° and the surrounding humidity is not controlled (time period 1 min and consecutive row distance in channel 23 µm).

- **Correct behavior** (made with water):

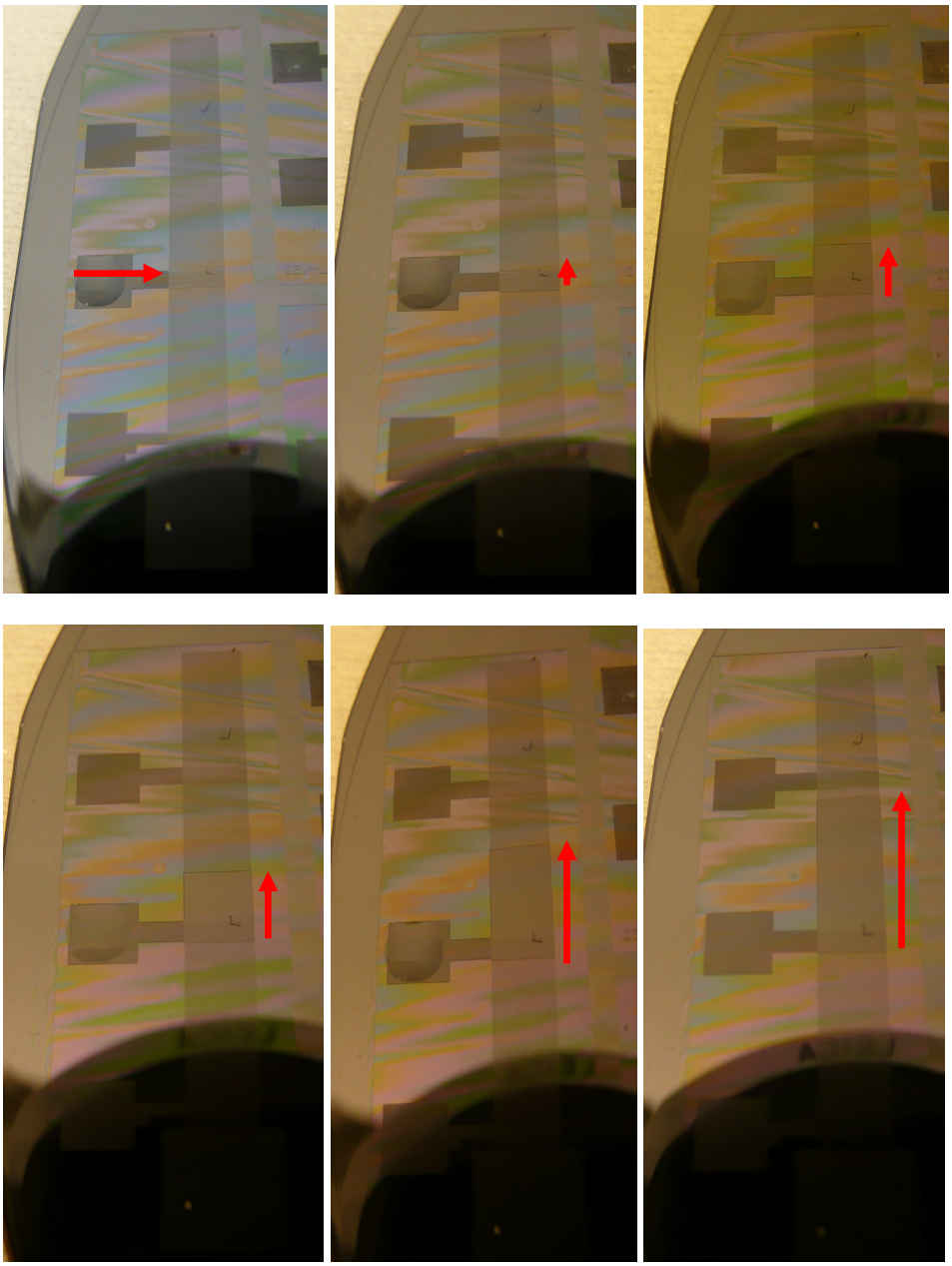

Figure 3. The water flows only upwards from the inlet when contact angle was 42°, SU-8 layer thickness 14.8 µm and the humidity under control (the red arrow indicates the current position of the proceeding liquid). Adapted from ref. [112].